GEOCHIMICA ET COSMOCHIMICA ACTA

UNIVERSITY OF HAWAII
LIBRARY
APR 4 '56

EDITORIAL ADVISORY BOARD

T. BARTH-OSLO · **N. L. BOWEN**-WASHINGTON, D.C. · **A. F. BUDDINGTON**-PRINCETON, N.J. **L. CAPDECOMME**-TOULOUSE · **E. J. CONWAY**-DUBLIN · **P. ESKOLA**-HELSINKI **P. GALLITELLI**-MODENA · **D. GUIMARÃES**-BELO HORIZONTE · **A. HADDING**-LUND **O. HAHN**-GÖTTINGEN · **H. W. HARVEY**-PLYMOUTH · **F. HEIDE**-JENA · **A. HOLMES**-EDINBURGH · **G. E. HUTCHINSON**-NEW HAVEN, CONN. · **W. Q. KENNEDY**-LEEDS **PH. H. KUENEN**-GRONINGEN · **S. LANDERGREN**-STOCKHOLM · **F. MACHATSCHKI**-VIENNA · **B. H. MASON**-NEW YORK · **A. MUIR**-HARPENDEN · **J. ORCEL**-PARIS **E. RAGUIN**-PARIS · **K. RANKAMA**-HELSINKI · **E. REINHARD**-BASLE · **TH. G. SAHAMA**-HELSINKI · **C. E. TILLEY**-CAMBRIDGE · **H. C. UREY**-CHICAGO · **T. VOGT**-TRONDHEIM **W. WAHL**-HELSINKI · **T. WATANABE**-TOKYO · **F. WHIPPLE**-CAMBRIDGE, MASS. **R. WILDT**-NEW HAVEN, CONN.

EDITORS

L. H. AHRENS — OXFORD
C. W. CORRENS — GÖTTINGEN
E. INGERSON — WASHINGTON
S. R. NOCKOLDS — CAMBRIDGE
F. A. PANETH — MAINZ
L. R. WAGER — OXFORD
F. E. WICKMAN — STOCKHOLM

VOLUME 6 Nos. 5/6

DECEMBER, 1954

PERGAMON PRESS LTD · LONDON & NEW YORK

Geochim. et Cosmochim. Acta

GEOCHIMICA ET COSMOCHIMICA ACTA

EDITORS

DR. L. H. AHRENS, *Department of Geology and Mineralogy, The University, Oxford, England.*

PROF. C. W. CORRENS, *Sedimentpetrographisches Institut der Universität, Lotzestr.* 13, *Göttingen, British Zone, Germany.*

DR. E. INGERSON, *United States Department of the Interior, U.S. Geological Survey, Washington* 25, *D.C., U.S.A.*

DR. S. R. NOCKOLDS, *Department of Mineralogy and Petrology, The University, Cambridge, England.*

PROF. F. A. PANETH, F.R.S., *Max-Planck-Institut für Chemie, Mainz, Saarstrasse* 23, *Germany.*

PROF. L. R. WAGER, F.R.S., *Department of Geology and Mineralogy, The University, Oxford, England.*

PROF. F. E. WICKMAN, *Naturhistoriska Riksmuseets, Mineralogiska Avdelning, Stockholm* 50, *Sweden.*

PERGAMON WAS THE NAME OF A GREEK TOWN IN ASIA MINOR, FAMOUS FOR ONE OF THE GREAT WORKS OF ART, THE ALTAR OF PERGAMON, DEDICATED TO ATHENA.

THE COLOPHON ON THE FRONT COVER IS A REPRODUCTION OF A COIN FOUND AT HERAKLEIA, DATING FROM ABOUT FOUR-HUNDRED B.C., SHOWING THE HEAD OF ATHENA.

VOLUME 6, NOS. 5/6 DECEMBER, 1954

CONTENTS

PAGE

G. BOATO: The isotopic composition of hydrogen and carbon in the carbonaceous chondrites 209

EDWARD P. HENDERSON and STUART H. PERRY: A discussion of the densities of iron meteorites 221

WILLI DANSGAARD: The O^{18}–abundance in fresh water 241

W. GENTNER and E. A. TRENDELENBURG: Experimentelle Untersuchungen über die Diffusion von Helium in Steinsalzen und Sylvinen 261

J. R. BUTLER: The geochemistry and mineralogy of rock weathering. (2) The Nordmarka Area, Oslo 268

HERBERT H. UHLIG: Contribution of metallurgy to the origin of meteorites. Part I —Structure of metallic meteorites, their composition and the effect of pressure . 282

Book review:

Minerals for the Chemical and Allied Industries by SYDNEY J. JOHNSTONE (reviewed by C. F. DAVIDSON) 302

Correction to a paper by H. G. THODE, R. K. WANLESS and R. WALLOUGH . 302

Publishing Offices: Pergamon Press Ltd., Maxwell House, Marylebone Road, London, N.W.1 (AMB 3421).

Subscription per volume (including postage) £4 10s. (U.S.A. $12.60).

Distributors: Lange, Maxwell & Springer Ltd., Maxwell House, Marylebone Road, London, N.W.1.

and Pergamon Press Inc., 122 East 55th Street, New York 22, N.Y.

PERGAMON PRESS LTD., MAXWELL HOUSE, MARYLEBONE ROAD, LONDON, N.W.1
PERGAMON PRESS INC., 122 EAST 55TH STREET, NEW YORK 22, N.Y.

Geochimica et Cosmochimica Acta, 1954, Vol. 6, pp. 209 to 220. Pergamon Press Ltd., London

The isotopic composition of hydrogen and carbon in the carbonaceous chondrites[1]

Giovanni Boato[2]
Institute for Nuclear Studies, University of Chicago

(*Received* 18 *June* 1954)

ABSTRACT

A number of carbonaceous chondrites have been analyzed for hydrogen and carbon content and for the isotopic composition of these elements. Two types of these meteorites are found, the one containing about 10% of water and 2% of carbon and the other about 1% of water and 0·3–0·8% of carbon. The isotopic compositions of these elements in both groups are not much different from terrestrial sources. Four stones show a deuterium content definitely outside the range of terrestrial values; this fact and a series of experiments showed that the extracted hydrogen was truly meteoritic. Thus for the first time an experimental value for the isotopic composition of the hydrogen of an extraterrestrial material has been obtained. It appears that no large isotopic fractionation of the hydrogen isotopes has occurred in the planetary system; therefore, the terrestrial deuterium abundance is probably well representative of the primeval cosmic abundance.

Three groups of chondrites are apparent on the basis of carbon results; they correspond to progressively higher values for total carbon and C^{13} content. The results are discussed in the light of present theories on the formation of the planetary system and on the origin of meteorites.

Introduction

The carbonaceous chondrites are a rare type of stony meteorite of high carbon and water content and little or no metallic iron; they are poorly described in the literature and some general information about their occurrence and properties will first be discussed.

Twenty carbonaceous chondrites are known at the present time; all of these were observed to fall and were collected shortly afterwards. The names and dates of fall are shown in Table 1 together with the localities of the falls; it is interesting to note that they have fallen all over the earth and with a uniform rate of fall.

Most of the carbonaceous chondrites are very similar in appearance and physical properties. At the surface they show a thin fusion crust, due to the heat developed during the fall through the earth's atmosphere, but a few millimetres below, the stone is completely unaltered. The inner material is grey-black with a few small chondrules, and its behaviour and appearance are those of a heavily compressed powder. Chemical analyses have been made in only a few cases and unfortunately most of them are of very poor quality. They have been tabulated in a recent article by Urey and Craig (1953, Table 7). The main peculiarity of the carbonaceous chondrites is the high percentage of carbon and water and a highly oxidized state for the iron. Organic substances have been reported by several authors; the subject has been discussed recently by G. Müller (1953), who carefully studied the organic complex contained in the Cold Bokkeveld meteorite. He reported about one per cent of organic matter containing nitrogen, chlorine, and sulphur. In the small specimens at my disposal it was not possible to separate

[1] Part of this paper was presented at the A.A.A.S. Conference on the Origin of Meteorites, held in Boston, Mass., on December 30, 1953.

[2] Present address: Universita' di Genova, Istituto di Fisica, Genova, Italy.

workable amounts of organic substances by extraction at the boiling point of benzene; in three different stones which were processed, a slight amount of a colourless, oily, spicy-smelling substance mixed with a few crystals of sulphur was obtained in each case. If one heats the powdered meteorites at about 250°–300°C, a colourless sublimate of the same nature is often observed. The sublimate can be re-evaporated without any decomposition. It appears likely that traces of organic substances are present in variable amounts in all these meteorites.

Table 1. *Carbonaceous chondrites with locality and date of fall*

Alais, France, 1806	Mighei, Ukraine, 1889
Cold Bokkeveld, South Africa, 1838	Mokoia, New Zealand, 1908
Crescent, United States, 1936	Murray, United States, 1950
Felix, United States, 1900	Nawapali, India, 1890
Grazac, France, 1885	Nogoya, Argentina, 1879
Haripura, India, 1921	Orgueil, France, 1864
Indarch, Russia, 1891	Santa Cruz, United States, 1939
Ivuna, Tanganyika, 1931	Simonod, France, 1835
Kaba, Hungary, 1857	Staroye Boriskino, Russia, 1930
Lancé, France, 1872	Tonk, India, 1911

The mineralogical structure of the carbonaceous meteorites is not known because the very fine grained material and amorphous carbon hinder greatly the microscopic observation of the ground mass.

It should be noted that the carbonaceous chondrites have never been heated above a temperature of 300°–400°C since their formation. At this temperature one begins to notice a strong modification of the general properties of the stone, as has been shown by Müller (1953) and other observers. Water, for example, is given off irreversibly and organic compounds are distilled out or decomposed.

Because of this and other properties so similar to those expected for low temperature accumulation products, these particular stones were chosen by Urey (1952a) as the cosmic material nearest to the "primordial dust" from which the planetary system was formed. Volatile elements[1], such as hydrogen and carbon, were preserved in carbonaceous meteorites and were probably carried to the forming earth by means of objects of this kind during the accumulation process.

The origin of the carbonaceous chondrites is still uncertain. Urey and Craig (1953) had difficulty in including them in their theory of the formation of meteorites by the collision of two small asteroids. In this theory one place for them would be in the interior of the body of the asteroids. This assumption is consistent with the general course of events advanced by Urey (1952b) for the preservation of carbon, nitrogen, and water during the formation of the solar system.

The aim of the present research was to study the volatile elements hydrogen and carbon, to determine their isotopic composition in comparison with the ordinary chondrites and the earth's crustal material, with the hope of finding some general indication as to the origin of meteorites and the process of formation of the planetary system, and to solve the particular question as to whether the deuterium content of meteorites is different from that of the earth.

[1] Volatile elements are those possessing some stable volatile compound at low temperature.

Samples

Fragments of twelve carbonaceous chondrites were made available through the courtesy of many museums, institutions, and private persons. A specification of the specimens follows.

British Museum of Natural History, London, England	Cold Bokkeveld
Muséum National d'Histoire Naturelle, Paris, France	Cold Bokkeveld Orgueil Lancé
Wanganui Museum of Natural History, Wanganui, New Zealand	Mokoia
Geological Survey of India, Calcutta, India	Haripura Nawapali
Geological Survey of Tanganyika, Dar-es-Salaam, Tanganyika Territory	Ivuna
Mr. John R. Horan, Idaho Falls, Idaho	Murray
U.S. National Museum, Washington, D.C.	Felix
American Meteorite Museum (H. H. Nininger), Sedona, Arizona	Mokoia Santa Cruz
Chicago Natural History Museum, Chicago, Illinois	Mighei Indarch

Experimental Technique and Results

The specimens were analyzed for hydrogen and carbon with a combustion method very similar to an ordinary combustion train for organic micro-analysis. A thoroughly quantitative procedure of extraction is necessary not only to obtain an exact determination of the H and C content of the meteorite but also to prevent isotopic fractionation during the processing. Precautions have to be taken also to avoid any possibility of contamination of the sample with foreign H and C, both from material adsorbed on the walls and in the reagents and from exchange processes.

The apparatus is shown in Fig. 1. The meteorite sample (about 0·2 gms) placed in a small boat (*A*), is first gently heated in a vacuum to 180°C, in order to give off the water physically adsorbed on the surface of the meteorite. The temperature of 180°C was chosen on the basis of experiments which will be described later. A pure oxygen stream at reduced pressure (~50 cm Hg) is then allowed to pass through the Vycor combustion tube, at the rate of 5–8 cc per minute. The sample is heated with a Bunsen burner to total combustion. The uncombusted gases are completely oxidized in *B* on a Pt catalyst at 800°C, which has the additional purpose of converting the SO_2 to SO_3. The silver gauze contained in the furnace *C*, along which a temperature gradient from 300 to 450°C is established, takes up all the halogens as silver halides and all the sulphur as $AgSO_4$. The only residual condensible combustion products, water and carbon dioxide, are trapped in *D* and *F* with dry ice and liquid oxygen. The MnO_2 filled tube *E* (room temperature) adsorbs the SO_2 not oxidized in *B*.

When enough time has elapsed to insure complete combustion of the sample and total condensation of H_2O and CO_2, the stop-cocks 1 and 4 are closed, a vacuum is made in the manifold through 5 and the H_2O and CO_2 can be distilled out, measured, and collected in sample tubes. H_2O is totally converted to H_2 with Zn at 400°C. The per cent of water in the meteorite is determined by measuring the pressure of the hydrogen in a known volume. The hydrogen is transferred to this volume and to the sample tube by an automatic Toepler pump.

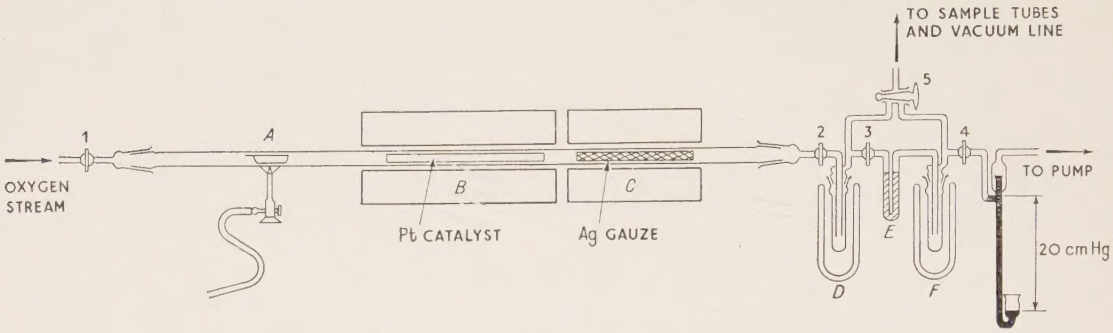

Fig. 1. The combustion apparatus.

The mass spectrometers used for this investigation were those of H. C. UREY'S group (MCKINNEY *et al.*, 1950). The instrument for carbon is the same as that used by CRAIG (1953) and reference is made to his paper for a complete discussion of the errors of measurement and of the precautions to be taken for good reproducibility of results. The standard used for comparison is CRAIG'S.

The hydrogen mass spectrometer is described by FRIEDMAN (1953). The standard used was again Lake Michigan water, but a new calibration of the instrument was made with water samples of known deuterium content. These additional standards were prepared from the original one, adding to it accurately measured amounts of pure heavy water. Our main standard differs from FRIEDMAN'S by containing 0·5% more deuterium. The overall error of the hydrogen results is usually less than ±0·5%.

The isotopic data presented in this paper are expressed in the conventional way, i.e.

Hydrogen

$$\delta \text{ D in } \% = \left[\frac{\text{D/H sample} - \text{D/H standard}}{\text{D/H standard}}\right] \times 100$$

Carbon

$$\delta \text{ C}^{13} \text{ in } ‰ = \left[\frac{\text{C}^{13}/\text{C}^{12} \text{ sample} - \text{C}^{13}/\text{C}^{12} \text{ standard}}{\text{C}^{13}/\text{C}^{12} \text{ standard}}\right] \times 1000$$

Table 2 lists the weight per cent of hydrogen (as water) and carbon and their isotopic analyses for the investigated chondrites. The first column shows the percentage of water given off by the meteorite in a vacuum at 180°C; in the third column the amount of water produced during the combustion of the sample after the vacuum treatment is given. The second and fourth columns show the corresponding isotopic composition of hydrogen.

According to the ranges in carbon and total water content, the carbonaceous chondrites analyzed were divided in two groups: the first corresponds to 9–12% total water and 1·6–3·3% carbon, the second 1·0–1·5% water and 0·3–0·8% carbon.

Carbon content and isotopic composition of two ordinary chondrites are also given. Many chemical analyses have shown ordinary chondrites to contain 0·2% water and less than 0·1% carbon.

In two cases analyses are given for specimens of the same stone from two different museums; the measured isotopic compositions are similar in the case of Mokoia, but definitely different in the case of Cold Bokkeveld. This difference may result from the two specimens of Cold Bokkeveld representing different stones from the same meteoritic shower.

Table 2. Hydrogen and carbon content and isotopic composition of chondrites

Type	Name	Per cent H_2O at 180°C	$\delta D(‰)$	Per cent combined water	$\delta D(‰)$	Per cent carbon	$\delta C^{13}(‰)$
Type I Carbonaceous Chondrites	Cold Bokkeveld (British Museum)	2·1	−7·6	7·8	−13.0	1·55	−9·4
	Cold Bokkeveld (Paris)	2·6	−3·7	8·0	−5·8	1·6	−5·2
	Haripura	2·4	−1·1	7·3	−3·3	1·6	−3·7
	Ivuna	4·7	−1·0	7·0	+35·8	3·3	−6·6
	Mighei	1·7	−4·2	8·6	−6·4	2·6	−9·9
	Murray	2·3	−8·9	6·8	+9·6	1·9	−3·9
	Nawapali	3·0	−4·2	9·0	−7·2	1·9	−10·0
	Orgueil	4·0	+1·5	7·3	+29·0	2·8	−11·4
	Santa Cruz	1·8	−8·0	8·4	−0·7	2·2	−4·3
Type II Carbonaceous Chondrites	Felix	(1·0)	—	—	—	0·47	−16·4
	Indarch	0·7	−7·3	0·3	−10·7	0·4	−12·9
	Lancé	0·6	−6·3	0·9	−7·7	0·34	−15·7
	Mokoia (Nininger)	0·3	−6·8	0·8	+25·9	0·84	−17·4
	Mokoia (Wanganui)	0·25	−7·2	0·75	+23·5	0·65	−18·8
Ordinary Chondrites	Richardton	(0·1)	—	—	—	0·02	−24·6
	Forest City	—	—	—	—	0·08	−24·3

The figures in Table 2 represent generally the average of two or three determinations carried out on different parts of the same specimen. The difference between two such measurements was found in several cases (in the meteorites of the first group) to be slightly outside the overall error of the experimental procedure. It appears that the carbonaceous meteorites are not always homogeneous throughout their mass as far as hydrogen and carbon are concerned. This point will be considered further in the discussion of carbon results.

The two groups of carbonaceous chondrites are seen in Table 2 to be clearly divisible on the basis of water content, carbon content, and carbon isotopic composition; they are also definitely different from a broader point of view. The first group, here designated as Type I carbonaceous chondrites, are structurally all very similar to one another and correspond closely to the general description given in

the introduction. With the exception of Ivuna, Murray, and Santa Cruz, all these Type I stones have been described in the literature; they are classed in COULSON'S catalogue (1940) as carbonaceous chondrites, characterized by the presence of free carbon and the near or total absence of nickel-iron.

The second group, for which the designation Type II carbonaceous chondrites is here proposed, consists of four stones. Three of these, Indarch, Felix, and Lancé, are classed by COULSON as spherical carbonaceous chondrites, distinguished from the ordinary carbonaceous chondrites by the presence of metallic nickel-iron, and of hard, radiated chondri. Indarch, in particular, is additionally specified as "veined," the veins being nickel-iron. Indarch is a very hard stone, and, on the basis of its general characteristics, is most likely an enstatite chondrite, as PRIOR (1916) pointed out long ago. Felix and Lancé, friable grey stones, are immediately distinguishable from the Type I stones, even by inexperienced observers. Mokoia is structurally the most similar to the Type I stones, and indeed is classed by COULSON as an ordinary carbonaceous chondrite; however, it contains so much less water and carbon that it must be put in the second group.

DISCUSSION OF THE RESULTS

Hydrogen

The described procedure for extraction of the water was adopted after a series of experiments was carried out to establish the nature and the amount of contamination with terrestrial water. First, it was found that the water given off in a vacuum at low temperature was strictly related to the isotopic composition of the atmospheric water vapour. Thus meteorites analyzed during winter time—Cold Bokkeveld (British Museum), Murray, Santa Cruz, Indarch—showed lower values for the D content than those analyzed during the summer, an observation which correlates with the fact that Chicago snows always have several per cent less deuterium than Chicago summer rains (H. CRAIG, unpublished data; FRIEDMAN, 1953). Secondly, exchange experiments were carried out by leaving samples of powdered carbonaceous chondrites in contact with water vapour of known deuterium content for periods of a week or more. It was found that the higher the temperature of extraction of the water in vacuum, the less was the observed exchange of deuterium in comparison with the original value. Moreover, the water collected in the subsequent oxidation of the sample approached nearer and nearer the initial composition. The temperature of 180°C was chosen as that corresponding to a minimum of contamination of terrestrial water in the water obtained during the combustion process. The water extracted at 180°C in a vacuum is presumed to contain all the superficially absorbed water, which can exchange completely with external water. An exchange experiment carried out on the Murray stone for a six months period showed that the exchange with the remaining water, which in Table 2 is called "combined" water, is practically absent. The experiment was effected in a saturated water vapour environment to insure conditions much worse than those present in a museum. The isotopic composition of the "combined" water is assumed to be representative of the original hydrogen isotopic composition of the meteorite. It is interesting to note that most of the total water is extracted during the combustion process, and in a constant proportion.

To clear up this point, and to check the possible contribution to this high temperature water from other hydrogenated compounds, several stones were heated gradually in a vacuum up to 900°C, collecting the fractions of water given off between six different temperatures. Two typical cases are shown in Table 3 and the corresponding isotopic compositions are given.

Table 3. Water fractions extracted in vacuum at different temperatures from carbonaceous chondrites, in weight per cent of meteorite sample

Temperatures	Ivuna		Cold Bokkeveld (Paris)	
	Per cent water	δD(‰)	Per cent water	δD(‰)
25°–180°C	6·0	+1·8	2·6	−2·8
180°–260°C	1·1	+11·4	1·1	−5·6
260°–325°C	0·7	+19·5	1·2	−9·8
325°–400°C	0·8	+31·5	1·9	−8·6
400°–500°C	1·2	+37·9	2·4	−3·8
500°–800°C	3·1	+42·0	1·6	−2·1
Total combined water (180°–800°C)	6·9	+30·0	8·2	−5·7

It appears that a remarkable amount of water is bound in the stone even at 500°C; the total amount of water given off above 180°C is about the same as in the combustion process, thus excluding the presence of important quantities of other volatile hydrogenated materials, such as organic compounds. If organic-like compounds are present in large amount they must decompose totally into water before distilling out from the stone.

Table 4. Deuterium content of terrestrial waters (δD in per cent with respect to Lake Michigan standard water)

Average ocean[1]	+4·7
Rain and snow[1]	−14·4 to +4·8
Atmospheric water vapour[2]	down to −13·5
Rivers and lakes[1]	−10·3 to +4·1
Hot spring waters[3]	−13·0 to +3·2
Hekla lava[2]	−15·0

[1] H. Craig, manuscript in preparation.
[2] G. Boato, unpublished data.
[3] H. Craig and G. Boato, manuscript in preparation.

We do not yet know with certainty the chemical form in which the water exists in the carbonaceous chondrites, but the present data indicate that it is mainly combined as hydrated minerals.[1]

[1] A. N. Zavaritzky and L. G. Kvasha (The Meteorites of U.S.S.R., Moscow, 1952) report about 8·5% of combined water in Staroye Boriskino and Mighei, in good agreement with our results. They claim these meteorites contain "chloritic minerals" and that they have seen chlorite crystals under the microscope.

Before discussing the isotopic data of Table 2, it is worthwhile to compare them with the natural variations in the isotopic composition of terrestrial waters, which are briefly summed up in Table 4. No surface water analyzed mass-spectrometrically has yet been found with a deuterium content more than 5% higher than Lake Michigan water.

The isotopic composition of the water extracted at 180°C from carbonaceous chondrites falls always in the range of the terrestrial variations; this confirms the conclusion drawn previously that this water is mostly of terrestrial origin. The water obtained at higher temperature has a much greater range of variation and in four cases is definitely outside the terrestrial range. It seems established, therefore, that at least in four cases the measured isotopic composition cannot be ascribed to water exchange or adsorption taking place on the earth after the fall of the meteorite, i.e., it has to be ascribed to true meteoritic water.

The relatively small enrichment in deuterium of this meteoritic water (some 30%) can be explained with single stage fractionation processes. However, it is very difficult to explain the observed effect with fractionation processes on the earth because there is no relation between isotopic composition and date of fall, and, moreover, the stones are all very similar one to the other, as was pointed out earlier; thus there is no plausible way to explain the large range of meteoritic variation with terrestrial fractionation processes.

It is concluded that the observed variations can only be explained with single stage fractionation processes which happened before the fall of the meteorites on the earth, probably during the formation of the stones themselves. The implications of this result with respect to the genesis of the solar system have been discussed elsewhere (BOATO, 1954), and need not be repeated in detail. One is led to the conclusion that the terrestrial or meteorite abundance is our closest estimate for the primordial cosmic abundance of deuterium, and that the much lower deuterium concentration in the sun is due to its consumption as nuclear fuel during the course of time since the formation of the planets and the asteroids.

The meaning of the large range of variation of the isotopic composition of hydrogen is not clear. Two kinds of behaviour are apparent from the water extraction processes in vacuum, although they are not sharply defined. High deuterium stones behave like Ivuna (see Table 3); the deuterium content of the different water fractions increases continuously with the temperature; low deuterium stones show a minimum of deuterium at a temperature around 300–400°C; Cold Bokkeveld is a typical example of this. Whether the effect is due to contamination of external water or whether it is a property of the meteorites themselves could not be determined.

The apparently random variations of the content and isotopic composition of hydrogen will be discussed in the next section together with the carbon results.

Carbon

In columns 5 and 6 of Table 2, the percentage and isotopic composition of carbon in the carbonaceous chondrites, and in two ordinary chondrites, are given.

The two groups of carbonaceous chondrites, defined on the basis of carbon and water content as noted previously, are seen to be distinguishable also on the basis

of carbon isotope composition. In the Type I group, highest in carbon and water content, the C^{13} concentration is a maximum, δ ranging from -3 to $-12‰$. In the Type II group, the lower carbon and water content is accompanied by a lower C^{13} concentration, δC^{13} ranging from -13 to $-18‰$. Finally, in the ordinary chondrites, lowest of all in carbon and water, the C^{13}/C^{12} ratio is also lowest, δ being about $-24‰$ as shown by the two data and from less accurate analyses by Murphey and Nier (1941), and Trofimov (1950). The isotopic composition of carbon in the ordinary chondrites here analyzed falls just in the range of the carbon in the terrestrial igneous rocks analyzed by Craig (1953, p. 80).

Thus, in the chondrites, one finds three associated trends: decrease of carbon and water content, decrease of C^{13} concentration in the carbon, and increase in nickel-iron content. The variation in isotopic composition of the carbon may well reflect the history of these stones with respect to their volatile material, that is, it may have been produced by whatever processes caused the associated differences in water and carbon content. If the two types of carbonaceous chondrites have been derived from one fundamental material, then certainly Type I is much closer in bulk composition to the original material; it would be extremely difficult to devise a mechanism which would produce the Type I stones from the Type II group. However, it does not appear possible to devise a simple genetic relationship between these three types of chondrites based only on heating, loss of carbon and water, and reduction of iron by carbon. In fact, the ordinary chondrites, at least, must have had a more complicated history, since they are agglomerates of fragmental material and chondrules. Moreover, the increase in nickel-iron content in going from Type II carbonaceous chondrites to ordinary chondrites is certainly so much greater than the increase in going from Type I to Type II carbonaceous chondrites, that another reducing agent, most probably hydrogen, must have been involved.

Whatever the actual processes were which finally produced these various types of chondrites, the decrease in C^{13} content with decreasing water and carbon, may reflect an isotopic effect during the particular process by which the volatiles were lost. It is interesting, in this connection, to note that Craig (1953) found a $15‰$ depletion in C^{13} to result from the process by which the organic material of marine plants and animals is concentrated to form petroleum and the carbonaceous material in black shales. The carbonaceous material in the meteorites is, of course, not derived from living sources, but it is noteworthy that the range of variation in C^{13} in the meteorites is of the order of the depletion observed in a terrestrial process involving loss of volatile carbon compounds. Such a depletion of C^{13} may represent an actual isotopic fractionation process, or may represent loss of compounds which possessed an isotopic composition heavier than that of the material retained, as was postulated by Craig to explain the petroleum composition.

On the other hand, it should be noted that the correlation of carbon content with isotopic composition in the meteorites may be due to an original accumulation in varying proportions of different carbon compounds such as amorphous carbon, graphite, and organic material. Craig (1953, p. 83) found that graphite and iron carbide in the Canyon Diablo iron meteorite differed considerably in C^{13} content. His value for the iron carbide ($-17{\cdot}9‰$) falls nicely in the range of the Type II

group, while his value for graphite (−6·3‰) is very close to the average of the Type I stones. Amorphous carbon is certainly present in carbonaceous chondrites and has been reported by many authors; graphite is doubtful, as X-ray diagrams do not show the corresponding lines. A small amount of organic compounds is certainly present, but it is not possible to infer any conclusions about them at the present time.

It is interesting, in any case, to compare the meteoritic and terrestrial C^{13} concentration. The range of variation is pretty much the same; an average value was estimated by Craig (1953, p. 87) for the earth's crust from the isotopic composition of shales and limestones, the two most abundant deposits of carbon; this value is about −12‰ on the scale we are using. It is difficult to calculate a similar average for the meteorites, because of the present lack of data, but a rough estimate seems to be not much different from the terrestrial value, if one takes into account the carbonaceous chondrites. If one assumes that the carbonaceous chondrites represent 2% of the total chondrites with −7‰ average C^{13} concentration, one gets about −16·5‰ for the desired average. It is not possible to compare the meteoritic and terrestrial isotopic data more precisely without some knowledge of how the different groups of meteorites should be weighted.

No other correlation but that mentioned above is evident from the results on carbon content and isotopic composition; in the first group of carbonaceous chondrites, high carbon percentage and high δ do not correlate at all. Nor is there evidence of any relationship between carbon and hydrogen values.

Surely we are too short of data to draw definite conclusions, but it is possible that this random distribution of values has some meaning. Attention should be drawn to the fact, already mentioned, that different parts of the same stone sometimes show slightly different results, outside the experimental errors. As an example, one may note the data obtained for the two meteorites for which the discrepancies were the most remarkable:

Mighei	Combined water	δD (%)	= −5·4, −7·4
	Carbon	δC^{13}(‰)	= −9·1, −11·8, −8·7
Cold Bokkeveld	Combined water	δD(%)	= −5·7, −5·9
(Paris)	Carbon	δC^{13} (‰)	= −5·0, −6·3, −4·4

While these differences might be explained in the case of hydrogen by terrestrial contamination, the matter is different when carbon results are considered: exchange is not possible in this case and adsorption of carbonaceous substances on the earth is very unlikely. Moreover our method of isotopic analysis for carbon is reproducible within 0·2‰, as has been shown in many experiments with homogeneous materials.

It is certain therefore that the effect is due to an inhomogenity of the meteorites themselves. This is not a surprising conclusion, as it is well known that meteorites are the product of an accumulation process which produced a physical mixture of silicate and metal fragments and chondrules in varying proportions. However, the differences found for both carbon content and isotopic composition are much greater than the ordinary variations met for non-volatile elements. It appears then

that during the history of the carbonaceous chondrites some kinetic process was operative for carbon compounds (and probably for water), such as escape of carbon or chemical reactions. It is possible, of course, that several carbon compounds were present at the time of accumulation.

At present amorphous carbon is supposed to be the only important compound in the Type I carbonaceous chondrites, while organic compounds are present in trace amounts, but it is possible that in the future more accurate chemical analyses will shed more light on this point.

Conclusion

Precision isotopic analysis has again proved to be useful for problems in geochemistry and cosmochemistry. The present data on carbonaceous chondrites contribute to the explanation of some interesting questions.

First, it was shown that the highly volatile elements, hydrogen and carbon, underwent no large isotopic fractionation during the formation of the planetary system. This statement is made on the presumption that carbonaceous meteorites, and ordinary ones, are parts of the solar system and originated with it.

Secondly, it was concluded that the primeval cosmic D/H ratio was not much different from the present ratio on the earth.

Finally, a correlation between the carbon content and the C^{13}/C^{12} ratio was found, possibly representing preferential loss of C^{13} during the process in which the volatiles were lost from the original material from which the various groups of chondrites were formed. Type I carbonaceous chondrites are probably closest in bulk composition to this original material. On the other hand, accumulation in varying proportions of isotopically different carbon compounds cannot be ruled out as an explanation.

It is hoped that a larger number of analyses, extended also to sulphur and nitrogen, and to all types of meteorites, will help us to understand more thoroughly the fundamental question of the history of the volatile elements during the formation of the planetary system.

Acknowledgments

I wish to thank Dr. Harold C. Urey, who suggested the search for deuterium in meteorites, for his advice and helpful interest in this work. It is also a pleasure to thank Dr. Harmon Craig, with whom every point of this paper has been discussed.

I wish to acknowledge the help of Dr. George Edwards, Mrs. Toshiko Mayeda, and Mr. Arthur Gropen for many services in the laboratory. I am deeply indebted to the following persons for furnishing meteorite specimens: Dr. W. Campbell Smith, British Museum (Natural History), London; Dr. J. Orcel, Museum National d'Histoire Naturelle, Paris; Dr. M. J. G. Smart, Wanganui Museum, New Zealand; the Directors of the Geological Survey of India and Tanganyika; Mr. John R. Horan; Dr. E. P. Henderson, U.S. National Museum, Washington; Dr. H. H. Nininger, American Meteorite Museum, Sedona, Arizona; Dr. Sharat Roy, Museum of Natural History, Chicago.

I am personally indebted to the Department of State of the U.S. Government for having granted me a fellowship which made possible my travel and stay in the United States.

The isotope research programme in Dr. Urey's laboratories was financed in part by the Atomic Energy Commission under Contract No. AT(11–1)—101 during the time in which this work was done.

References

Boato, G. (1954) Phys. Rev. **93,** 640
Coulson, A. L. (1940) Memoirs Geol. Survey India 75
Craig, H. (1953) Geochim. et Cosmochim. Acta **3,** 53
Friedman, I. (1953) Geochim. et Cosmochim. Acta **4,** 89
McKinney, C. R., McCrea, J. M., Epstein, S., Allen, H. A., and Urey, H. C. (1950) Rev. Sci. Instrum. **21,** 724
Müller, G. (1953) Geochim. et Cosmochim. Acta **4,** 1
Murphey, B. F., and Nier, A. O. (1941) Phys. Rev. **59,** 771
Prior, G. T. (1916) Mineral. Mag. **18,** 26
Trofimov, A. V. (1950) Doklady Akad. Nauk S.S.S.R. **72,** 663
Urey, H. C. (1952a) Williams Bay Conference on Atomic Abundances
Urey, H. C. (1952b) The Planets (Yale University Press)
Urey, H. C., and Craig, H. (1953) Geochim. et Cosmochim. Acta **4,** 36

Geochimica et Cosmochimica Acta, 1954, Vol. 6, pp. 221 to 240. Pergamon Press Ltd., London

A discussion of the densities of iron meteorites

Edward P. Henderson
U.S. National Museum, Washington 25, D.C.

and

Stuart H. Perry
Adrian, Michigan

Published by permission of the Secretary of the Smithsonian Institution

ABSTRACT

The density of iron meteorites is an important property so its determination should be as accurate as possible. This study shows that the density of meteoritic iron increases with the nickel content so closely that a density can be calculated from the analysis. Thus, it is possible to co-ordinate the superior analyses and density measurements of the iron meteorites. The average measured density of hexahedrites is 7·91 which is higher than the 7·870 reported by Jette and Foote (1936) based on an X-ray study of kamacite. Plotting the composition of these meteorites on Owen and Liu's Ni-Fe diagram (1949) we find the hexahedrites and coarsest octahedrites do not fall where they should. Either their diagram does not apply to the conditions under which meteoritic iron formed or these meteorites were rapidly cooled from a temperature of about 450°C, and therefore are not in equilibrium. H. H. Uhlig independently noticed this disagreement and is presenting a possible explanation for the difference based on the effect of high pressure.

The density determinations reported in the older descriptions of iron meteorites are lower than that of pure iron. Since all meteorites contain appreciable quantities of nickel, an element whose density is higher than iron, something is wrong with the recorded densities of meteoritic iron.

Daly (1943) in discussing the measured and calculated densities of three different types of iron meteorites, found rather consistent differences (2·5; 2·6; 2·7) between the determined and calculated densities and considered this to indicate that meteorites are porous.

Daly probably obtained his data from Farrington (1907), whose compilation included seventy-three different iron meteorites. But Farrington's purpose was to assemble all the published information rather than be selective. Buddhue (1946) discussed 114 density determinations all of which he said "were carried out to the third figure beyond the decimal in hopes that they would be more accurate." Buddhue gave 7·677 as the average of these densities. He further attempted to relate the density to the percentage of nickel and to the different classes of iron meteorites but had only limited success.

Buddhue referred to Huntington's (1887) study of the Coahuila, Mexico, iron where twenty-one density determinations were made on many pieces. The average density for the Coahuila meteorite reported by Huntington is 7·717. This value is above the average density given by Buddhue but is far below the density we found for the Coahuila iron. (See Tables 2 and 3.)

Had Buddhue critically examined these 114 densities he would have found 50 per cent were between 7·755 and 7·852. The data he cited should have indicated that an average density of 7·677 was meaningless. Apparently the old information was taken at its face value because he says, "errors should give high values as well as low ones."

It is unfortunate that he believed a reliable figure could be obtained by averaging densities. We believe it is impossible to get the correct density by averaging data, because the errors in the density measurements on an iron meteorite are more likely to give low values. A high value could only be obtained through a careless mistake while a low density probably represents measurements on altered material.

Probably the most frequent error, in measuring the density of meteoritic iron arises through the use of oxidized material. Apparently little attention has been given to the fundamental point of getting a fresh sample. Perhaps it was falsely assumed that if the density was measured on a large sample a little oxide would make no difference. This is not the case and examples are cited below which show a much higher density on the unaltered meteoritic iron than on a slightly altered sample obtained from near the surface of the meteorite.

The following illustrates how a small amount of oxidation lowers the density. The chemical analysis of the Bruno, Canada, meteorite (Nininger, 1936) seemed to be good but no density was given. Since our slice was thin and was free from large inclusions, it was suitable for a density measurement. Although some oxide occurred on the edge of this slice, the amount looked insignificant and one could assume that there was not enough to make any difference. So the density was measured with the oxide in place and after it was removed. The two densities were 7·719 and 7·869, respectively. Obviously the lower figure is worthless. The higher value agrees rather well with the densities of the other meteorites in Table 2.

The density of the Smithsonia, Georgia, meteorite was given by Roy and Wyant (1950) as 7·76 but this value does not agree with the other irons of the same type. The slice of this iron in the U.S. National Museum shows that weathering has penetrated the mass very deeply, thus their density probably was measured on a weathered sample. In private communications Roy and Wyant reported the redetermined density to be 7·829. Although the second value is higher it is still too low for a meteorite of this type and they said, "in view of the extreme degree of oxidization within the Smithsonia it is doubtful that a specimen 100 per cent fresh can be obtained."

Two densities were measured on the Mayodan, North Carolina, meteorite (Henderson and Perry, 1953) one on a piece from near the surface yet sufficiently free from alteration that a chemist would regard it as suitable for study, and the other from near the centre of the mass. The density from near the centre was 7·910 while the material from near the surface was 7·820.

A density determination seems like a simple operation and most investigators who report these low values understand the technique and precautions one should take. It is inexcusable that so many density measurements have been so carelessly made. Since the recorded data are essentially inaccurate for the real density of meteoritic iron, we believe a few points about the errors that are likely to be made should be mentioned;

(1) First, cut a slice from the iron that is not more than 0·5 cm thick, then select an area where the structure properly represents the meteorite and one which contains no conspicuous inclusions. Since alteration penetrates these irons much deeper than most investigators realize, be certain that the sample selected comes from below the zone of alteration. A sample containing either the hydrous iron

oxide from weathering or the anhydrous iron oxide from flight has a lower density than the unaltered iron. Also the commonly included minerals, schreibersite, troilite and cohenite, have lower densities than meteoritic iron, hence included minerals must never be present in greater proportions than they occur in the meteorite. When an irregular chunk is used in a density measurement one rarely can be sure that it is free from included minerals or oxide.

(2) If water is used in the density determinations another probable source of trouble is introduced, especially if the specimen is rough and irregular because it is difficult to wet the sample properly. A correction should be made for the temperature of the water displaced.

(3) Caley (1952) found when one measures the density of small objects that it is important to reduce, as far as possible, the error caused by the adherence of the surface film of water to the suspension wire. He also mentioned another refinement not available to earlier investigators, "the addition of a drop or two of a dilute aqueous solution of any common wetting agent to the surface of the water. This addition makes no significant change in the density of the water."

Table 1. *The density and nickel determinations of meteorites studied by the authors*

Name	*Density*	*Nickel, %*	*Type of meteorite*
Ballinger, Texas	7·868	6·89	Coarsest Octahedrite
Coolac, Australia	7·849	6·78	Coarsest Octahedrite
El Burro, Mexico	7·884	6·02	Coarsest Octahedrite
Loreto, Mexico	7·822	7·75	Coarsest Octahedrite
Pittsburgh, Pa.	7·791	6·77	Coarsest Octahedrite
Aggie Creek, Alaska	8·004	8·54	Medium Octahedrite
Breece, New Mexico	7·865	9·26	Medium Octahedrite
Drum Mts., Utah	7·857	8·59	Medium Octahedrite
Mertzon, Texas	7·88	9·61	Medium Octahedrite
Morito, Mexico	7·87	7·67	Medium Octahedrite
Edmonton, Ky.	7·945	12·57	Fine Octahedrite
Social Circle, Ga.	7·89	7·44	Fine Octahedrite
Coahuila, Mexico	7·922	5·59	Hexahedrite
Mayodan, N.C.	7·910	5·63	Hexahedrite
Puripica, Chile	7·835	5·77	Hexahedrite
Dayton, Ohio	8·018	18·10	Nickel-rich-ataxite
Weaver, Arizona	8·074	18·03	Nickel-rich-ataxite
Cincinnati, Ohio	7·71	5·33	Nickel-poor-ataxite
Pima Co., Arizona	7·695	5·64	Nickel-poor-ataxite
Soper, Oklahoma	7·644	5·66	Nickel-poor-ataxite
Wathena, Kansas	7·590	5·56	Nickel-poor-ataxite

Density measurements usually are routine determinations in the descriptions of iron meteorites. Those in Table 1 were obtained when the irons were being investigated in the Museum's laboratory, using samples believed to be representative of the meteorite as well as suitable for all the measurements made. This investigation was started after the data in Table 1 had been obtained and shows

that several of the samples were not so good as we originally thought. However, that was not known until the densities in Table 1 were plotted (see Fig. 1).

The average density of meteoritic iron is of no importance but since Buddhue (1946) gave 7·677 as the average of many reported densities including all types of meteorites it was of interest to see how the average density from Table 1 agreed with his figure. The average density in Table 1 is 7·85 which is close enough to the density of iron to show that meteoritic iron is not porous nor is the density of meteoritic iron as low as it is so frequently reported.

In all the density measurements we made for this study the sample was suspended in carbon tetrachloride, either by a wire or in a wire sling. However, some of the results in Table 1 were obtained on specimens we analyzed before we started gathering data for this study but in each case a sample had been specially prepared for analysis hence a density measured on such a piece is better than a density determination made on a casually selected portion. In a few cases we had to be satisfied by measuring the density on the best available material although it was known to be somewhat unsatisfactory. Thus, some of the results in Table 1 probably are slightly lower than they should be.

The density of iron has been measured many times, and Buddhue (1946) gave references for these densities, 7·887, 7·858, 7·868, 7·867, 7·854, 7·864, 7·871, 7·870. The average for these is 7·867. But in meteoritic iron some of the iron is replaced by nickel, an element of higher density, so we do not believe the density of any meteorite should ever be less than that of pure iron (see Table 6).

Had Daly or Buddhue critically examined the series of densities Cohen (1903) gave they would have found 85 per cent of those measurements were between 7·70 and 7·90.

The density of both iron and nickel will vary depending upon how the metal was prepared or treated before the density was measured. Rolled and cast metal have different densities, and likewise the densities of steel can be changed by the amount of work done on it. Since we are not discussing the changes which take place when metals are treated, neither references nor a discussion of this point is given herein.

In Fig. 1 the densities of the meteorites from Table 1 are plotted against their nickel content, and the general grouping of the points indicates there is a relationship between the Ni and the density; but since the points are scattered, apparently something is wrong. Either the samples studied were not prepared with sufficient care or other factors need to be considered.

Actually it is unrealistic to think that the density measurements of a random series of meteorites would have a direct relationship to their Ni content because the chemical analyses show that varying amounts of included minerals are present in the samples.

The densities below the horizontal line 7·80 in Fig. 1 are on meteorites that have structures which indicate that the material has been reheated. Although the densities in Table 1 are as reliable as one is likely to get from the literature, there are not enough determinations on one type of meteorite to establish the range in densities for a particular group.

Probably the density of meteoritic iron, like artificial iron, can be changed by

the treatment the meteor has undergone since it cooled. Although density is directly related to the number and weight of the atoms in the unit cell, which can be determined by X-ray measurements, it is impossible to make such an examination on the sample someone has analyzed.

The formula by which calculated densities are given in this paper is outlined in Table 3. Since the measured and calculated densities for some of the irons that were analyzed on carefully selected material agree so closely this method of calculating the density apparently provides a means of appraising the quality of old analyses

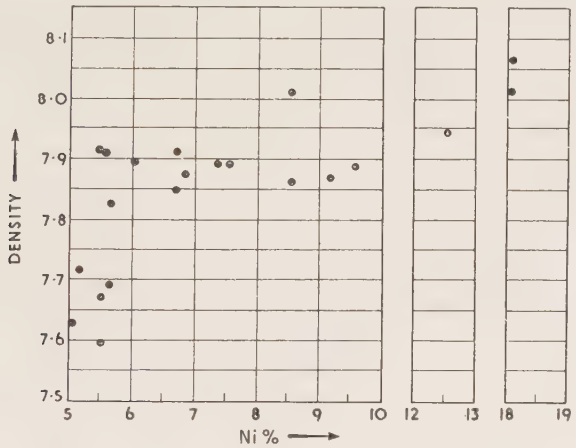

Fig. 1. Density-nickel content of meteorites in Table 1.

and densities. After that was known an attempt was made to measure the densities of several meteorites from the same group to see how consistently they agreed.

Hexahedrites are the logical group to investigate because they usually are homogeneous and have the lowest nickel content so they probably have the lowest density. Since the nickel-rich ataxites contain the highest percentages of nickel they should have the highest density. The densities of the other types of iron meteorites should fall between these groups.

The hexahedrite analyses which were selected represented those we regarded as being reliable and which had the highest recorded densities for this group of meteorites. Even though the measured densities of these 17 irons apparently agree their range, 7·792 to 7·92 seems to be greater than it should be for such a homogeneous type of meteorite. The phosphorus in these irons when calculated to schreibersite represents between 1 and 2 per cent of that mineral and since its density is lower than Ni-Fe, a correction for the schreibersite must be made.

The percentages of the principal elements in the analyses are listed and only these were used in calculating the density of the meteorite. Other elements are present which are not reported by the analyst and these analyses also show traces of carbon, copper, insoluble matter and other constituents, but percentagewise all of these make up such a small part of the meteorite that chemically they are unimportant. How these traces will influence the measured density is unknown. By neglecting them we have introduced an error but it is impossible to correct properly

for all the elements which occur in such small percentages. On the other hand, we do not know that the densities in the literature were measured on sample that was analyzed but the densities in this investigation were calculated on the figures the analyst gave and using the elements given in the respective tables after the figures were adjusted to 100 per cent.

The analyses could have been recalculated to 100 per cent by distributing the difference over the Ni, Co, and P, but Henderson (1941) showed the nickel content in hexahedrites was rather constant. The selected analyses were taken because there was agreement between the Ni. Goldberg (1951) not only confirmed the nickel content of these meteorites but established the cobalt values. Usually when nickel is below 5·5 per cent cobalt will be higher than 0·5 per cent and as both have the same density these analytical errors compensate.

We believe the iron determinations include the largest errors, because iron commonly makes up more than 90 per cent of the sample. At least, it has been our experience that it is more difficult to make iron determinations agree than it is the Ni and Co determinations.

The determined density is measured on 100 per cent of the material so if an analysis totaling more or less than 100 per cent is used to calculate the density an error is introduced. Thus, the reported values for the four principal elements in the meteorite were taken and recalculated to 100 per cent by adding the percentages of Ni, Co, and P, and deducting them from 100 per cent to give the percentage of Fe. The calculated densities were then obtained on the adjusted values shown in the tables.

Our purpose is to test this method of calculating densities, Table 3, and see how closely the results would agree with the measured densities. When the difference between the two values exceeds 0·05 we suspect something is wrong and on investigating a reason is usually found.

It is our experience that the chemical analyses usually more reliably represent the compositions of the meteorites than the reported measured densities represent the true densities of the meteorites. Unfortunately authors rarely tell how the samples they study were selected, prepared or how the density was measured. Judging from the number of low densities it appears that many investigators either used altered material or took little care with their density determinations.

Since the calculated density is based upon the analyses the most reliable results are those obtained on analyses whose summation is within $\pm 0{\cdot}3$ of 100 per cent, and those which came to within those limits are given in Table 4. Incidentally the average summation of the selected analyses is 100·02.

Discussion of Data in Table 2

Obviously we can only speculate on the density determinations selected from the literature. The densities measured on superior material are consistently close to 7·90 and the calculated densities also essentially agree with that value so perhaps the lowest measured densities in this table were obtained on altered samples.

The difference between the two densities in the Hollands Store iron is high and Cohen (1905) noted a network of hair-like cracks in the sample indicating his specimen was not entirely fresh.

Table 2. Density and analyses of selected hexahedrites

	Density			Composition					
	Det.	*Cal.*	*Diff.*	*Fe*	*Ni*	*Co*	*P*	*Sch.†*	*Sum*
1. *Boguslavka, Siberia	7·920	—	—	94·05	5·48	—	—	—	99·53
2. Braunau, Czech.	7·851	7·901	+0·050	93·62	5·21	0·92	0·24	—	99·99
				92·68	4·81	0·91	—	1·60	100·00
3. Bruno, Canada	7·867	7·900	+0·033	93·30	5·79	0·29	0·20	—	99·58
				93·00	5·39	0·28	—	1·33	100·00
4. *Coahuila, Mexico	7·922	7·894	−0·028	93·59	5·59	0·78	0·32	—	100·28
				92·04	5·06	0·77	—	2·13	100·00
5. Hex River, S. Africa	7·822	7·892	−0·070	93·59	5·68	0·66	0·25	—	100·18
				92·42	5·27	0·65	—	1·66	100·00
6. Hollands Store, Ga.	7·801	7·895	+0·094	93·06	5·35	1·00	0·31	—	99·72
				92·10	4·85	0·99	—	2·06	100·00
7. *Keen Mt., Va.‡	7·908	7·904	−0·004	93·33	5·65	0·77	0·19	—	99·94
				92·64	5·34	0·76	—	1·26	100·00
8. Lick Creek, N.C.	7·860	7·882	+0·022	93·00	5·74	0·52	0·36	—	99·62
				91·96	5·14	0·50	—	2·40	100·00
9. *Mayodan, N.C.	7·910	7·906	−0·004	93·70	5·63	0·49	0·17	—	99·99
				93·14	5·38	0·48	—	1·00	100·00
10. Navajo 1, Ariz.	7·820	7·892	+0·072	93·62	5·37	0·41	0·28	—	99·68
				92·83	4·91	0·40	—	1·86	100·00
11. Navajo 2, Ariz.	7·820	7·893	+0·073	93·34	5·60	0·47	0·30	—	99·71
				92·34	5·20	0·46	—	2·00	100·00
12. Negrillos, Chile	7·896	7·895	−0·001	93·94	5·32	0·35	0·22	—	99·83
				93·24	4·96	0·34	—	1·46	100·00
13. Nenntmannsdorf, Ger.	7·824	7·895	+0·071	94·33	5·48	0·71	0·29	—	100·81
				92·37	5·00	0·70	—	1·93	100·00
14. Puripica, Chile	7·835	7·901	+0·066	93·83	5·77	0·26	0·19	—	100·05
				93·03	5·46	0·25	—	1·26	100·00
15. Scottsville, Ky.	7·795	7·901	+0·106	94·03	5·33	0·95	0·23	—	100·54
				92·58	4·95	0·94	—	1·53	100·00
16. Smithsonia, Ga.	7·828	7·900	+0·072	93·42	5·58	0·60	0·20	—	99·80
				92·90	5·18	0·59	—	1·33	100·00
17. Uwet, Nigeria	7·862	7·900	+0·038	93·36	5·78	0·75	0·25	—	100·14
				92·23	5·37	0·74	—	1·66	100·00

* Sample studied came from below the zone of alteration.
† Schreibersite, calculated from P.
‡ Unpublished data.

Number of analysis	*Reference*	
1, 4, 12, 14	Henderson	1941
9	Henderson and Perry	1953
7	Henderson and Perry	unpublished
2, 5, 6, 15	Cohen	1905
13	Cohen	1897
3	Nininger	1936
8	Hidden	1880
10, 11	Roy and Wyant	1949
16	Roy and Wyant	1950
17	Prior	1914

Since the Navajo individuals are so large it was not convenient to get a good sample from either specimen. The measured density on this iron probably was obtained on a piece from the surface, hence the material studied was not of the best quality.

The difference between the two densities of the Nenntmannsdorf meteorite is large and something may be wrong with both the measured and calculated densities. The iron, in this analysis, is the highest in this table but had it been obtained by difference it would have been 92.37. The original analysis totals more than it should so possibly it is open to question.

The low measured density of the Scottsville iron, 7·795, likely was obtained on partly altered material. Although this analysis generally agrees with the others it totals 100·54. The nickel is lower than the average in this table and the cobalt is high but these differences may compensate. Had the iron been determined by difference it would have been 92·58 and this value was used to calculate the density.

The Smithsonia meteorite was previously discussed.

Calculation of Density

It is comparatively simple to calculate the density of a meteorite from an analysis. As hexahedrites often contain schreibersite, it is necessary to make corrections for this mineral and the composition of schreibersite varies within certain limits. The Coahuila meteorite was selected to show the steps in the calculation.

This meteorite was selected because Huntington (1887) had made a series of density measurements on it and, as we have already shown, his results did not agree with ours. The piece we studied came from below the zone of penetration for either alteration or heat so a reliable density can be obtained on it.

The percentage of schreibersite in iron meteorites can be calculated from the total phosphorus because it all comes from that mineral. The analyses of schreibersite have established its phosphorus content as about 15 per cent.

Since Ni replaces Fe in schreibersite we arbitrarily assumed Ni made up 25 per cent of this mineral. The cobalt in schreibersite analyses averages 2·1 per cent of the Ni so this proportion was used in the calculations. The iron was obtained by

difference from the calculated percentage of schreibersite. Obviously it is not accurate to assume that schreibersite has a fixed composition but as long as the amount that is present is between 1 and 2·5 per cent the error introduced will not make much difference in the calculated density.

The density of schreibersite probably varies with its composition and if there is any appreciable range in its density another error has been introduced because all the calculations were made with 7·0 as the density for this mineral.

The formula to use in calculating the density of a meteorite from its analysis is the same as SHARWOOD (1912) used to calculate densities from analyses of rocks or ores and is,

$$\text{Density} = \frac{100}{\frac{\%\text{ of A}}{\text{Density of A}} + \frac{\%\text{ of B}}{\text{Density of B}} + \text{- - -} + \text{- - -}}$$

The steps in calculating the density of a meteorite from an analysis are given in

Table 3. *Calculation of density from the chemical analysis of the Coahuila meteorite*

Analysis	*Composition of schreibersite to be deducted*	*Adjusted analysis*	*Adjusted analysis* 100%		*Density of metal*	
Fe 93·59	1·27	92·32	92·04*	÷ 7·86	11·709	
Ni 5·59	0·53	5·06	5·06	÷ 8·90	0·568	
Co 0·78	0·01	0·77	0·77	÷ 8·90	0·086	
P 0·32	0·32	—				
Schreibersite		2·13	2·13	÷ 7·0	0·304	
Total	2·13	100·28	100·00		12·667	$= \frac{100{\cdot}00}{12{\cdot}652} = 7{\cdot}894$

The calculated density of the Coahuila meteorite—7·894

* In recalculating analyses of meteorites we recommend that all the error be assigned to the iron determination and not distribute the error to the other elements.

Although the densities measured on samples taken from near the outside of a meteorite vary and sometimes are found to be lower than the density of metallic iron, the densities on material taken from near the centres of four hexahedrites are remarkably constant, (see Table 4). The densities of meteorites, containing more nickel than the hexahedrites, frequently are reported as less than 7·9 so something may be wrong with those values. Most likely the low values are due to oxidization, to included minerals, but perhaps the density of the outside zone of iron meteorites is lowered by a thermal change which occurred during the flight of the mass through our atmosphere.

The measured densities in Table 4 were determined on carefully selected samples free from appreciable inclusions and oxidization. The calculated densities were obtained on the adjusted analyses in Table 2.

Table 4. The best of the measured and calculated densities from Table 2

Meteorite	*Measured density*	*Calculated density*
Boguslavka, Russia	7·920	
Braunau, Czech.		7·901
Coahuila, Mexico	7·922	7·894
Hex River, S. Africa		7·892
Keen Mt., Virginia	7·908	7·904
Mayodan, N. Carolina	7·910	7·906
Navajo 2, Arizona		7·893
Negrillos, Chile		7·895
Puripica, Chile		7·901
Smithsonia, Georgia		7·900
Uwet, Nigeria		7·900
Average	7·914	7·898

Changes in Density by Thermal Treatment

Since the lowest densities in Table 1 are on irons where there was evidence of reheating, it is necessary to see how the density of a meteoritic iron is changed by heat treatment.

Samples were taken from below the surface of four different hexahedrites. These irons were chosen because they are homogeneous—essentially kamacitic iron. Meteorites containing plessite were avoided because plessite is in an arrested state of transformation; i.e., it may have been quenched during a density change.

The samples were cut into rectangular blocks and all sides were ground smooth. After the density of each block was obtained, the pieces were packed in freshly calcined CaO and heated in an electric oven for 100 hours, then slowly cooled in the oven.

Since there was some air in the CaO the surfaces of these blocks become slightly oxidized by the treatment, but all surfaces were refinished before the density was determined. Then the samples were repacked in calcined CaO and heated to 750°C for 100 hours.

Table 5. Density changes made by heat treating hexahedrites (kamacite)

	Original density	*Density after 100 hrs at 450°C*	*Density after 100 hrs at 750°C*	*Total diff.*
Artificial metal	7·895	7·889	7·878	−0·017
Mayodan, N.C.	7·910	7·900	7·875	−0·035
Boguslavka, Russia	7·920	7·883	7·875	−0·045
Coahuila, Mexico	7·922	7·902	7·873	−0·049
Negrillos, Chile	7·896	7·900	7·894	−0·002

It is important that the sides of these blocks be smooth at the start because the oxide films can be removed by grinding but if a surface is irregular some oxide will remain in the low places. Following the 450°C treatment about 1·5 mm of metal was ground off, but after 750°C nearly twice that amount had to be removed.

The artificial metal was supplied by Dr. G. A. Ellinger of the National Bureau of Standards. We were fortunate in getting an alloy with 3 per cent Ni, about half the nickel in hexahedrites, to determine if it would behave the same as meteoritic iron in the heat tests.

Although the density of three of the meteorites and the alloy was decreased by the termal treatment the changes are not uniform. Although the other meteorite showed a slight change in density during its treatment, the change was in the third decimal place so we considered that it underwent no change during the heating.

These heat treatments were carried to 750°C because according to Owen and Liu's (1949) Ni-Fe diagram alpha iron with 5·5 per cent Ni enters the alpha-gamma zone at 470°C and is still in that zone at 750°C. We proposed to see if a detectable change in density occurred and if the change would be permanent in a sample that was heated to such temperatures and slowly cooled.

Since the measured density of the selected material in Table 4 averages 7·914 and the calculated density of the analyses averages 7·904 we believe the density of hexahedrites must be very close to 7·91. Thus, we report 7·91 $\pm$0·005 as the density of kamacite, even though it does not agree with the calculated density of alpha iron for the amounts of nickel given by Jette and Foote (1936) whose results appear in Table 6.

Table 6. *Calculated density of alpha iron with different percentages of nickel* (*data by* Jette *and* Foote)

Atomic % of nickel	*Density*	*Atomic % of nickel*	*Density*
0	7·8661	4	7·8638
1	7·8634	5	7·8647
2	7·8628	6	7·8658
3	7·8631		

Furthermore, Malmqvist (1946-48) states that from Jette and Foote's study on alpha iron which contained 5·41 (wt. per cent Ni) and with a lattice constant $a = 2{\cdot}8634$ A the calculated density was 7·870 gr. cc.

The average measured density of hexahedrites 7·91, is 0·04 higher than the 7·870 value obtained by calculating the density from X-ray measurements on kamacite. The density obtained on selected samples from within the meteorites was lowered by heat treatment, the loss of density of three out of the four samples averaged 0·043.

There may be no relationship between the two sets of differences but since the calculated density, 7·870, is 0·04 lower than our direct measurements, there is a possibility that the kamacite measured by X-ray was obtained from near the

surface and was expanded by heat during the flight of the meteor through our atmosphere.

Owen, Yates, and Sully (1937) investigated the density of Ni-Fe alloys and reported that the densities of three different alloys, in the alpha phase, decreased when the alloy was heated at 200°, 400°, and 600°C. Their values are given in Table 7.

Table 7. Densities of pure Fe-Ni alloys at various temperatures
(Owen, Yates, and Sully, 1937)

Ni content atom %	*Temperature*			*Decrease in density*
	200°C	400°C	600°C	
8·8	7·83	7·77	7·70	0·13
3·1	7·81	7·75	7·76	0·05
0·0 Alpha Fe	7·81	7·74	7·66	0·15

Our investigations showed that the densities of iron meteorites are lowered by the heat treatment we gave them, but we did not find the decrease in density that Owen, Yates, and Sully reported on their prepared alloys. Their densities were calculated from parameter values obtained at these temperatures while our values were direct measurements.

We cannot account for the increase in density that Frankel and Tammann (1908) reported on the Damara* iron. They gave the density as 7·908 before heating, and after it was heated until the structure disappeared (1300°C) and cooled the density was 7·938, an increase of 0·030.

Calculation of Density on an Octahedrite containing Plessite

Octahedrites, which make up the largest group of meteorites, contain appreciable amounts of taenite and plessite so it was important to see if their density could be calculated as accurately as the hexahedrites and the coarse octahedrites. Fortunately Malmqvist (1946-48, page 302) measured the density of the Muonionalusta meteorite and he also determined the percentage abundance of the kamacite, taenite and plessite. All the figures in Table 8 were taken from Malmqvist's description, except the calculated density.

Table 8. Muonionalusta, Sweden, Meteorite (R. Mauzelius, *analyst*)

			Abundance	*Density*
Fe	91·10	Kamacite	80·8	7·87
Ni	8·02	Taenite	4·0	8·16
Co	0·69	Plessite	15·2	8·015
Cu	0·01	*Density of the meteorite*		
Cr	0·01	Measured density	7·893	
P	0·05	Calculated density	7·934	
	99·88	Difference	0·041	

* We were unable to identify the Damara meteorite; it is not listed in our records nor in the 1953 British Museum's Catalogue of Meteorites, 2nd Edition, by Max H. Hey.

JETTE and FOOTE (1936) studied four taenites with 25·75, 29·62, 34·92, 40·31 per cent of nickel, and MALMQVIST (1946-48, page 303) gave the density of these taenites as 8·185, 8·182, 8·129, 8·144, and selected the mean, 8·160, for the density of taenite. Then MALMQVIST assumed that plessite was a 50-50 mixture of kamacite and taenite and by averaging the densities of kamacite and taenite reported 8·015 as the density of plessite.

Plessite is not necessarily a 50-50 mixture of kamacite and taenite, so perhaps a better density for the plessite in the Muonionalusta iron can be obtained by using the abundance figures MALMQVIST gave for the kamacite, taenite, and plessite, and his measured density for the meteorite. The average density of kamacite from Table 4 is used in the following calculation along with MALMQVIST's calculated density for taenite, and the density of plessite is the unknown.

$$7{\cdot}891 = \frac{100}{\frac{80{\cdot}8}{7{\cdot}91} + \frac{4{\cdot}00}{8{\cdot}16} + \frac{15{\cdot}2}{X}\ (\text{density of plessite})}$$

Density of plessite is 7·788

This density is different from what MALMQVIST gave for plessite but we do not know that it is any more accurate. Since plessite does not have a fixed composition its density should vary. Thus, the octahedrites containing appreciable amounts of plessite may not lend themselves to a density calculation as well as the hexahedrites.

COARSEST OCTAHEDRITES

It is not always possible to make a clear distinction between hexahedrites and some of the coarsest octahedrites, but chemically the latter group contains more nickel than will dissolve in kamacite so the excess must separate as taenite or plessite. Hexahedrites occasionally have plessite areas although theoretically they should not and perhaps there would not be any if the rate of cooling had been slower. Rapid cooling will preserve some of the mixed phase which normally would have transformed into kamacite.

When meteorites are made up of large areas of kamacite iron, each displaying well developed Neumann lines, and the composition agrees with other hexahedrites we believe they should be so classified even if they have a few areas of plessite.

Usually the iron meteorites with a nickel content of about 6 per cent or slightly higher, instead of being similar to hexahedrites with an occasional spot of plessite, have a coarse granular texture. Such irons are made up of large irregular rounded kamacite areas so disposed that the irregularities of the separate pieces interlock. Each area has prominent Neumann lines. Since the nickel content of these irons is higher than that of the hexahedrites we have classified them as coarsest octahedrites, regardless of the fact most of them do not show the orderly pattern of an octahedrite.

Several such irons have been examined during this investigation. Unlike the hexahedrites there were not enough of these analyses to make a critical selection of the best ones, and, furthermore, the quality of the material that was available for density measurements was not as good as we had in the case of the hexahedrites.

Frequently iron oxide partly fills the fractures between the kamacite masses in the coarsest octahedrites. But in selecting a sample for study, if one avoids these fractures the area taken will be essentially kamacite and the analysis will be

Table 9. Density of coarsest octahedrites

	Density			Composition					
	Det.	*Cal.*	*Diff.*	*Fe*	*Ni*	*Co*	*P*	*Sch.**	*Sum*
1. Annaheim, Canada	7·873	7·926	+0·053	91·51	7·84	0·46	0·22	—	100·03
				90·61	7·48	0·45	—	1·46	100·00
2. Ballinger, Texas	7·873	7·961	+0·088	92·37	6·93	0·54	0·03	—	99·87
				92·25	6·88	0·54	—	0·02	100·00
3. Coolac, Austral.	7·849	7·930	+0·081	92·31	6·78	0·87	0·03	—	99·99
				92·19	6·73	0·87	—	0·20	100·00
4. El Burro, Mex.	7·884	7·893	+0·009	93·10	6·02	0·34	0·32	—	99·78
				92·05	5·59	0·33	—	2·13	100·00
5. Morito, Mex.	7·870	7·921	+0·051	91·76	7·67	0·56	0·01	—	100·00
6. Nelson Co., Ky.	7·824	7·900	+0·076	91·90	6·78	0·34	0·21	—	99·23
				91·84	6·43	0·33	—	1·40	100·00
7. Pittsburgh, Pa.	7·791	7·914	+0·123	92·15	6·99	0·67	0·22	—	100·03
				91·25	6·63	0·66	—	1·46	100·00
8. Yenberrie, Austral.	7·934	7·932	−0·002	92·15	7·07	0·67	—	—	99·89
				92·26	7·07	0·67	—	—	100·00

* Sch. schreibersite calculated from P.

Number of analyses	*Reference*	
1	Johnston and Ellsworth	1908
2, 5, 6, 7, 8	Henderson and Perry	unpublished
3	Henderson	1951
4	Henderson	1941

similar to a hexahedrite because most of the taenite occurs in these cracks. Thus, the agreement between the measured and calculated densities of the coarsest octahedrites, Table 9, is not as good as it was for the hexahedrites and probably the calculated density in this table is superior to the measured density.

Discussion of the Data in Table 9

The cobalt determinations on the El Burro and Nelson Co. irons are believed to be low. When these analyses were made our interest was in the nickel, we knew that the figures for cobalt were not as accurate as those for nickel. Since then studies by Goldberg and others (1951) as well as additional work in this laboratory have independently shown that the old low values are probably incorrect and meteorites usually have about 0·5 per cent cobalt.

The density of the Pittsburgh iron was measured on the sample we restudied, but previously it had been granulated by reheating. Furthermore, the piece we had was partly oxidized, thus the measured density has no scientific value other than show the condition of the material restudied. The density we obtained was higher than Genth (1875) reported, 7·741, and also above the density given by Shepard (1951), 7·38.

The Yenberrie meteorite was recently re-examined and as the Museum's sample was large it was possible to get a specimen from below the zone of alteration. Probably this piece was the most carefully selected one in Table 9 because this reinvestigation was made after this density study was started. The fact the two densities for the Yenberrie iron agree so closely is significant.

Nickel-rich Ataxites

This group contains the highest percentage of nickel of all the iron meteorites; these should, therefore have the highest densities. There is a greater range in the nickel content of these meteorites than in either the hexahedrites or coarse octahedrites, so irons with these structures will have a wider range in their densities.

Explanations to Table 10

The Freda iron is a small specimen with beautifully orientated structures and well developed flight markings. The measured density is low because it was obtained on the entire mass rather than on a prepared sample. Here a decision had to be made, either to preserve the markings and forgo the density or to sacrifice the exhibition value of the specimen and determine the density. We decided that science would be better served if the sample were preserved, and we hope that some day a meteorite with a similar composition will be found on which a good determination of density can be made.

This iron weighed 268 grams and was well covered with fusion crust. Percentagewise, the crust appears to make up such a small proportion of the mass that one might think the density determination on it would be very close to the correct value. However, the determined density is much lower than the calculated value, about three times the average difference of those listed in Table 10, and we attribute the difference to the fusion crust.

Our redetermination of the density of the Klondike iron was 8·005 which is much higher than the density given in the literature (7·566). However, the calculated density, based on the original analysis, is 8·039, only 0·034 above our measured density.

The density of the Shingle Springs iron has been determined many times. Jackson (1872) gave 7·905; Shepard (1872) reported 7·80 on turnings from this

iron; Silliman (1873) on a 750 gram specimen got 7·875 but also he reports the density of 8·024 on some shavings. Cohen (1899) reports 7·894 and a "theoretical" density of 7·921. The average of these values, 7·924, is 0·091 below our determination, 8·015.

Table 10. *Density of nickel-rich ataxites*

	Density			*Composition*					
	Det.	*Cal.*	*Diff.*	*Fe*	*Ni*	*Co*	*P*	*Sch.*†	*Sum*
1. Dayton, Ohio	8·018	8·038	+0·020	81·09	18·10	0·81	0·001	—	100·001
2. Freda, N. Dakota	7·962	8·077	+0·115	75·82	23·49	0·66	0·15	—	100·12
				75·06	23·29	0·65	—	1·00	100·00
3. Klondike, Canada	8·005	8·034	+0·028	80·65	18·20	0·91	0·19	—	99·95
				78·95	18·89	0·90	—	1·26	100·00
4. Shingle Springs, Cal.	8·015	8·000	−0·015	82·21	16·69	0·65	0·34	—	99·89
				80·87	16·23	0·64	—	2·26	100·00
5. Tawallah, Austral.	8·001	8·033	+0·032	82·29	16·90	1·09	—	—	100·28
				82·01	16·90	1·09	—	—	100·00
6. Tchinge, Mongolia	7·937	8·021	+0·084	82·36	16·71	0·40	tr.	—	99·47
				82·89	16·71	0·40	—	—	100·00
7. Weaver, Ariz.	8·074	8·033	−0·041	80·54	18·03	0·91	0·07	—	99·55
				80·71	17·92	0·91	—	0·46	100·00
8. Wedderburn, Austral.	8·025	8·019	−0·006	74·35	23·95	0·50	0·78	—	99·58
				71·68	22·65	0·47	—	5·20	100·00

† Sch. = schreibersite calculated from P.

Number of analysis	*Reference*	
1	Henderson and Perry	unpublished
2	Henderson	1942
7	Henderson	1951
3	Johnston	1915
4	Cohen	1899
5	Hodge-Smith and Edwards	1941
6	Pehram	1923
8	Edwards	1953

The measured density of the Tchinge (Chinga) iron was first reported as 7·868 but we got 7·937 and both values are lower than the calculated density.

The measured density of the Weaver iron, 8·074, is higher than the calculated value but this partial analysis totals 99·55 which also is low. The iron in that

analysis was determined and when the analysis was completed there was no reason to challenge the results, but now by comparing the calculated and determined densities it appears that the percentage of iron reported was slightly low.

Edwards (1953) in discussing the density of the Wedderburn iron said, "The specific gravity of the main portion of the meteorite is 8·025 and it is probable that the specific gravity of the fresh iron is a little higher than this. With its rust coating untouched the fragment had a specific gravity of 7·899 and after a further grinding to 7·94 some rusted iron was still present."

The analysis of Wedderburn iron gives 0·78 per cent P the highest value in Table 10. When converted into schreibersite this corresponds to 5·20 per cent. The analysis also given S 0·16 which corresponds to 0·40 per cent troilite. The density calculated from the analysis after correcting for these amounts to phosphide and sulphide comes to 8·019.

No further discussion is needed to show how useful density measurements are in appraising analyses of iron meteorites. Conversely, a good analysis is a check on the density. The inspection of Tables 2, 4, 9, 10 shows that the measured and calculated densities should be very close. When an iron meteorite is prepared for study, the density should be one of the first determinations made, because it helps establish the quality of the sample being studied and later will assist in appraising the accuracy of the analysis. If the piece selected for study is known to be fresh, a low density betrays some inclusions and in the course of the investigation the reasons for the low density should be found.

Hexahedrites and Coarsest Octahedrites compared with the Ni-Fe Diagram

The hexahedrites when placed on Owen and Liu's Ni-Fe diagram (1949) lie too far to the left in the single phase area, kamacite. Also the coarsest octahedrites are partly within the single phase zone although this group should lie just to the right of the AB line if the diagram explains the structures in iron meteorites. Since the hexahedrites and the coarsest octahedrites are to the left of where they should be on this diagram, their position could be explained if these meteorites cooled rapidly from a temperature near 400°C.

If Owen and Liu's diagram, Fig. 2, holds for meteoritic iron it is possible for some hexahedrites to contain 7 per cent Ni. Such a meteorite has not been found and since all hexahedrites are so much alike chemically it indicates that these irons probably had a common origin rather than coming from several different places.

By adhering to Owen and Liu's diagram and accepting the limited range for nickel shown in Table 2 for hexahedrites, we can explain their position to the left of the AB line by assuming that the melt from which they formed contained no more than about 5·8 per cent nickel. However, the earlier diagram of Owen and Sully (1939) shows the AB line bending to the left below 400°C which made that diagram consistent with meteoritic iron, but the bend to the left on the AB line was not well established.

Another reason has been proposed which accounts for hexahedrites being found so far to the left of the AB line in the Ni-Fe diagram and H. H. Uhlig (1954) is discussing this point in another paper.

Several of the coarsest octahedrites in Table 9 when plotted on the Ni-Fe diagram of Fig. 2 appear to indicate rapid cooling below a temperature of about 400°C, because rapid cooling would preserve the mixed phases which existed at higher temperatures. According to Owen and Liu's diagram these coarsest octahedrites could not have cooled slowly to low temperatures, for if this had happened, there would be hexahedrites with nickel percentages in the range of these coarsest octahedrites. Although about forty-five hexahedrites are known, none contain such a percentage of nickel.

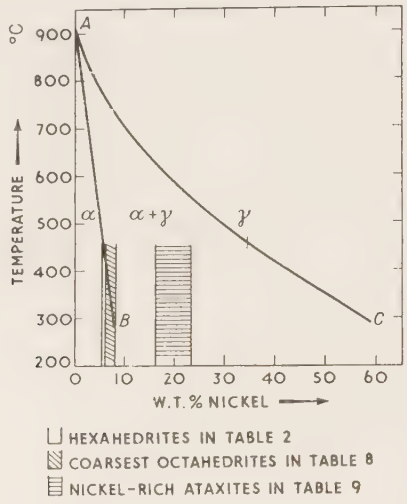

Fig. 2. Phase diagram for Fe-Ni alloys (Owen and Lui).

Rapid cooling of a large body is impossible, especially if the metal represents segregations from some basic magma, because the core would be blanketed by insulating silicates. Rapid cooling of such a body would result if the planet-like mass was fragmented. So, to explain meteoritic iron by Owen and Liu's diagram, we are practically required to assume that the metal slowly cooled to approximately 450°C, when some drastic event such as an explosion occurred which made rapid cooling possible.

By another line of reasoning one should consider the composition of the taenite which has been studied from about twenty meteorites, most of which are medium octahedrites; their abundance over the coarse octahedrites is of the order of 2 to 1. The percentage of nickel in these taenite analyses varies widely and probably many of the analyses are not reliable by present standards. Only a few of these analyses show as little as 14 per cent Ni; most of them have between 24 and 36 per cent Ni yet there is no reason why some taenites should not contain higher percentages of nickel; possibly some will be found which have between 40 and 50 per cent Ni.

If we speculate about the composition of taenite our guess would be that it should average more nickel than those mentioned above. We tentatively would place the average Ni as near 35 per cent. Such a point falls on the AC line in Fig. 2 about 450°C at the point marked |. Our reasoning is conjectural; we regard the

estimates as qualitative, indicating that the end of the transformation occurred at about the temperature where some of these coarsest octahedrites entered the alpha or kamacitic field. Thus, the areas where these hexahedrites, coarsest octahedrites and nickel-rich ataxites from Tables 2, 9 and 10 fall on Fig. 2 were extended upward until about the level of the 450°C line.

Summary

This study shows that the densities of meteoritic irons are higher than previously reported and that the density of a meteorite offers a simple method of selecting reliable analyses from the masses of analytical data. However, we recognize that some meteorites are so heterogeneous in character that a small piece cannot properly represent the nature of the meteorite. Thus, one must not assume that every low density is inaccurate or that it was determined on altered material even though most of the old densities actually are incorrect (low). If the density calculated from the analysis does not agree with the determined density, or is different from what it should be for that type of meteorites, the description of the iron should tell why.

The average of the measured densities for selected kamacite, Table 4, is 7·914. The average of the selected hexahedrites, Table 2, is 7·855 but since Table 2 contains several densities believed to have been obtained on altered samples the evidence here presented implies that Jette and Foote's density for kamacite iron, 7·870, is lower than it should be.

The analyses of hexahedrites and coarsest octahedrites in Tables 2 and 9 when located on Owen and Liu's diagram are too far to the left, so if this diagram is applicable to iron meteorites these irons must have cooled rapidly from about 450°C. Rapid cooling can best be explained by a planet-like body exploding. The close agreement in the composition of hexahedrites is suggestive of a single origin for such meteorites.

Acknowledgments—We wish to express our appreciation to Prof. H. H. Uhlig of of Massachusetts Institute of Technology; Dr. G. A. Ellinger, National Bureau of Standards; Drs. S. K. Roy and R. K. Wyant, Chicago Museum of Natural History; Dr. Walter Corvello, Museu Nacional, Rio De Janeiro, Brasil; and Dr. Earl Ingerson, U.S. Geological Survey, for various assistance which they have given us in this investigation.

References

Buddhue, J. D. (1946) The specific gravity of meteoritic iron. Pop. Astron. **54,** 541–544

Caley, E. R. (1952) Estimation of compositions of ancient metal objects. Anal. Chem. **24,** 676–681

Cohen, E. (1897) Meteoreisen-Studien V. Ann. k. k. naturhist, Hofmus **12,** 42–62

Cohen, E. (1899) Meteoreisen-Studien IX. Ann. k. k. naturhist, Hofmus **13,** 473–486

Cohen, E. (1903) Meteoritenkunde. II Heft. Strukturformen, Stuttgart, pp. 209–210

Cohen, E. (1905) Meteoritenkunde. III Heft. Klassifikation und Nomenklature, Stuttgart, pp. 217–220

Daly, R. A. (1943) Meteorites and an earth-model. Bull. Geol. Soc. Amer. **54,** 401–455

Edwards, A. B. (1953) The Wedderburn meteoritic iron. Proc. Roy. Soc. Victoria (N.S) (2) **64,** 73–76

Farrington, O. C. (1907) Analyses of iron meteorites compiled and classified. Field Museum Nat. Hist., Geol. Ser. 3, No. 5, 57–110

Fraenkel, W., and Tammann, G. (1908) Über meteorisches Eisen. Zeit. Anorg. Chem. **60,** 416–435

Genth, F. A. (1875) Second preliminary report on the mineralogy of Pennsylvania. Pa. Geol. Survey Rpt. **6**

Goldberg, E., Uchiyama, A., and Brown, H. (1951) The distribution of nickel, cobalt, gallium, palladium and gold in iron meteorites. Geochim. et Cosmochim. Acta **2,** No. 1, 1–25

Henderson, E. P. (1941) Chilean hexahedrites and the composition of all hexahedrites. Amer. Mineral. **26,** 546–550

Henderson, E. P. (1941) El Burro, Coahuila, Mexico, meteorite. Amer. Mineral. **26,** 655–656

Henderson, E. P. (1951) A restudy of the Coolac, New South Wales, Australia, meteorite. Pop. Astron. **59,** No. 4, 205–209

Henderson, E. P., and Perry, S. H. (1942) The Freda, North Dakota, meteorite: a nickel-rich ataxite. Proc. U.S. Natl. Museum **92,** No. 3134, 21–23

Henderson, E. P., and Perry, S. H. (1951) A reinvestigation of the Weaver Mountains, Arizona, meteorite. Pop. Astron. **59,** No. 5, 263–266

Henderson, E. P., and Perry, S. H. (1953) The Mayodan meteorite, Rockingham County, North Carolina. Amer. Mineral. **38,** 1026–1040

Hidden, W. E. (1880) A new meteoritic iron from North Carolina. Amer. J. Sci. (3) **20,** 324–326

Hodge-Smith, T., and Edwards, A. B. (1941) The Tawallah Valley meteorite. Records, Australian Museum **21,** 1–8

Huntington, O. W. (1887) On the Coahuila meteorites. Amer. J. Sci. (3) **33,** 115–118

Jackson, C. T. (1872) Analysis of the meteoric iron of Los Angeles, California. Amer. J. Sci. (3) **4,** 495–496

Jette, E. R., and Foote, R. (1936) X-ray study of iron-nickel alloys. A.I.M.E. Trans. **120,** 259–272

Johnston, R. A. A. (1915) Gay Gulch and Skookum meteorites. Museum Bull. Geol. Survey Canada, Geol. Ser. No. 26, No. 15, 1–8

Johnston, R. A. A., and Ellsworth, H. V. (1908) The Annaheim meteorite. Trans. Roy. Soc. Canada **60,** 416–435

Malmqvist, D. (1946–1948) Structure of Muonionalusta iron meteorite and method of determining the orientation of lamellae of octahedrites. Geol. Inst. Upsala Bull. **32,** 277–328

Nininger, H. H (1936) The Bruno meteorite. Amer. J. Sci. (5) **31,** 209–222

Owen, E. A., and Liu, J. H. (1949) Further X-ray study of equilibrium diagram of the Fe-Ni system. J. Iron Steel Inst. **163,** 132–137

Owen, E. A., and Sully, A. H. (1939) The equilibrium diagram of iron-nickel alloys. Phil. Mag. (7) **27,** 614–636

Owen, E. A., Yates, E. L., and Sully, A. H. (1937) An X-ray investigation of pure iron-nickel alloys, Part 4: Variation of lattice-parameter with composition. Proc. Phys. Soc. (London) **49,** (Pt. 4), 315–322

Pehram, G. (1923) Über ein Nickeleisen aus Tannuola. Acta. Acad. Aboensis, Math. Phys. **3,** No. 1, 12

Prior, G. T. (1914) The meteorites of Uwet, Kota Kota, and Angela: redeterminations of nickel and iron in the Baroti and Wittekrantz meteoric stones. Mineralog. Mag. **17,** No. 80, 123–134

Roy, S. K., and Wyant, R. K. (1949) The Navajo meteorite. Field Museum Nat. Hist., Geol. Ser. **7,** No. 8, 113–127

Roy, S. K., and Wyant, R. K. (1950) The Smithsonia meteorite. Field Museum Nat. Hist., Geol. Ser. **7,** No. 9, 129–134

Sharwood, W. J. (1912) The specific gravities of mixtures; a discussion. Econ. Geol. **7,** 588–590

Shepard, C. U. (1851) On meteorites. Amer. J. Sci. (2) **11,** 36–40

Shepard, C. U. (1872) On a meteoritic iron lately found in El Dorado County, California. Amer. J. Sci (3) **3,** 438 pp.

Silliman, B. (1873) On the meteoric iron found near Shingle Springs, El Dorado County, California. Amer. J. Sci. (3) **6,** 18–22

Uhlig, H. H. (1954) Contributions of metallurgy to the origin of meteorites; Part I, Structures of metallic meteorites, their composition and the effect of pressure. Geochim. et Cosmochim. Acta **6,** 276.

Geochimica et Cosmochimica Acta, 1954, Vol. 6, pp. 241 to 260. Pergamon Press Ltd., London

The O^{18}-abundance in fresh water

Willi Dansgaard
Universitetets biofysiske laboratorium, København, Denmark.

ABSTRACT

Fresh water of various origins as distinct from ocean water shows great variations in O^{18}-abundance. Proceeding from the temperate towards the colder climates a considerable decrease is noticeable.

It is demonstrated that the O^{18}-abundance in atmospheric water vapour is dependent on (a) the precipitation temperature, (b) the origin of the vapour and (c) the average cooling of the vapour during the circulation of the water in nature, whereas the O^{18}-abundance in a certain precipitation, further, depends on (d) the condensation temperature, (e) the cooling since the beginning of the condensation of the vapour in question, and (f) the evaporation during the fall of the precipitation from cloud to ground. Furthermore, the O^{18}-abundance in ground water from a certain locality depends on (g) the evaporation from the precipitation since its reaching the ground and (h) the possible exchange of O^{18} between the water and oxygenic substances in the ground.

Computations on this basis and on measurements of the O^{18}-abundance of ocean water are in agreement with measurements of fresh water of various origins.

In this journal Epstein and Mayeda (1953) have published a long series of mass-spectrometric measurements of the O^{18}-abundance, a_o, in ocean water. From these measurements it may be deduced that

1. Addition of fresh water reduces the a_o (owing to the very low O^{18}-abundance of fresh water),

2. Ocean water without fresh water has an a_o value at the water surface slightly higher than the average value (owing to the fact that mainly H_2O^{16} escapes by the evaporation),

3. Ocean water containing meltwater has an a_o value slightly lower at the surface than the average value (probably due to the fact that meltwater, being poor in O^{18}-abundance, is mainly to be found in the surface water because of its low density).

In this work, in principle conducted on the lines employed by Epstein and Mayeda, some fresh-water samples of various origins have been tested, and the results show considerably greater variations in O^{18}-abundance than the samples of ocean water.

The Absolute Value of the O^{18}-Abundance of the Samples

A knowledge of the absolute value of the O^{18}-abundances of the samples proved to be essential for the discussion set forth in the following.

Four samples of water were prepared of hydrogen and atmospheric oxygen. After shaking CO_2 for equalization with the samples in excess, the difference in O^{18}-abundance of the CO_2 samples and the Danish CO_2 standard was found to be: $(89{\cdot}0 \pm 0{\cdot}2) \cdot 10^{-4}$ atom %. Comparing this result with Nier's (1950) measurements of atmospheric oxygen, 0·2039 atom %, the O^{18}-abundance of the Danish standard should be 0·1950 atom %

Tests of 17 ocean samples gave $(+41{\cdot}0 \pm 0{\cdot}3) \cdot 10^{-4}$ atom %. Consequently the O^{18}-abundance of unmixed ocean water should be 0·1991 atom %.

The Selection of Fresh-Water Samples

Investigations on the natural circulation of the heavy oxygen isotope should be based on the collection of samples of water and vapour of widely differing origin. The samples, naturally, should be representative of the characteristic features of a certain phase of the circulation. One important source of error in this connection is the evaporation. Referring to Riesenfeld and Chang (1936), the proportion $\frac{p_0^{16}}{p_0^{18}}$ of the pressure of the saturated vapour of H_2O^{16} and H_2O^{18} is determined by:

$$\log_{10}\left(\frac{p_0^{16}}{p_0^{18}}\right) = \frac{2{\cdot}74}{T} - 0{\cdot}0056 \qquad (1)$$

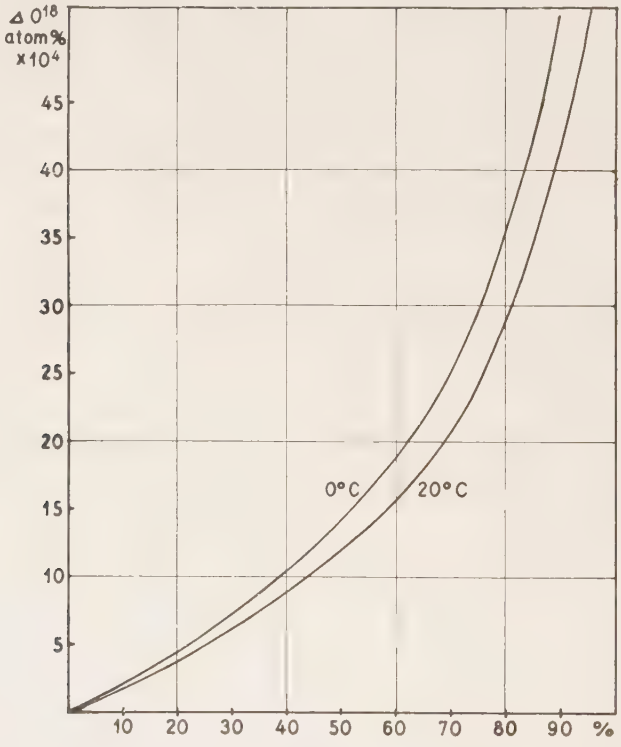

Fig. 1. The increase in the O^{18}-abundance in the remaining volume of water after evaporation of a certain fraction of the original volume.

T being the absolute temperature, hence always higher than unity, which means that H_2O^{16} is relatively volatile, and that a final volume of water exposed to evaporation gains a steadily increasing O^{18}-abundance. The value of this change may be computed from Raleigh's distillation formula:

$$\frac{p_0^{18}}{p_{H_2O}} \cong \frac{p_0^{18}}{p_0^{16}} = 1 - \frac{\log\,(a/a^\circ)}{\log\,(v_0/v)}\,, \qquad (2)$$

a° and a respectively representing the O^{18}-abundance before and after the distillation, and v_0 and v representing the corresponding volumes of water. In Fig. 1

is shown ΔO^{18}, the change in the O^{18}-abundance in the water remaining after evaporation, expressed in per cent of the original volume of water.

It will be seen that even 2 per cent evaporation is evident in the test result, when the reproducibility of the measurements as in this instance, is $0{\cdot}5 \cdot 10^{-4}$ atom %.

The evaporation from fresh water being considerable in dry and warm climates it also there affects the O^{18}-abundance. Representative samples, which have not been exposed to casual local evaporation, should be looked for in large reservoirs, where the water is constantly being replaced. In the towns tap water is undoubtedly suitable, while in nature river water is to be preferred to lake water. After the collection no evaporation from the sample should take place.

Other important sources of error become evident in the measurement of precipitation. The O^{18}-abundance in the precipitation of a certain locality cannot be taken as representative from a few odd samples. As will be shown later, the samples of precipitation show such great variations that many tests must be made before it is possible to speak of a representative average value.

Tests on Fresh Water

Table 1 shows measurements of fresh water of various origins. ΔO^{18} here indicates deviations from the Danish standard. A point directly following a final digit indicates the increase of this digit by one half. Following the climatic classification used by Köppen (1936), the samples are grouped according to the climate of their place of collection (or, in the case of river water, the area of drainage). The average values for the samples in question are stated opposite their climatic type. The figures in parentheses are not taken up in the computation of the average values. Thus, only one of the five measured Danish samples of tap water has been taken into account in the calculations, because of the relatively close proximity of the places of collection. The results indicate a considerable decrease in the O^{18}-abundance when moving towards colder climates. This fact, as might be expected, is not evident until areas are reached where the evaporation is insignificant compared with the precipitation; i.e., among the climates from Cfb to EF. Here, apart from the samples of precipitation, the spread in the test results is only slight. It should be noted that the samples from Argentina (comprising the climatic types from Cwa to ET) closely agree with samples of corresponding climatic types of other origin.

Also among the climatic types from Af and Aw the divergences are small. This is explainable by the fact that all the samples in this group were collected during the rainy season, when evaporation could not have set in to any appreciable extent. In the Aw group, Foy's Lake, Pakistan, No. 20 was not taken up in the calculation of the mean value, inasmuch as the evaporation from the lake is considerable compared with the outflow. In other words, this is a case of an unusual circulation of water similar to the process taking place in the Dead Sea, where the O^{18}-abundance in the water is the highest measured.

A considerably wider divergence is to be found in the groups of Cwa and Cfa, where the smaller volume of precipitation and the heavy evaporation make the

Table 1

Sample No.	*Climate and locality*	*Ground or flow water*		*Precipitation*	
		ΔO^{18} atom % . 10^4	*Collecting date*	ΔO^{18} atom % . 10^4	*Date*
	A. TROPICAL RAINY CLIMATES				
	Af *Rain Forest Climate*, mean	25		(26·)	
	Philippines				
1	Pasig River, Manila	32			
2	River Water Minglasulla, Cebu	23	53.8.7		
3	Cold Spring Water, Guanos	24·	8.7		
4	Hot Spring Water, Manit, Mingl.	23	8.7		
5	Lake Water, Guason, Mingl.	23	8.7		
6	Pasay			27·	53.7.19
7	Cebu			22	7.25
	Malaya				
8	Water Fall, Maxwill, Taiping	24	7.19		
9	Timor Estate, Johore Bahra	28	7.16		
10	Mount Austin, Johore Bahra	27·	7.21		
11	Waterfall Gardens, Penang	23	8.1		
12	Mount Erskine, Penang	25	7.30		
13	Ravine Water, Pedang, Meiha Estate, Pedang Serai, S. Kedah,	25·			
14	Taiping			31	53.7.16
	Am *Tropical Monsoon Climate* India,				
15	Bombay			36	53.7.12
	Aw *Tropical Savanna Climate*, mean	22			
	Siam				
16	Ground Water, Prae	22·	53.6.27		
17	Me-Yome River, Prae	22·	6.29		
18	River Water, Bankok	21	9.30		
	Pakistan				
19	Hoogly River, Ganges	22·	8.12		
20	Foy's Lake, Pahartalli, Dt-Chittagong	(34)	7.9		
21	Calcutta			28	53.8.27
22	Calcutta			21	9.9
	C. WARM TEMPERATE RAINY CLIMATES				
	Cwa *Winter dry, hot summers*, mean	29			
	Pakistan				
23	Ravi River, Madhopur	27	53.7.8		
	South Africa				
24	Ground Water, Welcom Orange	25	8.14		
25	Spring Water, near Johannesburg	36·	10.14		
26	Spring Water, Klip Riviersberg	38·	10.12		

Table 1

Sample No.	*Climate and locality*	*Ground or flow water*		*Precipitation*	
		ΔO^{18} atom % . 10^4	*Collecting date*	ΔO^{18} atom % . 10^4	*Date*
27	Spring Water, North of Doornkop	29	53.9.10		
28	Little Fugela, Winterton, Natal	31	54.1.14		
29	7 mile Stream, Hilton Road, Natal	32	1.31		
30	Ukamba Stream, Natal National Park	32	1.14		
	Br. Central Africa				
31	Mulunguzi Stream, Zomba Plateau, Nyasaland	29	53.6.7		
32	Namadzi Stream, Nyondtwe	25·	6.14		
33	Nambola Spring	25	6.14		
	Argentina				
34	Perana River, Posadas Misiones	30	10.6		
	China				
35	Hongkong			25	
	Cfa *Without dry season, hot summers*, mean	34			
	Argentina				
36	Ground Water, near Buenos Aires	28·	53.10.13		
37	River Water, San Nicolas, near Buenos Aires	32	9.11		
38	Lujan River, Delta of Tigra	32	10.12		
39	San Juan River, Rosario, Santa Fe	42·	9.11		
	Csa *Summer dry, hot summers*	26			
	Italy				
40	Roma tap water	26	54.4.17		
41	Napoli tap water	26·	4.15		
42	Assisi tap water	25	4.13		
43	Firenze tap water	26·	4.14		
	Cfb *Without dry season, warm summers*, mean	20·			
	Argentina				
44	Lake Nahuel, Huapsi, Neuquen, near Chile	20	53.9.8		
45	Ground Water, San Carlos de Bariloche, Neuquen	15·	9.8		
	Canada				
46	Lake on Br. Properties, West Vancouver	18·	6.19		
47	Mosquito Creek, North Vancouver	17	6.19		

Table 1

Sample No.	*Climate and locality*	*Ground or flow water*		*Precipitation*	
		ΔO^{18} atom % . 10^4	*Collecting date*	ΔO^{18} atom % . 10^4	*Date*
	Denmark				
78	Copenhagen tap water	(23)	52.10.6		
49	Copenhagen tap water	22	53.7.27		
50	Copenhagen tap water	(22)	54.3.12		
51	Naestved tap water	(22)	2.19		
52	Møn tap water	(22)	3.4		
53–115	63 samples of precipitation, mean			22	
	Germany				
116	Grossenbrode tap water	23·	4.10		
117	München tap water	25	4.24		
	Italy				
118	Milano tap water	21	4.11		
119	Venezia tap water	22	4.22		
	D. COOL SNOW FOREST CLIMATES				
	Dfc *With cool summers*				
	Finland				
120	Helsinki tap water	16·	54.5.6		
	E. POLAR CLIMATES				
	ET *Tundra Climate*, mean	8·		(10·)	
	Argentina				
121	River Water, Salta	8·	53.11.20		
122	River Water, Salta	10·			
	Greenland				
123	Red River, Godhavn	8·	52.11.20		
124	Spring, Godhavn	6	11.16		
125	Spring, Godhavn	8·	3.10		
126	Godhavn			13·	52.11.4
127	Godhavn			5	10.31
128	Godhavn			14·	11.5
129	Godhavn			18	11.20
130	Godhavn			4	3.29
	EF *Frost Climate*, mean			(—17)	
	Greenland				
131	Ice cap			—17	
132	Ice cap			—23	
133	Ice cap			—12·	

O^{18}-abundance highly dependent on local conditions and on the samples being collected in or outside the rainy season.

The findings from the above have been grouped in Table 2, where the average values of the O^{18} of the various climatic types are listed:

Table 2

Climate	ΔO^{18}	O^{18} atom %
A		
Cwa	21–42	depending on the season
Cfa		0·1971–0·1992
Cfb	20·	0·1970·
ET	8·	0·1958·
EF	(−17)	(0·1933)

The O^{18}-abundance in Atmospheric Water Vapour

In order to explain this dependence on climatic conditions it is essential to explore the entire circulatory course of the water.

As stated in Dansgaard (1953) the immediate O^{18}-abundance in atmospheric water vapour depends on the pre-history of the vapour.

The following sources of variation were mentioned:

(a) the temperature of the evaporation,

(b) the origin of the vapour,

(c) earlier precipitation of water owing to cooling.

(a) *The temperature of the evaporation*

From equation (1) it will be seen that the O^{18}-abundance in vapour (hereinafter called a_v) from ocean water is somewhat less than the O^{18}-abundance in the ocean water, and that it is dependent, besides, on the evaporation temperature. Applying Raoult's Law on the equilibrium between vapour and sea water we get, after the elimination of insignificant terms (cf. Dansgaard, 1953):

$$a_{vo} = a_o \frac{{p_0}^{18}}{{p_0}^{16}} \tag{3}$$

From equation (1) and the value 0·1991 atom % for a_o we arrive at the a_{vo} values in Table 3.

Table 3

t°C	T°K	a_{vo} atom %
0	273	$0{\cdot}1971_1$
5	278	$0{\cdot}1971_8$
10	283	$0{\cdot}1972_5$
15	288	0.1973_2
20	293	$0{\cdot}1973_8$
25	298	$0{\cdot}1974_5$
mean		0·1973

Hence, a_{vo} is approximately 0·0018 atom % less than a_o.

The small variations are noticeable but far from sufficient to explain the wide variations in the O^{18}-abundance in fresh water (hereinafter called a_f).

A comparison with Table 1 shows agreement between the a_{vo} and a_f of fresh water from warm and temperate climates. On the basis of this agreement, the O^{18}-abundance in fresh water has been explained, simply, by the fresh water being condensed ocean-water vapour.

(b) *The origin of the vapour*

Since $\frac{p_0^{18}}{p_0^{16}}$, according to equation (1) differs only about 1 per cent from unity, it will be seen from equation (3) that the a_{vf} of vapour from fresh water must be just as much below the values of a_{vo} listed in Table 3 as a_f is below a_o. Since

$$a_o - a_f \cong 0{\cdot}1991 - 0{\cdot}1970{\cdot} = 0{\cdot}0020{\cdot} \text{ atom } \%$$

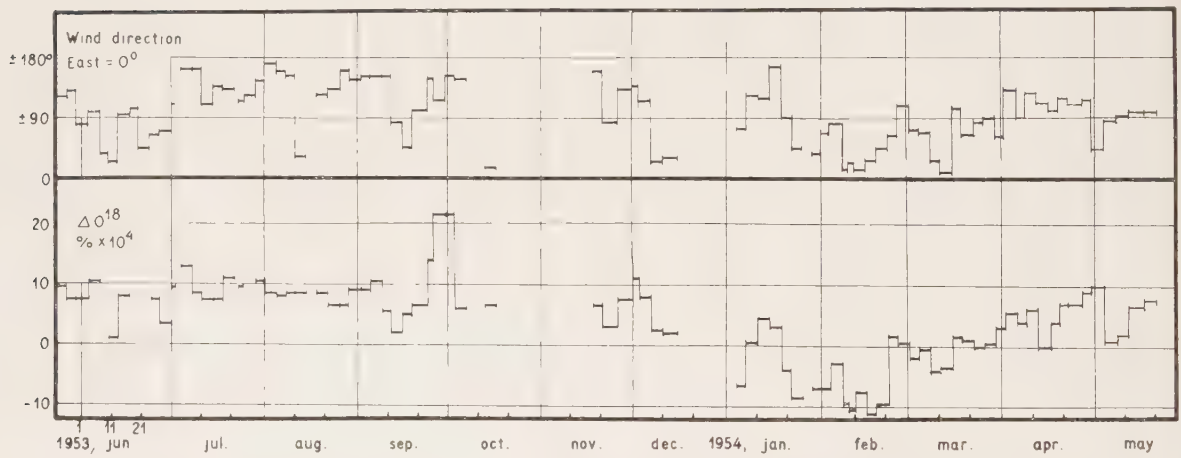

Fig. 2. In the lower part is shown deviations from the Danish standard of the O^{18}-abundance in samples of water vapour collected in 3 to 4 day periods. In the upper part for the same periods is shown the average deviation of the wind from the east point direction.

in temperate zones, this is also the difference between a_{vo} and a_{vf}. According to Table 3, the highest absolute value of a_{vo} in the temperate zones should be about 0·1974 atom %, which should obtain in pure ocean-water vapour that, in moving from the place of evaporation to the place of collection, has not by condensation separated any volume of water worth considering. On the other hand, for the reasons stated under (c), the lower limit of a_v is not easy to determine.

At Copenhagen, in the period of May 23, 1953, till May 21, 1954—apart from some periods of short duration—atmospheric water vapour was collected in a trap cooled by means of dry ice and alcohol. The trap was emptied twice a week. Thus each sample represented the average O^{18}-abundance in atmospheric water vapour for a period of three or four days. The a_v was tested with CO_2 equalized with the thawed water from the trap. The difference of a_v and the Danish standard is plotted in the lower part of Fig. 2, while the deviations from the east point of the

average direction of the wind are shown in the upper part, plotted into the corresponding intervals of time. The correlation between the two curves is evident and indicates that the easterly winds in Denmark contain more fresh-water vapour than the westerly winds. This fact is not surprising considering the situation of Denmark, bordering on the ocean and the continent; nor is it surprising that the correlation is incomplete; for example, with regard to the last mentioned fact, it is quite possible that easterly winds in special circumstances may contain water vapour principally of maritime origin.

It is astonishing, however, in two periods only (Sept. 26 to 30 and Sept. 30 to Oct. 3) was a_v as high as 0·1971 atom %; hence, apparently, almost purely maritime. The explanation of this phenomenon is given under (c) below.

Furthermore, an annual variation in the a_v is worthy of note. Table 4 shows the average values of the a_v month by month.

Table 4

Period	ΔO^{18} atom % . 10^4	a_v atom %
May	6·6	0·19566
1953, June	8.2	582
July	10·1	601
Aug.	8·2	582
Sept.	10·3	603
Nov. 18–Dec. 15	5·6	566
1954, Jan.	−2·9	471
Feb.	−5·8	442
March	−0.6	494
Apr.	5·1	0·19551
mean for the year	4·7	0·19547
mean of precipitative vapour: a_{vp}	5·5	0·19555

At bottom, in Table 4, is stated the result of a computation of the O^{18}-abundance, a_{vp}, in precipitative vapour. This a_{vp} is found from the summation of the products of the quantity of the precipitation in the 3 or 4 day periods, and the corresponding a_v values divided by the total quantity of the precipitation. The fact that the a_{vp} is slightly higher than the mean value for a_v computed in the usual way, merely implies that the precipitative vapour in Denmark is of maritime origin to a greater extent than the average vapour.

(c) *Precipitation released by cooling*

In Dansgaard (1953) it was shown that the O^{18}-abundance in a given volume of atmospheric water vapour will decrease gradually with the separation by cooling of water vapour, since the H_2O^{18}, on account of its relatively low vapour pressure, is

condensed in a degree disproportionate to its abundance in the vapour. Thus the a_r in the remaining water vapour is less than the a_r in the initial water vapour, and also less than the H_2O^{18}-abundance in the precipitation (hereinafter called a_p).

For the determination of the gradual decrease in a_v during the cooling process, an equation is employed, derived from Dansgaard (1953), expressing a_v as a function of T, the temperature and a_r at the beginning of the condensation being T_0 and a_v° respectively:

$$a_v = K \,.\, T^{-C_1} \,.\, \exp\left(C_2 T - \frac{C_3}{T}\right)$$

K, C_1, C_2, and C_3 being constants. C_1 and C_2 depend on the heat of evaporation of the water and its variation in temperature. C_3 at the same time is dependent on $\frac{p_0^{18}}{p_0^{16}}$ and its variation with the temperature, whereas K depends on a_v^0 and the other constants.

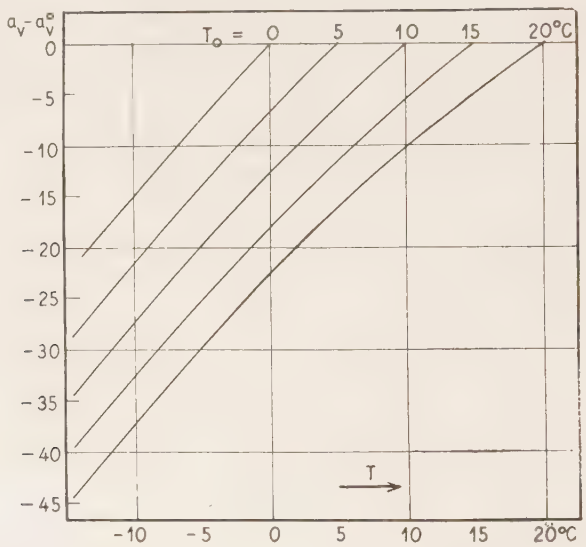

Fig. 3. The increase in O^{18}-abundance in a quantity of vapour from which water has been separated by cooling from T_0 to T.

$a_v - a_v^\circ$ is shown in Fig. 3 plotted as the function of T at various T_0; hence the changes taking place in the O^{18}-abundance of saturated vapour in cooling from T_0 to T°. In the calculation is employed the a_v° value, 0·1973 atom %, corresponding to pure ocean vapour. A recalculation on the basis of the a_v° value for fresh-water vapour, 0·1952· atom %, even in cooling by 35°C, gave deviations from the values shown in Fig. 3 of less than 0·00005 atom %. This is of the same size as the accuracy of the measurements. Hence, the values in Fig. 3 may be regarded as valid for any kind of vapour. The curves,

$$a_r - a_v^\circ = f(T - T_0)$$

may be approximated by the straight line

$$a_v - a_v^\circ = 1{\cdot}28 \,.\, 10^{-4}\,(T - T_0) \qquad (4)$$

with an accuracy which, by cooling from all temperatures of $T_0 \leqq 17°C$ down to $-10°C$, is better than $\pm 0{\cdot}0002$ atom %.

Since, for the O^{18}-abundance, a_c, in the cloud droplets formed by condensation during cooling, we have $a_c \cong a_v \frac{p_0^{16}}{p_0^{18}}$, we get with $\frac{p_0^{16}}{p_0^{18}} = 1{\cdot}01$:

$$a_c(T) - a_c(T_0) = 1{\cdot}29 \,.\, 10^{-4}(T - T_0).$$

Supposing saturated, pure ocean vapour to be cooled from T_0 to T, the remaining vapour, according to the above, should have an a_v lower than the original vapour. When the air upon being heated to $T_0°$ has again absorbed ocean vapour to saturation, the vapour mixture will also have an a_v lower than the original. Hence a decrease in a_v takes place in the air passing through the following circulatory process:

1. Air saturated with ocean vapour at $T_0°$ gives off precipitation when cooled to $T_1°$,
2. The air again is heated to $T_0°$,
3. The air is saturated with ocean vapour at $T_0°$.

The decrease in a_v may be determined in the following way: where 1 m^3 of saturated air at $T°$ contains $M(T)$ grammes of water vapour, the quantity of H_2O^{18} in the same volume is

$$A = \frac{20}{18} M(T) \,.\, \frac{a_v(T)}{100} \text{ grammes.}$$

With $T = T_1$ this may be taken to express the remaining quantity of H_2O^{18} per m^3 after the first part process. During the third part process is absorbed

$$\frac{20}{1800} (M(T_0) - M(T_1)) \,.\, a_v(T_0) \text{ grammes of } H_2O^{18}.$$

Thus, on completion of the whole circulatory process, the new a_v of the vapour is

$$a_v' = \frac{M(T_1) \,.\, a_v(T_1) + (M(T_0) - M(T_1)) \,.\, a_v(T_0)}{M(T_0)}$$

or

$$a_v' = a_v(T_0) \,.\, \frac{M(T_1)}{M(T_0)} (a_v(T_0) - a_v(T_1)).$$

Since

$$M(T) = 288 \frac{E(T)}{T},$$

$E(T)$ being the pressure of saturated water vapour at $T°$, the change taking place in a_v in the entire circulatory process can be expressed thus:

$$\Delta a_v = a_v'(T_1) - a_v(T_0) = - \frac{E(T_1) \,.\, T_0}{E(T_0) T_1} \,.\, 1{\cdot}28 \,.\, 10^{-4}(T_0 - T_1) \qquad (5)$$

Fig. 4 is a diagram of Δa_v as a function of $(T_0 - T_1)$. Continuing the curves towards the right side, these must finally reach ordinate $\Delta a_v = 0$. It should be

noted that any circulatory process where $T_0 - T$ is within the interval of $7° < T_0 - T_1 < 23°$C will cause a decrease in a_v of $-0{\cdot}0006 \cdot \pm 0{\cdot}0001$ atom %. In nature, naturally, "equilibrium" is soon readjusted. Where it is a matter of ocean vapour exclusively, the "equilibrium" value is of such order that the average value of a_v is just so much below the a_v value of maritime vapour, 0·1973 atom %, that the decrease in a_v during the first part process is equalized by the increase in a_v during the third part process. The equilibrium value of a_v, after the air has passed

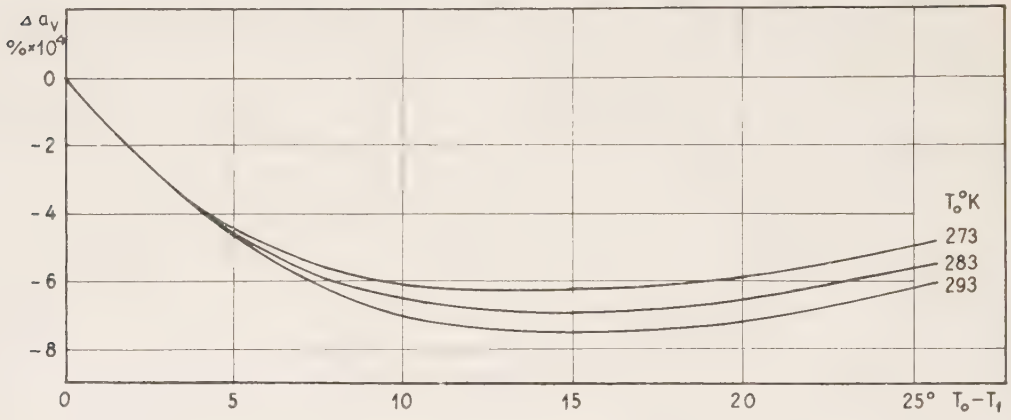

Fig. 4. The increase in O^{18}-abundance in vapour which has passed through a circulatory process of (1) separation of water due to cooling from T_0 to T, (2) heating to T_0, and (3) saturation at T_0 by vapour from the original composition.

through an infinite number of circulatory processes, cooling down from $T_0°$ to $T°$, is $a_{ve}(T_1, T_0)$. Vapour of this O^{18}-abundance after the first part process has an O^{18}-abundance of

$$x_v(T_1) = a_{ve}(T_0, T_1) - 1{\cdot}28 \,.\, 10^{-4}(T_0 - T_1) \tag{6}$$

After the third part process, the O^{18}-abundance is again $a_{ve}(T_0, T_1)$. Reasoning as in the working out of (5), we find that,

$$a_{ve}(T_0, T_1) = \frac{x_v(T_1) \,.\, M(T_1) + (M(T_0) - M(T_1))a_{vo}(T_0)}{M(T_0)}$$

Hence

$$a_{ve}(T_0, T_1) = x_v(T_1)\frac{M(T_1)}{M(T_0)} + \left(1 - \frac{M(T_1)}{M(T_0)}\right) \cdot a_{vo}(T_0)$$

Inserting (6), with f representing $M(T_1)/M(T_0)$, we get

$$a_{ve}(T_0, T_1) = a_{vo}(T_0) - 1{\cdot}28 \,.\, 10^{-4} \,.\, (T_0 - T) \,.\, \frac{f}{1 - f}$$

Hence the difference of the O^{18}-abundance of ocean vapour and equilibrium vapour is

$$a_v(T_0) - a_{ve}(T_0, T_1) = 1{\cdot}28 \,.\, 10^{-4}(T_0 - T_1)\frac{f}{1 - f}.$$

This equation is shown graphically in Fig. 5. Hence, a long series of circulatory processes, cooling down $T_0 - T_1°$, will yield an equalization vapour of an O^{18}

value lower than the abundance present in the additional vapour. The smaller the $T_0 - T_1$ value the greater, according to Fig. 5, the fractionation, or, in other words, the lower will be the O^{18} abundance of the equalization vapour.

Thus, in the main, the fact is explained that the average O^{18}-abundance of atmospheric water vapour, according to Table 4, is as low as 0·19547‰. The a_v of

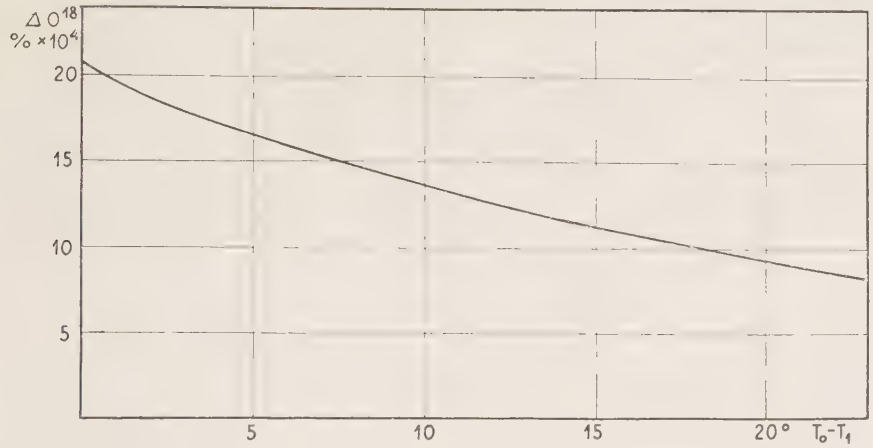

Fig. 5. The difference in O^{18}-abundance of the additional vapour and the equilibrium vapour produced after passing through numerous circulatory processes by cooling from T_0 to T.

pure ocean vapour, according to Table 3, is 0·1973‰, whereas the a_v of pure fresh-water vapour of climatic type C is approximately 0·1952·‰.

The Vertical Distribution of H_2O^{18}

Vertical air currents produce a mixing of the water vapour in the atmosphere. Since the gravitation plays no part in this connection, these currents only bring

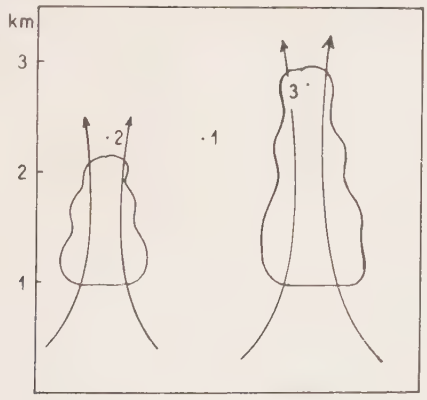

Fig. 6. Cumulus clouds with tracks of air particles 1, 2, and 3 indicate the places of collection.

about fractionation upon forming clouds. In that event, fractionation goes on in the usual way, the H_2O^{18} having the greater tendency to condensation. Consequently the a_v of an air mass with cumulus clouds, formed by powerful vertical air

currents, should decrease on the upgrade and be the lowest in value immediately above the clouds, where the casual blending with the surrounding air is still of little consequence.

This fact was experimentally demonstrated by the measuring of samples collected by means of an airplane, on September 17, 1951. The air was drawn in through a trap, in which the water was condensed. Fig. 6 shows cumulus clouds with tracks of currents and places of collection, while Table 5 shows the results obtained.

Table 5

Sample No.	Altitude	ΔO^{18} atom % . 10^4
1	2300 m	−15·
2	2300 m	−29·
3	2800 m	+0·

The high value of sample 3 is no doubt due to the fact that this sample consisted of frozen cloud droplets as well as of condensed vapour. The values of the two first samples are far below the very lowest a_v value measured at ground level.

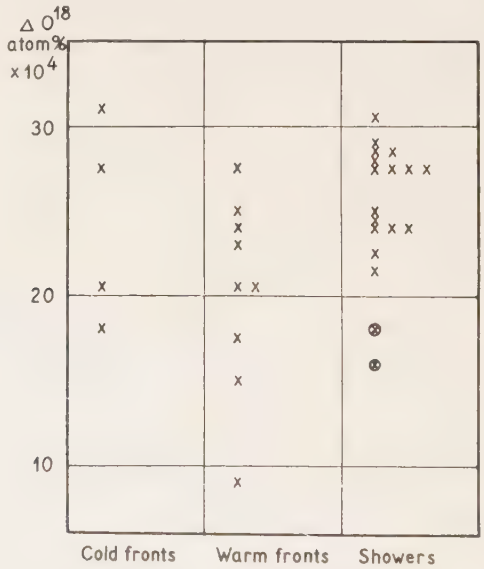

Fig. 7. Deviations from the Danish standard of samples of special types of precipitation.

For the further elucidation of these facts, we here mention some measurements made on special kinds of precipitation. Fig. 7 shows that precipitation from showers, produced by the above stated process, have a relatively high O^{18}-abundance. The lowest two encircled marks refer to hail formed, for the most part, in the topmost layers of the high level clouds.

The process going on in the cumulus clouds, where falling rain drops pass through ascending water vapour, essentially corresponds to the process employed in tall distillation columns for the artificial enrichment of the O^{18} in water.

The O^{18}-Abundance in Fresh Water

Since fresh water, for the most part, is derived from atmospheric water vapour, it is obvious that the O^{18}-abundance of fresh water (a_f) will depend, inter alia, on the same factors as the a_v. The a_p of a certain precipitation is

$$a_p \cong a_v \frac{{p_0}^{16}}{{p_0}^{18}}$$

where a_v, as mentioned, depends on

(a) the precipitation temperature,

(b) the origin of the vapour,

(c) the average cooling the circulatory process,

whereas the $\frac{{p_0}^{16}}{{p_0}^{18}}$ depends on

(d) the condensation temperature.

The a_p, furthermore, depends on

(e) the cooling since the beginning of the condensation in question

plus an effect owing to

(f) the evaporation during the fall from cloud to ground.

The a_f for a certain locality, further, depends on

(g) the magnitude of the evaporation from the precipitation since its reaching the ground

(h) the possible exchange of O^{18} between the water and oxygenic substances in the ground.

The significance of these factors will be discussed singly in the following, particularly in relation to fresh water in Denmark. Attempts will be made to conform the measured a_f value for Danish fresh water to a value worked out partly on the basis of measurements of the O^{18} abundance in ocean water, fresh water, precipitation and atmospheric vapour, and partly on the basis of meteorological observations and reasonable estimates of evaporation and condensation temperatures.

Fig. 8 is a sketchy representation of the movements of the air during a typical circulatory process. The evaporation, which never or very seldom, according to meteorological observations, goes on to saturation, takes place at $T_e{}^\circ$ at A. On cooling to $T_0{}^\circ$ over the interval of AB, condensation commences at B. When the air reaches the place of collection C, the temperature has dropped to $T_2{}^\circ$, and at D, at condensation temperature T_1, the air is returned to A, where heating and evaporation takes place. For practical reasons, pure ocean vapour

$$a_v = 0{\cdot}1991 \left(\frac{{p_0}^{18}}{{p_0}^{16}}\right)_{T_e} = 0{\cdot}1973\,\%$$

is assumed for the evaporation temperature $T_e = 286^\circ\mathrm{K}$.

(a)

The evaporation temperature may require a correction, k_a, to the above value, which at most, according to Table 3, can be of the order of $\pm 0{\cdot}0002\%$. It is difficult, naturally, to assess the actual value for a certain locality. For temperate climates it may be placed at $0{\cdot}0000 \pm 0{\cdot}0000{\cdot}\%$ corresponding to the average temperature of

$$T_e = 13 \pm 4°\text{C}.$$

(b)

The vapour not being exclusively of oceanic origin, a negative correction k_b, which numerically, at most, can be equal to the difference of a_o and the a_f of the relevant climatic type, hence for the temperate zones $0{\cdot}1991 - 0{\cdot}1970{\cdot} = 0{\cdot}0020{\cdot}\%$.

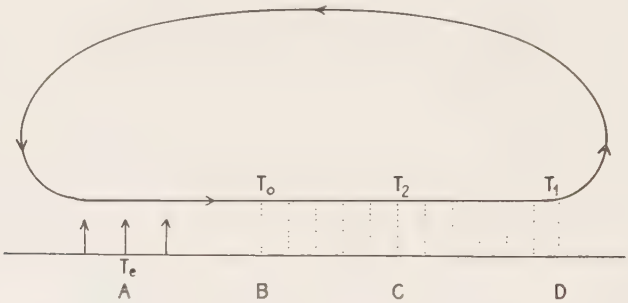

Fig. 8. A sketchy representation of the movements of the air during a typical circulatory process. The evaporation takes place at T_e at A. On cooling to T_0 over the interval of AB, condensation commences at B. When the air reaches the place of collection C, the temperature has dropped to T_2, and at D, at condensation temperature T_1, the air is returned to A.

This maximum is to be multiplied by the relative proportion of the fresh-water vapour in the average vapour of the locality in question. This factor, naturally, much depends on the climatic conditions, and for Denmark it should be equal to $0{\cdot}2 \pm 0{\cdot}1$. Consequently, the k_b for Denmark is taken to be

$$-0{\cdot}0020{\cdot} \times 0{\cdot}2 = -0{\cdot}0004 \pm 0{\cdot}0002\%$$

(c)

The correction, k_c, due to the passage of the vapour through numerous circulatory processes, is not determinable independent of the other corrections, inasmuch as the average cooling, $T_0 - T_1$, since the beginning of the precipitation of the water, is unknown. In Denmark the vapour equilibrium is

$$a_k{}^\circ = 0{\cdot}1973 + k_a + k_b + k_c = 0{\cdot}1954{\cdot} \qquad (7)$$

the last figure representing the value of atmospheric vapour measured for one year Hence

$$k_c = 0{\cdot}1954{\cdot} - 0{\cdot}1973 - k_a - k_b = -0{\cdot}0014{\cdot} \pm 0{\cdot}0004\%.$$

The rather great inaccuracy of this figure is mainly owing to the value 0·1973 for

a_{vo}, because of its deriving from a_o through multiplication by the relatively indefinite $p_0{}^{18}/p_0{}^{16}$.

(d)

$a_{ve}{}^{\circ}$, representing the vapour equilibrium before condensation, may be written

$$a_{ve}{}^{\circ} = 0{\cdot}1991 \,.\, \left(\frac{p_0{}^{18}}{p_0{}^{16}}\right)_{T_e} + \Delta a,$$

$\Delta a = k_a + k_b + k_c$, which according to (7) is: $-0{\cdot}0018{\cdot}‰$. After the beginning of the precipitation, at $T_0{}^{\circ}$, we have according to (4)

$$a_{ve} = 0{\cdot}1991 \,.\, \left(\frac{p_0{}^{18}}{p_0{}^{16}}\right)_{T_e} + \Delta a - 1{\cdot}28 \,.\, 10^{4}{\cdot}(T_0 - T)$$

from which water is condensed of

$$a_p = a_{ve}\left(\frac{p_0{}^{16}}{p_0{}^{18}}\right)_{T_2} = 0{\cdot}1991 \,.\, \left(\frac{p_0{}^{18}}{p_0{}^{16}}\right)_{T_e} \cdot \left(\frac{p_0{}^{16}}{p_0{}^{18}}\right)_{T_2} + (\Delta a - 1{\cdot}28 \,.\, 10^{-4}(T_0 - T_2)) \,.\, \left(\frac{p_0{}^{16}}{p_0{}^{18}}\right). \tag{8}$$

Approximating equation (1) to a straight line $\left(\frac{p_0{}^{16}}{p_0{}^{18}}\right) = a - bT$, we get

$$\left(\frac{p_0{}^{18}}{p_0{}^{16}}\right)_{T_e} \cdot \left(\frac{p_0{}^{16}}{p_0{}^{18}}\right)_{T_2} = \frac{a - bT_2}{a - bT_e} = 1 + \frac{b(T_e - T_2)}{a - bT_e} \cong 1 + 1{\cdot}01{\cdot}(T_e - T_2) \,.\, b \tag{9}$$

with $b = 7{\cdot}80 \,.\, 10^{-5}$.

Hence, according to (8) and (9), the correction, k_d, presumed because of the different evaporation and condensation temperatures, is

$$k_d = 0{\cdot}1991 \,.\, 1{\cdot}01(T_e - T_2)b \tag{10}$$

For Denmark T_e is taken as 286°K. As regards T_2, it may be assumed that the precipitation in Denmark is condensed at the altitude of 1 to 3 km. The mean temperature at ground level is approximately 6·5°C, and calculating on a rising temperature gradient of −0·65°C per 100 m, we get 0° and −13° at the altitudes of 1 and 3 km respectively. No great error is committed by figuring on an average condensation temperature of $T_2 = 267$°K. Inserting T_e and T_2 in equation (10) we get

$$k_d = 0{\cdot}0003 \pm 0{\cdot}0001‰$$

(e)

Hence, with $\left(\frac{p_0{}^{16}}{p_0{}^{18}}\right)_{T_2} = 1{\cdot}01$, equation (8) may be written

$$a_p = 0{\cdot}1975{\cdot} - 1{\cdot}29 \,.\, 10^{-4}(T_0 - T_2) \tag{11}$$

calling the last term k_r, due to the part of the cooling of the air which took place before its arrival at the place of collection which caused precipitation.

On the supposition of a fairly equal, vertical temperature gradient and about equal cloud elevations at B and C in Fig. 8, $T_0 - T_2$ is equal to the differences of the temperatures at the ground at B and C, called T_B and T_C. The lower limit for $T_B - T_C$ is 0°; the upper limit being $T_e - T_C$, which in Denmark is about 6°C. Hence $T_0 - T_2 = T_B - T_C = 3 \pm 2$°C, and we get

$$k_e = -0{\cdot}0004 \pm 0{\cdot}0002{\cdot}‰.$$

(f)

Owing to evaporation while falling, the precipitation that reaches the ground may have a greater O^{18}-abundance than the precipitation at the moment of separating from the cloud. This fact has been demonstrated in Dansgaard (1953), where the k_f of the precipitation from the uppermost layer of a very high warm front was no less than 0·0008‰. Naturally, only the drops separated in the beginning of the precipitation are subject to any appreciable increase in O^{18}-abundance during the fall. Gradually, the air is saturated and, at any rate, during rains of long duration and/or great violence the phenomenon is insignificant. In Denmark, therefore, the k_f of the total volume of rain is practically equal to 0.

(g) and (h)

According to equation (2) the evaporation from fresh water on the ground requires a positive correction, k_g, which must be expected to increase in the direction of warmer and drier climates. In regions having dry seasons, the k_g should increase in the dry periods.

The correction for the exchange with oxygenic substances in the ground being k_h, the $k_g + k_h$ of a given locality and at a certain time may be found by comparing the a_p for the total volume of precipitation with the a_f for the available fresh water.

In Denmark tests have been made of 63 samples of precipitation representing 304 mm of rain and equal to 48% of the average annual precipitation. The samples were drawn in fairly even distribution throughout the four seasons; nevertheless, it was not possible during the year to prove any definite seasonal changes in the a_p. The average deviation from the standard was 0·00223‰. Comparing this figure with the values listed in Table 1 for Danish fresh water, we get

$$k_g + k_h = 0{\cdot}0000 \pm 0{\cdot}0000{\cdot}‰$$

Hence, the following findings for Danish fresh water:

$$a_f = 0{\cdot}1991 + \sum_{a}^{h} k = 0{\cdot}1971{\cdot} \pm 0{\cdot}0005‰$$

corresponding to

$$\Delta O^{18} = (21{\cdot} \pm 5) \,.\, 10^{-4}‰ \qquad (12)$$

in accordance with the measured value of 0·1972‰.

The value of (12) practically agrees with the test results listed in Table 1 of samples of climatic type Cfb, where the variations in general correspond to the variations in the temperature in the particular zones; thus, the highest ΔO^{18} is in water from the warmest regions. Exceptions are samples of tap water from Milano

and Venezia. This is explained by the fact that these waters are of alpine origin, corresponding to higher latitudes.

Naturally, regarding the climatic types ET and EF, it is not possible without extensive measurements of precipitation and vapour to enter into such details as in the above. However, if one tries in the same way to calculate the a_f for Godhavn, Greenland, from the supposition that the air there has made circulatory processes equal to those of the air in Denmark, one gets the figures of correction expressed in per cent . 10^4 which are listed in Table 6. By temperature at ground is

Table 6

Climate	Temp. at ground	k_a	k_b	k_c	k_d	k_e	$k_f+k_g+k_h$	calc. a_f	obs. a_f
ET	−7.5°C	−1	−4	−14·	4·	−14	0	0.1961·	0.1957·

meant the mean temperature of the drainage area of the river and springs in Godhavn. It is estimated to be −7·5°C at a height of 600 m above sea level, the temperature at sea level being −4°C. In this calculation T_e has been estimated as 280°K. The observed a_f lies within the error of the computation of the calculated value.

With regard to the other climatic types, of which many measurements are available, the evaporation plays so great a part that a rational result by computation cannot be expected.

In certain areas on the Greenland Ice Cap is a distinct layer formation caused by melting in the summer season. On the supposition that the character of the circulatory processes, in all essentials, have not varied over a long period of time, the above, in the opinion of this author, offers the possibility by measurements of the a_f in these layers of ice to determine climatic changes over a period of time of several hundred years of the past. According to equation (11), a change in temperature of 1°C results in a variation in a_f of 1·3 . 10^{-4}‰, which indicates an absolutely measurable variation. The exchange of water between the layers may constitute a source of error, which, however, may be ascertained by a closer investigation of the layers. Evaporation has hardly played any great role, particularly not in the northern regions of Greenland, which should be made the choice for investigation, as there the layers of ice are the thinnest, because of the slight annual precipitation.

An investigation will be undertaken as soon as an opportunity offers.

In conclusion I wish to express my gratitude for the interest and assistance rendered to me from so many sides in collecting samples of water. First and foremost my thanks are due to H.R.H. Prince Axel, at whose initiative the staffs of the East Asiatic Company's branches in Argentina, South Africa, Pakistan, the Far East, and Canada have done much valuable work. My thanks and appreciation are also extended to Dr. phill. A. F. Bruun, of the Copenhagen Zoological Museum,

to Professor K. Rankama, of Helsinki, and to Mrs. Rigmor Thomsen, of Copenhagen. I am indebted and very grateful to Colonel C. C. Lassen, of Vaerlose air base, for his kindness in placing at my disposal an airplane for the collection of vapour samples from cumulus clouds.

Last but not least I wish to thank Mr. Søren Brogaard, M.S., for his very valuable assistance in the making of numerous measurements.

References

Dansgaard, W. (1953) Tellus **5,** 461
Epstein, S., and Mayeda, T. (1953) Geochim. et Cosmochim. Acta **4,** 213
Køppen-Geiger (1936) Handbuch der Klimatologie, Vol. **1C,** Berlin
Nier, A. O. (1950) Phys. Rev. **77,** 789
Riesenfeld, E. H., and Chang, T. L. (1936) Z. phys. Chem. **B 33,** 127

Geochimica et Cosmochimica Acta, 1954, Vol. 6, pp. 261 to 267. Pergamon Press Ltd., London

Experimentelle Untersuchungen über die Diffusion von Helium in Steinsalzen und Sylvinen

W. Gentner und E. A. Trendelenburg
Physikalisches Institut der Universität Freiburg i.Br.

(*Received* 26 *July* 1954)

ABSTRACT

Measurements with a mass-spectrometer gave diffusion constants of helium in pure NaCl and in a sylvin mixture (45% NaCl and 55% KCl) in the temperature region between 500 and 650°C. An extrapolation of the measured values to the temperature region between 40 and 80°C showed good agreement with the values obtained from calculated corrections in age determinations. (Extrapolated values $D_{He(80°C)} = 4{\cdot}0 \times 10^{-17}$ cm^2/sec; $D_{He(40°C)} = 3{\cdot}2 \times 10^{-19}$ cm^2/sec; from age determinations $D_{He(80°C)} = 1{\cdot}2 \times 10^{-17}$ cm^2/sec; $D_{He(40°C)} = 1{\cdot}2 \times 10^{-19}$ cm /sec.)

A discussion is presented why these values differ from those derived by Thomson and Wardle. It was also shown that in sylvin, besides a pure volume diffusion, further processes of degassing occurred which were dependent upon the crystal structure.

An anderer Stelle (Gentner & Trendelenburg, 1954) wurde bereits beschrieben, in welcher Weise verhältnismässig kleine Diffusionskonstanten von Gasen in Festkörpern mit einer massenspektrometrischen Methode bestimmt werden können. Ausgehend von der Tatsache, dass schon vor einiger Zeit (Gentner *et al.*, 1953a, b; 1954) durch systematische Untersuchungen der Zusammenhänge zwischen mittlerer Kristallgrösse und gemessenem Alter an Sylvinen Abschätzungen über die Diffusionskonstanten von Helium und Argon vorgenommen werden konnten, sollte mit dieser Methode nun versucht werden, derartige Diffusionskonstanten direkt zu messen. Während die seinerzeit vorgenommenen Abschätzungen sich auf den Temperaturbereich von 40 bis 80°C bezogen und dabei als "Messzeit" die gesamte Lebensdauer des Salzlagers (25×10^6 Jahre) benutzt wurde, war es notwendig, die experimentellen Untersuchungen unter Ausnutzung des für Diffusionsvorgänge gültigen Temperaturgesetzes $D = D_0 \exp(-Q/RT)$ (Q = Aktivierungs-oder Ablöseenergie, R = Gaskonstante, T = absolute Temperatur) bei entsprechend höheren Temperaturen anzustellen. Durch eine Extrapolation in den vorher genannten Temperaturbereich sollten die so erhaltenen Werte dann mit den aus Beobachtungen bei der Altersbestimmung erhaltenen Daten verglichen werden. Des Weiteren sollte überprüft werden, ob es tatsächlich, wie zunächst angenommen war, zulässig ist, bei der Altersbestimmung nur Gasverluste durch Volumdiffusion anzunehmen.

Bei den Untersuchungen wurden Salzproben mit einem mittleren Heliumgehalt von 1×10^{-5} cm^3 (bezogen auf Atmosphärendruck) in einem Vakuumofen erhitzt und die austretende Gasmenge in einem registrierenden Massenspektrometer mit einer Nachweisempfindlichkeit von 2×10^{-10} cm^{3}He/sec in ihrem zeitlichen Verlauf analysiert. Messungen mit Argon wurden aus apparativen, später zu besprechenden Gründen noch nicht vorgenommen, sind aber geplant. Eine eingehendere Beschreibung der Messmethode wurde bereits in der erwähnten Veröffentlichung (Gentner & Trendelenburg, 1954 gegeben.

Mathematische Behandlung des Diffusionsvorgangs

Bei der mathematischen Behandlung wurde vom zweiten Fick'schen Gesetz $\partial c/\partial t$ div (D grad c) ausgegangen. Nimmt man an, dass die Diffusionskonstante D von der Konzentration c unabhängig ist, was bei kleinen Konzentrationen zulässig erscheint, so vereinfacht sich dieses Gesetz zu $\partial c/\partial t = D\Delta c$. Zur Untersuchung wie der zeitliche Abfall der einen Kristall pro Zeiteinheit verlassenden Gasmenge mit den Diffusionskonstanten verknüpft ist, wurden folgende Randbedingungen eingeführt:

1. Reine Volumdiffusion.
2. Aussendruck an den Grenzen des Diffusionsmediums konstant.
3. Diffusionsmedium isotrop.
4. Temperatur konstant.
5. Betrachteter Körper würfelförmig mit Kantenlänge d.
6. Gasmenge vor Anlaufen des Diffusionsvorganges in Kristall homogen verteilt.

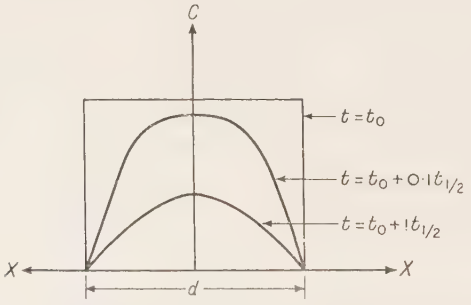

Abb. 1. Einschwingvorgang der Konzentrationsverteilung (c = Konzentration, d = Kristalldicke).

Es lässt sich nun durch Fourier-Zerlegung zeigen, dass sich bei anfangs homogener Gasverteilung in einer im Vergleich zur Dauer des Diffusionsvorganges kurzen Zeit die Konzentrationsverteilung rein sinusförmig einstellt (Abb. 1). Ist dies der Fall, dann wird von nun an in jedem Punkt des Kristalls die Gaskonzentration streng exponentiell mit der Zeit abfallen. Misst man nun die Halbwertszeit $t_{1/2}$ der dieser zeitlichen Konzentrationsänderung proportionalen pro Zeiteinheit den Kristall verlassenden Gasmenge, dann ergibt sich für die Diffusionskonstante der Wert $D = d^2/3\pi^2 t_{1/2} \ln 2$ cm^2/sec.

Ergebnisse

Da natürliche Sylvine stets aus einem Gemisch von NaCl– und KCl– Kristallen bestehen, ist es bei der Untersuchung der in derartigen Salzen auftretenden Diffusionsphänomene zweckmässig, von zwei verschiedenen Fragestellungen auszugehen. Erstens wird man die Diffusionsvorgänge an reinem NaCl und reinem KCl untersuchen müssen, und zweitens wird dann zu überprüfen sein, inweiweit sich die hier gefundenen Resultate auf Sylvine der verschiedensten Herkunft, Zusammensetzung und Struktur übertragen lassen. Im Folgenden soll nun über Untersuchungen an reinem NaCl und an zwei Gruppen von Sylvinen berichtet werden.

Untersuchungen an reinem NaCl:

Die Untersuchung an reinem NaCl wurde an Salzproben mit einem Kristalldurchmesser von $d = 0{\cdot}6$ und $d = 1{\cdot}3$ mm durchgeführt, die durch Zerschlagen und Sieben eines grossen natürlichen Einkristalls von besonderer Reinheit gewonnen wurden. Die Proben wurden vor der Messung jeweils zwölf Stunden bei einer Temperatur von 650°C in einer Helium-Luft Atmosphäre mit 10 Prozent Helium bei einem Druck von 500 Torr getempert. Diese Temperzeit war entsprechend den gemessenen Diffusionskonstanten mehr als ausreichend, um das gelöste Helium in den Kristalliten homogen zu verteilen. In den durch die Nachweisempfindlichkeit der Apparatur gegebenen Grenzen liessen sich im Temperaturbereich zwischen 500 und 650°C Diffusionskonstanten bestimmen. Die gefundenen

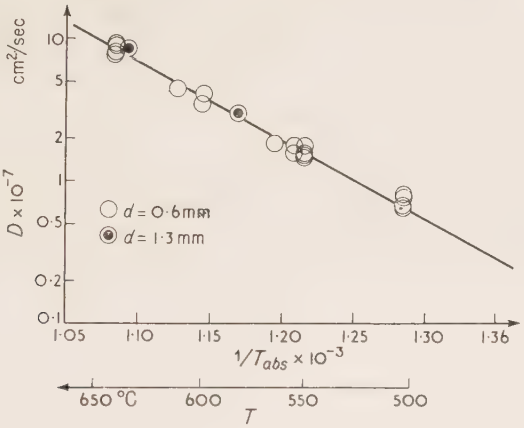

Abb. 2. Graphische Darstellung der für NaCl in Abhängigkeit von der reziproken Temperatur $1/T_{abs}$ gemessenen Diffusionskonstanten.

Werte sind in Abb. 2 in Abhängigkeit von $1/T_{abs}$ eingetragen. Da sich für verschiedene Kristallgrössen, bezogen auf gleiche Temperatur, gleiche Diffusionskonstanten ergaben, muss es sich um Volumdiffusion handeln.

Untersuchungen an Sylvinen:

Anschliessend wurden Untersuchungen an zwei Gruppen von Sylvinen vorgenommen, nämlich einerseits an einem in Übereinstimmung mit STURMFELS (1943) als E_0 bezeichneten Sylvin der Kaligewerkschaft Buggingen/Baden (45% KCl, 55% NaCl) und andererseits an einem im Folgenden als H 12 bezeichneten Sylvin der Grube Hattorf-Philipstal (Werra) der Wintershall A.G. (40% KCl, 60% NaCl).

Bei den Untersuchungen an E_0 wurden ausser einer Volumdiffusion im Bereich zwischen 500 und 600°C noch zwei weitere Vorgänge der Gasabgabe beobachtet. Zunächst wurden bereits im Temperaturbereich zwischen 220 und 250°C etwa 10 Prozent der gesamten Heliummenge abgegeben. Der gleichmässige exponentielle Abfall der Heliumabgabe lässt den Schluss zu, dass es sich hier ebenfalls um einen Diffusionsvorgang handelt. Es gelang jedoch nicht, den Vorgang quantitativ nach den Gesetzen der Volumdiffusion zu behandeln. Ein weiterer Vorgang der Gasabgabe trat im Bereich zwischen 420 und 450°C auf. Da die Gasabgabe hier

kurzzeitig ausserordentlich starke, unregelmässig verteilte Schwankungen aufweist, handelt es sich hierbei offensichtlich um Aufplatzvorgänge innerer Gaseinschlüsse (Abb. 3). Derartige Aufplatzvorgänge sind auch von anderen Mineralien (Dekrepetieren) her bekannt. Sie werden immer dann auftreten, wenn der Druck

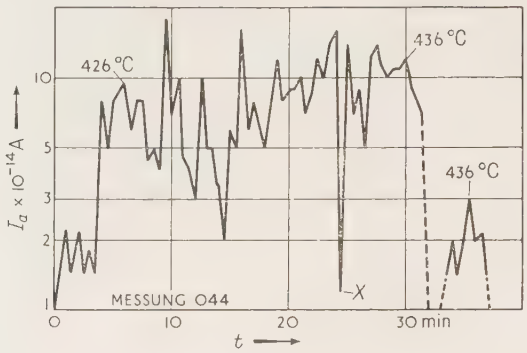

Abb. 3. Aufplatzvorgänge bei dem Bugginger Sylvin E_0 (I_α = Höhe der Heliumlinie).

in den Gaseinschlüssen durch Temperaturerhöhungen derart ansteigt, dass dadurch das Kristallgefüge gesprengt wird. Bei den für die Altersbestimmung zu berücksichtigenden Gasverlusten ist dieser Vorgang ohne Einfluss, da er erst bei Temperaturen einsetzt, denen die Salze seit ihrer Entstehung niemals ausgesetzt

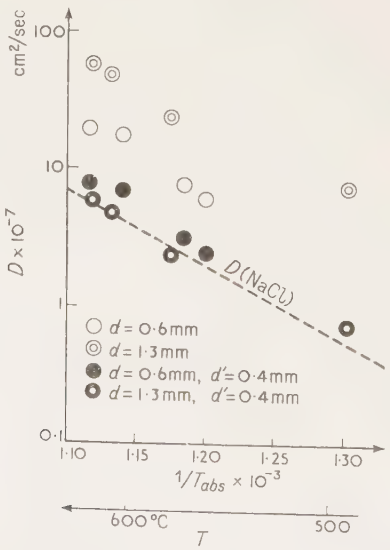

Abb. 4. Graphische Darstellung der für den Bugginger Sylvin E_0 gemessenen Diffusionskonstanten (d = vor der Messung bestimmter Kristalldurchmesser, d' = reduzierter Kristalldurchmesser).

waren. Er liefert jedoch eine Erklärung für die starke Streuung der für die Volumdiffusion an E_0 gemessenen Werte (Abb. 4). Durch die Aufplatzvorgänge wird nämlich die vor der Messung bestimmte Kristalldicke d in nicht messbarer Weise verringert. (Die Kristalle backen beim Erhitzen derart zusammen, dass sie nur

durch Lösung in Wasser aus dem Ofeneinsatz entfernt werden können). Macht man jedoch zunächst rein willkürlich die Annahme, dass die Kristalle völlig unabhängig von der ursprünglich gemessenen Kristallgrösse d nach Beendigung der Aufplatzvorgänge nur noch eine mittlere Kristallgrösse $d' = 0{\cdot}4$ mm aufweisen, dann passen sich die unter diesen Voraussetzungen für E_0 ermittelten Werte der Diffusionskonstanten sehr gut dem für reines NaCl ermittelten Verlauf an. Es erscheint also berechtigt, die an reinem NaCl ermittelten Werte auch für ein in beliebiger Weise aus NaCl und KCl gemischtes Salz als zumindest grössenordnungsmässig richtig anzusehen, wenn, wie es offenbar bei E_0 der Fall ist, der die Gasabgabe beherrschende Vorgang als Volumdiffusion anzusehen ist. Damit erscheint es zulässig, die an reinem NaCl ermittelten Werte in den Temperaturbereich zwischen 40 und 80°C zu extrapolieren und so mit den Werten zu vergleichen, die aus Beobachtungen bei der Altersbestimmung an Sylvinen gewonnen werden konnten. Die Werte seien hier gegenübergestellt:

Durch Extrapolation gewonnene Werte:	*Aus Beobachtungen bei der Altersbestimmung errechnete Werte* (Gentner *et al.* 1953a, 1954)
$D_{He(80°C)}$: $4{\cdot}0 \times 10^{-17}$ cm²/sec	$1{\cdot}2 \times 10^{-17}$ cm²/sec
$D_{He(40°C)}$: $3{\cdot}2 \times 10^{-19}$ cm²/sec	$1{\cdot}2 \times 10^{-19}$ cm²/sec

In Anbetracht der Tatsache, dass hier die Extrapolation der Diffusionskonstanten über zehn Grössenordnungen durchgeführt werden musste, ist die Übereinstimmung der auf völlig verschiedenen Wegen erzielten Resultate als überraschend gut zu bezeichnen. Es muss allerdings bemerkt werden, dass man bei einer derartigen Extrapolation bei der derzeitigen Messgenauigkeit der Apparatur dem extrapolierten Wert eine mögliche Fehlerbreite von ± 2 Zehnerpotenzen zuerkennen muss.

Bei den Untersuchungen an dem mitteldeutschen Sylvin H 12 konnte, von zwei nicht genau einzuordnenden Ausnahmen abgesehen, im Verlauf von 14 Messungen eine Heliumabgabe nur im Temperaturbereich zwischen 220 und 250°C beobachtet werden. Es gelang hier ebensowenig wie bei den in diesem Temperaturbereich an E_0 vorgenommenen Messungen quantitative Zusammenhänge zwischen Kristallgrösse, Temperatur und Diffusionskonstante zu finden. Offenbar ist bei diesem Diffusionsvorgang noch ein weiterer Parameter vorhanden, der von Probe zu Probe erhebliche Schwankungen aufweist. Es fällt bei der mikroskopischen Betrachtung von Kristallen des Sylvins H 12 auf, dass diese in grösserem Masse Strukturstörungen zeigen. Jedoch ist der Unterschied gegenüber der mikroskopischen Betrachtung von Kristallen des Salzes E_0 nicht so evident, dass man hierdurch in befriedigender Weise erklären könnte, warum bei E_0 nur 10 Prozent der gesamten Heliummenge bei dem hier besprochenen Vorgang verloren geht, während bei H 12 in diesem Bereich die gesamte Gasmenge frei wird. Man wird also annehmen müssen, dass bei H 12 auch in submikroskopischen Bereichen noch Aufbaustörungen vorliegen, die für die hier geschilderte offensichtlich strukturabhängige Diffusionskomponente verantwortlich zu machen sind. Es wird noch umfangreicher Untersuchungen an Salzen der verschiedensten

Herkunft und geologischen Geschichte bedürfen, um hier eine Klärung zu erzielen. Es lässt sich jedoch bereits jetzt sagen, dass es offensichtlich nicht zulässig ist, grundsätzlich bei der Altersbestimmung nur Gasverluste durch Volumdiffusion anzunehmen. Es wird daher im Zweifelsfalle zweckmässig sein zu überprüfen, ob die Diffusionseigenschaften der betreffenden Salzprobe es tatsächlich gestatten, die gemessenen Alterswerte unter dem Gesichtspunkte von durch Volumdiffusion eingetretenen Gasverlusten zu korrigieren.

Ausser Messungen an reinem KCl sollen ähnliche Untersuchungen auch mit Argon durchgeführt werden. Hier sind noch gewisse messtechnische Schwierigkeiten zu überwinden, da der massenspektrometrische Nachweis von kleinen Argonmengen durch die in diesem Massenbereich in besonderem Masse hervortretenden Kohlenwasserstofflinien gestört ist.

Diskussion der Ergebnisse:

Die hier mitgeteilten Ergebnisse stehen in einem gewissen Widerspruch zu Angaben, die von Thomson und Wardle (1954) für die Diffusionskonstante von Helium in NaCl gemacht wurden. Die Messung wurde von den Autoren so durchgeführt, dass eine Probe von violettem Steinsalz zunächst ganz fein pulverisiert wurde. Anschliessend wurde bei einer Temperatur von 25°C die zeitliche Abnahme des Heliumgehaltes dadurch bestimmt, dass jeweils im Abstand von einigen Tagen ein Teil der Probe auf seinen Heliumgehalt analysiert wurde. Aus dem zeitlichen Abfall des Heliumgehaltes und der hier ausserordentlich kleinen Dicke der Kristallite haben die Autoren dann die Diffusionskonstante für Helium in NaCl zu $D_{\mathrm{He}(25^\circ\mathrm{C})} = 3{\cdot}0 \times 10^{-15}$ cm²/sec bestimmt. Anschliessend haben sie diesen Wert auf die gesamte einige Meter betragende Dicke des Salzlagers extrapoliert. Sie konnten auf diese Weise die eingetretenen Gasverluste in befriedigendem Masse erklären. Es erscheint jedoch von vornherein fraglich, ob es zulässig ist, einen derartigen an Einkristallen gemessenen Wert auf das aus einer grossen Vielzahl von Kristallen zusammengesetzte Salzlager zu extrapolieren. Wir haben das schon früher (Gentner *et al.*, 1953a,b; 1954) für unzulässig gehalten und waren der Ansicht, dass ein Gasatom, das einen Kristall einmal verlassen hat, in einer im Vergleich zu dem geologischen Zeitraum sehr kurzen Zeitspanne aus dem gesamten polykristallinen Salzblock entweicht. Da wir unter dieser Annahme bereits seinerzeit befriedigende Korrekturen der Altersbestimmungen durchführen konnten und die dabei benutzten Werte für die Diffusionskonstanten von Helium in Sylvinen und Steinsalzen nun durch das Experiment als grössenordnungsmässig richtig bestätigt werden konnten, scheint tatsächlich die von Thomson und Wardle vorgenommene Extrapolation nicht zulässig zu sein.

Extrapoliert man nun im Gegensatz zu den Autoren ihren gemessenen Wert nur auf die im Mittel in einer Salzprobe herrschende Kristalldicke von z.B. $d = 10$ mm, dann ergibt sich für die Gasabgabe eine Halbwertszeit von rund 3×10^5 Jahren. Unter diesen Umständen wäre es völlig ausgeschlossen, Altersbestimmungen über einen längeren Zeitraum als etwa 10^6 Jahre durchzuführen, weil praktisch jedes vor diesem Zeitraum gebildete Gasatom den Kristall durch Diffusion verlassen haben müsste. Tatsächlich sind aber Altersbestimmungen an Steinsalzen und Sylvinen schon bis zu einer Grenze von etwa 250×10^6 Jahren durchgeführt

worden. Für noch grössere Zeiträume wird die Altersbestimmung auch unter Berücksichtigung der von uns gefundenen Werte für die Diffusionskonstanten problematisch (Oser, 1954) . Es scheint also, als ob der von Thomson und Wardle gefundene Wert, der etwa vier Grössenordnungen über den Werten liegt, die wir auf zwei unabhängigen Wegen finden konnten, nicht sehr plausibel ist.

Es entsteht daher die Frage, ob bei so weitgehender Pulverisierung, wie sie von Thomson und Wardle vorgenommen werden musste, überhaupt noch zuverlässige Angaben über den Diffusionsvorgang gemacht werden können. Die Störstellenverteilung in einem Kristall muss durchaus nicht homogen sein; es ist im Gegenteil anzunehmen, dass in kleinen Bereichen eine gewisse Störstellenschichtung vorliegt. Zerschlägt man nun einen Kristall, dann wird er vorzugsweise an seinen mechanisch schlechtesten Stellen aufplatzen, und das wird an solchen Störstellenschichten der Fall sein. Andererseits wird sich auch das gelöste Gas vorzugsweise in den Störstellen aufhalten. Nun umfasst die von den Autoren beobachtete Gasabnahme nur etwa 10 Prozent der in der betreffenden Salzprobe enthaltenen Heliummenge. Es ist daher durchaus denkbar, dass diese Gasabnahme nur durch das Abdiffundieren von Helium aus Störstellen bedingt ist, die nach der Pulverisierung an der Kristalloberfläche liegen. Unter diesen Umständen können natürlich keine Angaben über die Diffusionskonstante in grösseren Kristallen, bei denen dieser Diffusionsvorgang zu vernachlässigen ist, gemacht werden.

Herr H. Fechtig hat im Rahmen seiner Diplomarbeit einen Teil der Messungen selbstständig durchgeführt, wofür wir ihm auch an dieser Stelle danken. Ferner danken wir der Deutschen Forschungsgemeinschaft für die Gewährung von Sachbeihilfen sowie den Herren Dr. Simon (Kaligewerkschaft Buggingen/Baden) und Dr. Kühn (Kaliforschungsstelle Hannover), die uns die benötigten Salzproben zur Verfügung stellten.

Literatur

Gentner, W., Präg, R., und Göbel, K.	1954	Geochim. et Cosmochim. Acta **5,** 124
Gentner, W., Präg, R., und Smits, F.	1953a	Geochim. et Cosmochim. Acta **4,** 11
Gentner, W., Präg, R., und Smits, F.	1953b	Z.f. Naturforsch. **8a,** 216
Gentner, W., und Trendelenburg, E. A.	1954	Z.f. Naturforsch. **9a,** Heft 9
Oser, H.	1954	Diplomarbeit Freiburg
Sturmfels, E.	1943	Neues Jahrb. d. Min. A **78,** 131
Thomson, S. J., und Wardle, O.	1954	Geochim. et Cosmochim. Acta **5,** 169

Geochimica et Cosmochimica Acta, 1954, Vol. 6, pp. 268 to 281. Pergamon Press Ltd., London

The geochemistry and mineralogy of rock weathering.
(2) The Nordmarka area, Oslo

J. R. Butler*
Rothamsted Experimental Station, Harpenden, Herts

(*Received* 16 *August* 1954)

Introduction

To the petrologist the Permian igneous rocks of Oslo offer great variety and interest, and the researches of Brøgger have made the area a classic one. He recognized and described three rock series formed as the result of magmatic differentiation which occur in Nordmarka, a wooded area stretching to 40 km north of Oslo: the kjelsåsite-larvikite series, outcropping principally to the NNW of Oslo; the pulaskite-nordmarkite series, occupying a substantial area N of Oslo; and the ekerite series, which intrude into the latter; Palaeozoic and Pre-Cambrian sediments appear only near the eastern limits of Nordmarka. Unfortunately the effects of Quaternary glaciation have left but few localities where appreciable *in situ* weathering of these rocks occurs, and to the pedologist the area is not immediately rewarding. However, through the kindness of Professor Lâg, three suitable sites in Nordmarka were eventually found and the outcropping rocks together with the weathered material immediately overlying them were studied. The parent materials were (1) quartz-free alkali syenite, (2) hypersthene-monzonite, and (3) altered olivine-basalt. In addition, the weathering products of a Pre-Cambrian schist outcropping at Bleikan 60 km N of Oslo were also examined. The data in this article are frequently compared with those presented by the author (1953) in volume 4 of this journal.

Experimental Methods

The clay minerals were estimated by the methods previously described, but the samples (including the silts) were separated after using very dilute acqueous sodium hexametaphosphate (instead of NH_4OH) as dispersing agent. The elements Al, Ca, Fe, Mg, Mn, and Ti were determined spectrographically using a Zeiss Q24 spectrograph, and the method described by Kvalheim (1947) was followed, giving standard deviations of ±10 per cent. Dr. Kvalheim kindly allowed the author to use the working curves he had constructed for the above spectrograph. K and Na were estimated in solution by the Lundegårdh technique; standard deviations ±6 per cent for Na and ±5 per cent for K. The elements Ag, Ba, Be, Co, Cr, Cs, Cu, Ga, La, Li, Mn, Mo, Ni, Pb, Rb, Sn, Sr, Yt, V, and Zr were estimated by the method described before with, however, the following excitation conditions: Electrodes 3 mm diameter with cavity 4 mm deep by 1·5 mm diameter were used as cathodes, holding approximately 10 mg carbon: specimen (1 : 1) mixture: the material was burnt to completion at 7·5 amps with an arc-gap of 10 mm and the cathode layer 2 mm above the cathode was recorded. Be, Mo, and Sn were not found in any of the samples; the limits of detection were between 10 and 15 p.p.m. for these elements, and for the others as shown in Tables 9, 10, and 12. Fluorine was determined spectrographically as before.

Quartz-free Alkali Syenite

1. *Description of the rock*

East of the southern portion of Lake Katnosa an outcrop of medium- to coarse-grained rock occurs which consists principally of orthoclase (50–60 per

* Now at Department of Geology, Imperial College, London, S.W.7.

cent), albite (25–35 per cent), biotite (5–10 per cent), and hornblende (approximately 5 per cent). Neither quartz nor members of the nepheline group were identified, and the rock may thus be called a quartz-free alkali syenite. The orthoclase occurs in crystals up to 8 mm long, and in thin section usually shows a mottled brown cloudiness; very fine sericite is a probable alteration product, and albite has been exsolved along the (001) cleavage cracks. The remainder of the albite occurs as small discrete crystals which, in contrast to the orthoclase, are clear and fresh; occasionally albite borders orthoclase and may to some extent have replaced it. Biotite, occurring in plates up to 5 mm in diameter, gives the pleochroism $X = Y =$ black, $Z =$ light yellow-brown; inclusions of apatite and zircon are seen, but pleochroic haloes are absent, so are chloritic alteration products. Hornblende, occurring as elongated crystals up to 2 mm in length, gives the pleochroism $X =$ yellow-green, $Y =$ light olive-green, $Z =$ grass-green, and thus an alkali-rich amphibole is excluded.

The accessory minerals include, in order of decreasing abundance, sphene, ilmenite, magnetite, apatite, and zircon; chlorite is absent.

2. *Geochemistry of the rock*

The spectrochemical data for the rock (Table 8) can be compared with the chemical data by Brøgger (1933) for the pulaskite-nordmarkite series. The SiO_2 value (by difference) and the Fe/Mg (at.) ratio of the syenite lie between the values quoted for the end members pulaskite ($SiO_2 = 60$ per cent, Fe/Mg

Table 8

	18(*R*)	18(*H*)	18(*S*)	18(*C*)	19(*R*)	19(*S*)	19(*C*)	
SiO_2	(64)	—	(50–52)	(31)	(51–52)	(32–37)	(27–31)	SiO_2
Al_2O_3	20·0	3·0	15·0	16·0	15·0	13·0	13·0	Al_2O_3
TiO_2	0·40	>3·0	>3·0	2·9	2·7	2·0	1·5	TiO_2
Fe	1·7	18·0	13·0	18·0	7·0	17·0	24·0	Fe
MgO	0·50	12·0	3·4	4·1	3·2	13·0	9·5	MgO
MnO	0·10	0·96	0·84	0·90	0·16	0·19	0·43	MnO
Na_2O	6·8	—	3·3	1·5	4·0	0·72	<0·10	Na_2O
CaO	0·40	12·0	1·3	3·0	8·0	4·2	1·3	CaO
K_2O	5·7	—	3·7	2·4	2·7	1·0	0·90	K_2O
H_2O	0·21	—	0·64	6·2	0·20	3·65	6·23	H_2O
Ignition loss	0·67	—	4·6	11·85	0·70	9·40	11·62	Ignition loss
F	<0·03	1·0	—	0·20	<0·03	0·50	0·15	F

18(*R*) Quartz-free syenite, L. Katnosa, Nordmarka, Oslo.
18(*H*) Hornblende from quartz-free syenite, L. Katnosa.
18(*S*) Silt from disintegrated L. Katnosa syenite.
18(*C*) Ca-saturated clay from disintegrated L. Katnosa syenite.
19(*R*) Hypersthene-monzonite, SE of Heggelivatn, Nordmarka, Oslo.
19(*S*) Silt from disintegrated Heggelivatn hypersthene-monzonite.
19(*C*) Ca-saturated clay from disintegrated Heggelivatn hypersthene-monzonite.

Note: Except for H_2O- and Ignition loss values, the data in the Table are from spectrochemical results, SiO_2 being estimated by difference.

(at.) = 5·7), and nordmarkite (SiO_2 = 64 per cent; Fe/Mg (at.) = 6·5), and the percentages of the alkalies are close to those for pulaskite, with Na/K almost identical. Ca is anomalously low, however, and the ratio Na/Ca (at.) of 15 is more characteristic of the later igneous rocks nordmarkite and nordmarkite-ekerite. The minor elements Ba and Sr (Table 9) are approximately equal in concentration

Table 9

	A	*S*	18(*R*)	18(*H*)	18(*B*)	18(*WB*)	18(*S*)	18(*C*)	
Ga^{+3}	0·62	5	50	15	20	—	30	30	Ga
Cr^{+3}	0·63	1	1	30	8	—	*	*	Cr
Li^{+1}	0·68	1	55	20	480	240	380	210	Li
Ni^{+2}	0·69	1	*	5	*	—	1	2	Ni
Co^{+2}	0·72	5	*	*	*	—	*	*	Co
V^{+3}	0·74	10	*	*	*	—	*	*	V
Zr^{+4}	0·79	10	190	300	*	—	150	120	Zr
Mn^{+2}	0·80	10	780	5200	7400	—	6400	7000	Mn
Yt^{+2}	0·92	15	20	*	*	—	50	50	Yt
La^{+3}	1·14	100	*	*	*	—	125	125	La
Sr^{+2}	1·12	10	>1000	10	*	*	20	65	Sr
Pb^{+2}	1·20	15	*	*	85	—	*	20	Pb
Ba^{+2}	1·34	10	>1000	400	*	*	300	870	Ba
Rb^{+1}	1·47	50	690	*	2500	2200	1600	1150	Rb
Cs^{+1}	1·67	300	*	*	*	*	*	*	Cs
F^{-1}	1·33	300	*	1%	5000	5000	—	2000	F

A Ionic radius Å. After Ahrens, 1952.
S Sensitivity in p.p.m.
18(*R*) Quartz-free syenite, L. Katnosa, Nordmarka, Oslo (Ba and Sr approx. equal).
18(*H*) Hornblende from quartz-free syenite, L. Katnosa.
18(*B*) Biotite from quartz-free syenite, L. Katnosa. K_2O = 8·9 per cent.
18(*WB*) Weathered biotite from quartz-free syenite, L. Katnosa. K_2O = 4·8 per cent.
18(*S*) Silt from disintegrated L. Katnosa syenite; oven-dried basis.
18(*C*) Ca-saturated clay from disintegrated L. Katnosa syenite; oven-dried basis.
An asterisk (*) indicates below sensitivity, and a dash (–) absence of data.

and slightly exceed 1000 p.p.m. In contrast, the many values by Brøgger for the Permian igneous rocks show Ba/Sr (at.) usually above 5, and the concentration of Sr is frequently below 85 p.p.m.; it seems probable that the old chemical determinations have led to low values for Sr (*vide* Tables 10 and 12). The figure for Zr (180 p.p.m.), however, is not at variance with the older data (Brøgger, 1933; anal. Klüver). The concentration of Rb (690 p.p.m.) leads to a normal ratio of K/Rb for non-basic rocks, and the absence of Co and V can be correlated with the paucity of Fe.

3. *Geochemistry of the hornblende and biotite*

(a) *Hornblende.* The spectrochemical analysis (Table 8) shows Fe at 18 per cent, a figure between that expected for common hornblende from many plutonic rocks and that shown for, say, barkevikite, an alkali amphibole relatively poor in iron. CaO and MgO have usual values for common hornblende, and the ratio Fe/Mg

is indicative of a genesis from a non-basic magma. Al_2O_3 is unusually low. The value for F of 1 per cent is not an extreme one, and it is of interest to note that the associated biotite carries but half as much of that element.

Data for the minor elements (Table 9) show that the larger-sized ions are not abundant; Ba at 400 p.p.m. exceeds Sr by a factor of 40, and considering that Ca is the dominant ion in the *X* group, this is unusual. Further, the lack of Ba in the associated biotite is surprising. The remaining detectable minor elements substitute in the *Y* group, Cr and Ni being concentrated strongly from the magma. Ga at 15 p.p.m. is quite high, and the low Al value gives the small Al/Ga (at.) ratio of $2{\cdot}7 \times 10^3$. Nockolds and Mitchell (1948) report similar values for igneous hornblende however, and that from a granodioite gave the figure $3{\cdot}2 \times 10^3$.

(b) *Biotite.* An analysis of the hand-picked biotite for K_2O gave a value of 8·9 per cent (compatible with the fresh nature of the biotite), and this leads to a low spectrochemical summation for (Al, Fe, Mg, Mn, Ti) oxides (cf. Kvalheim, 1947, p. 591). The ratio Fe/Mg (at.) was, however, reliably estimated at 3·5, a figure contrasting with that found for biotites from hornblende-bearing *calc*-alkali rocks (Nockolds, 1947). Minor elements are not well represented in the biotite (Table 9), with the exception of Rb (and F). The ratio K/Rb (at.) of 65 is intermediate between those for the biotites from the adamellite and granodiorite-gneiss in Cornwall. Appreciable Rb (85 p.p.m.) is camouflaged in the intersheet (K^+) positions, and Li, not accepted by feldspars, is well concentrated at 480 p.p.m. in the octahedral positions; the competition for Cr by the hornblende is strong, and the biotite only holds 8 p.p.m.

4. *Weathering of the biotite*

The biotite weathers structurally and to some extent chemically in a manner analogous to the biotite from the adamellite in Cornwall. Chemically there is a pronounced drop in K_2O from 8·9 to 4·8 in weathered flakes, and structurally there is an expansion of the lattice in the *c* direction to a maximum of 14 kX. X-ray photographs of light-brown flakes, e.g., 1 mm in diameter, show a diffuse band between 10 kX and 14 kX with or without an intensity peak intermediately: e.g., at 11·8 kX. The collapse to 10 kX and the disappearance of the 14-kX line on heating at 550° for several hours excludes the presence of chlorite and confirms that of vermiculite. An associated weathering product of the Katnosa biotite, not recorded for the Cornish (or other) biotites, is lepidocrocite; the γ-iron hydroxide orientates itself with its (010) cleavage plane parallel to the (001) of the mica. A unit cell of lepidocrocite ($a_0 = 3{\cdot}87$, $b_0 = 12{\cdot}51$, $c_0 = 3{\cdot}06$ kX) in this orientation produces the maximum physical disruption between adjacent mica-cleavage planes. It is not clear what conditions govern the formation of lepidocrocite as opposed to (say) goethite (Marel, 1951), although it has been recorded in clays from soils under impeded drainage conditions (Brown, 1953). The Katnosa profile is, however, frozen during the winter and freely drained during the summer months.

5. *Mineralogy of the clay*

X-ray examination of the clay showed that illite, mica intermediate, and vermiculite constitute 95 per cent of the crystalline material (from which "free"

iron oxides had been removed; see Fig. 3). Kaolin is absent (i.e., below 5 per cent), indicating that albite and orthoclase are here more resistant to weathering than biotite. In clay-flake photographs a diffuse band extends from 10 kX to 14 kX with peaks at the extremes. The 14-kX reflection is due entirely to vermiculite, but that at 10 kX indicates either tri- or dioctahedral illite or both, i.e., biotite and sericite respectively. K_2O in the clay (Table 8), although substantial, limits the dioctahedral illite content to 40 per cent if that mineral is assumed to contain 6 per cent K_2O, and the MgO value (4·1 per cent) suggests that the trioctahedral mica is the more abundant (hornblende occurs only as an accessory). The F content (0·2 per cent) suggests not only that there is much trioctahedral mica in the clay but that, in contrast to the Cornish biotites, biotite here retains a substantial part of its fluorine content on weathering. Chemical weathering is thus less severe in the Katnosa profile, due, in part, to the different climatic conditions.

6. *Chemical changes on weathering*

Considering the change rock → silt → clay → and recalculating the analyses in Table 8 on an Al-constant basis, it can be shown that the anticipated decreases of Si and Na and the increase of Fe all occur. The preferential weathering of biotite causes Mg and Ti to increase (according with data for the adamellite). The values for K decrease but slightly and less markedly than for the adamellite changes, and, bearing in mind that the K content of both rocks is similar, this indicates again that chemical weathering is more pronounced in Cornwall. Ca is high in the silt due to appreciable hornblende, and its higher value in the clay is due to Ca-saturation and, possibly, presence of Ca phosphate formed during the flocculation of the clay.

The minor elements Li, Pb, Rb, and F behave as expected; these elements are conspicuously present in the fresh biotite and accompany its weathering product. Thus K/Rb (at.) for rock, fresh biotite, silt, and clay are 150, 65, 42, and 38 respectively. Cr is lost on weathering, Sr decreases sharply, and Ba less so, reflecting the paucity of feldspar in the clay.

Hypersthene-Monzonite

1. *Description of the rock*

1½ km SE of Lake Heggelivatn, in an area consisting predominantly of the kjelsåsite-larvikite series, an outcrop of a pyroxene-feldspar rock with nests of biotite occurs. The hand specimen suggests a basic or contaminated rock, but thin-section analyses show the approximate mode to be 50 per cent plagioclase (average An_{40}), 15 per cent orthoclase, 15 per cent rhombic pyroxene, 10 per cent monoclinic pyroxene, and 5 per cent biotite, with green amphibole, apatite, and iron ore as accessories. The rock may thus be called a hypersthene-monzonite. Plagioclase occurs as crystals up to 10 mm and shows both albite and pericline twinning. Zoning is uncommon, and sericitization, in contrast to that in the orthoclase, is not marked. The idiomorphic rhombic pyroxene shows slight pleochroism ($X = Y =$ very pale pink and $Z =$ green) and the high negative 2V

implies a variety of hypersthene. Occasionally the (001) partings contain a dark green-brown mineral of chloritic or vermiculitic appearance. Monoclinic pyroxene is colourless and diopsidic, and although crystals contain appreciable finely divided iron ore they are unaltered along cleavage cracks. Crystals frequently show a rim of light green amphibole whether adjacent to hypersthene or feldspar. Biotite, present as small clusters of crystals, shows the marked pleochroism $X = Y =$ black to very dark brown, $Z =$ very pale yellow-brown.

2. *Geochemistry of the rock*

By chance the major element composition of the monzonite (Table 8) is remarkably similar to that of the average essexite (=alkali gabbro) quoted by Brøgger (1933). Mineralogically, of course, the two rocks are very different and the minor element concentrations (Table 10) emphasize that the monzonite is

Table 10

	S	19(*R*)	19(*P*)	19(*B*)	19(L)	19(*S*)	19(*C*)	
Ga	5	15	5	15	*	25	10	Ga
Cr	1	2	*	*	10	*	10	Cr
Li	1	30	15	35	7	75	15	Li
Ni	1	10	20	2	45	3	1	Ni
Co	5	30	40	15	50	7	12	Co
V	10	55	110	105	95	*	20	V
Zr	10	400	250	20	High	125	55	Zr
Mn	10	1200	1200	900	High	1400	3300	Mn
Sr	10	1000	130	65	*	65	65	Sr
Pb	15	*	*	*	*	*	*	Pb
Ba	10	1000	*	1500	*	45	15	Ba
Rb	50	1000	*	4000	*	250	*	Rb
Cs	300	*	*	400	*	*	*	Cs
F	300	—	—	—	—	5000	1500	F

S Sensitivity p.p.m.
19(*R*) Hypersthene-monzonite, SE of Hegglevatn, Nordmarka, Oslo.
19(*P*) Monoclinic pyroxene from hypersthene-monzonite, SE Hegglevatn.
19(*B*) Biotite from hypersthene-monzonite, SE Hegglevatn (K_2O = 7·55 per cent; Na_2O = tr.)
19(*L*) Heavy minerals (s.g. > 3·3) from hypersthene-monzonite, SE Hegglevatn.
19(*S*) Silt from disintegrated Hegglevatn hypersthene-monzonite; oven-dried basis.
19(*C*) Ca-saturated clay from disintegrated Hegglevatn hypersthene-monzonite; oven-dried basis.

not a near derivative of a basic magma. Thus Cr (2 p.p.m.), V (55 p.p.m.), Ni (10 p.p.m.), and Co (30 p.p.m.) are all fairly low in comparison with Cr-200 p.p.m. and V-410 p.p.m. for Brøgger's essexites, and Ni-70–160 p.p.m. and Co-20–80 p.p.m. for gabbros generally. Further the Sr, Ba, and Rb values (all 1000 p.p.m.) are more akin to values for non-basic rocks.

3. *Geochemistry of the minerals*

(a) *Monoclinic pyroxene.* The separated mineral contained occluded iron ore, and the (uncorrected) values for trace-element content are shown in Table 10. The concentrations of Sr (130 p.p.m.) and Ba (below 10 p.p.m.) are similar to

those found by Wager and Mitchell (1951) for clino-pyroxene from the olivine gabbro of Skaergaard but distinct from those quoted by Nockolds and Mitchell (1948) for Caledonian augites. The values for V, Li, Co, and Ni are not unusual ones, although the ratio Ni/Co (at.) is low (0·5). Absence of Cr is significant, and recalls the low values for clino-pyroxene in later differentiates of the Skaergaard mass, e.g., in hortonolite ferro-gabbro.

(b) *Biotite.* The hand-picked mica was analyzed for alkalies and trace elements, with the results shown in Table 10. It is seen that the somewhat low K (in the X group) is augmented by Rb, Ba, Cs, and Sr in order of decreasing atomic concentration, and the ratio K/Rb is accordingly low. In comparison with the biotite from the quartz-free syenite (competing against hornblende), this biotite (competing against pyroxenes) captures Ba more effectively than the associated ferromagnesian minerals can camouflage it; it is probable, however, that the biotite from the monzonite crystallized some time after the pyroxenes and partly contemporaneously with the feldspars.

4. *Weathering of the biotite*

Both chemically and structurally the biotite weathers similarly to that from the quartz-free alkali syenite: thus lepidocrocite is associated with the altered mica and orientates itself as before with its cleavage-plane parallel to the (001) of the mica.

5. *Mineralogy of the clay*

X-ray diffraction data show the clay to be multimineralic, but with illite dominant (approximately 45 per cent, Fig. 3); kaolin and talc are estimated to be equally abundant (about 15 per cent). Dry or glycerol-treated clay-flakes show a diffuse X-ray diffraction band between 10 kX and 14-kX spacings, with customary peaks at the extremes but none intermediately. On heating at 550°C for several hours and re-photographing, a line appears at 12·0 kX, both the 10 kX and 14-kX lines remain, whilst the diffuseness intermediately is conspicuously lessened. Chlorite is thus confirmed (estimated at about 5 to 7 per cent) and the 12-kX spacing characterizes a mineral having alternate layers of chlorite and vermiculite (Walker, 1952). The diffuseness existing between the 10 kX and 14-kX spacings for the unheated flake may thus be due to mixed layer chlorite-illite or vermiculite-illite material. The rhombic pyroxene in thin section was seen to contain a dark green-brown mineral along its (001) partings, and it is possible that the weathering change hypersthene→ mixed-layer chlorite-vermiculite mineral occurs. Any excess of Mg released could contribute to the formation of talc, a mineral absent from the fresh monzonite. The spectrochemical composition of the clay (Table 8) shows the anticipated high Mg and Fe but rather low K_2O (0·90 per cent) indicating that the estimate of 45 per cent for illites may be excessive (dioctahedral and trioctahedral illite were not distinguished).

6. *Chemical changes on weathering*

Major elements showing a decrease relative to Al in the change rock → clay through silt are Na, Ca, K, Ti, and Si, in order of diminishing magnitude; Fe,

Mn, and Mg show an increase. In Cornwall the serpentine and hornblende-schist lost considerable amounts of Mg on weathering, and climatic differences may account for its retention here. The same two Cornish rocks also lost more Mg relative to Ni, but for the monzonite weathering to clay Mg/Ni increases. However, the fall of Sr to its value in the clay follows the general trend, and there is a similar fall for Ba.

Altered Olivine-Basalt

1. *Description of the rock*

The rock outcrops about 15 km N of Oslo on the eastern banks of Lake Movatn. In hand-specimen it shows numerous iron-stained spots set in a fine-grained greenish ground mass. Thin sections show the rock to be considerably altered; fresh olivine is absent but thought to be represented (5–10 per cent) by chlorite pseudomorphs partially enclosed in iron ore with some ore in the original positions of parting. Feldspar (up to 10 per cent) occurs in the ground mass of chlorite, but lath-shaped phenocrysts (30–40 per cent) of chlorite and calcite are presumed to be after feldspar. The mode is approximately 70 per cent chlorite, 10 per cent feldspar, 10–15 per cent calcite, and 5–7 per cent iron ore; accessory sphene occurs and talc (but not chrysotile) was confirmed by X-ray diffraction analysis.

2. *Geochemistry of the rock*

The composition of the altered basalt (Table 11) is fairly comparable with that of a normal olivine-basalt, and only the relatively high Na_2O suggests affinities to, say, Brøgger's essexite. The basic nature of the rock is reflected in the values

Table 11

	20(*R*)	20(*S*)	20(*C*)	21(*R*)	21(*S*)	21(*C*)	
SiO_2	—	(34–35)	(39–40)	—	(45–47)	(44–45)	SiO_2
Al_2O_3	12·0	17·0	12·0	7·6	26·0	25·0	Al_2O_3
TiO_2	3·4	1·4	0·85	1·3	1·2	0·80	TiO_2
Fe	12·0	11·0	7·0	4·9	7·6	7·7	Fe
MgO	9·0	22·0	17·0	4·5	1·4	1·3	MgO
MnO	0·20	0·25	0·50	0·31	0·76	0·13	MnO
Na_2O	3·2	0·79	<0·10	<0·20	<0·20	<0·20	Na_2O
CaO	11·0	1·5	1·4	>20·0	1·3	0·36	CaO
K_2O	1·1	0·73	0·85	2·1	6·4	5·5	K_2O
H_2O-	0·27	1·73	6·50	3·1	1·40	2·90	H_2O-
Ignition loss	—	8·81	16·40	—	6·35	10·50	Ignition loss
F	—	—	—	<0·03	0·15	<0·03	F

20(*R*) Altered olivine-basalt, Movatn, Nordmarka, Oslo; CO_3 present.
20(*S*) Silt from disintegrated Movatn olivine-basalt.
20(*C*) Ca-saturated clay from disintegrated Movatn olivine-basalt.
21(*R*) Muscovite-schist, Bleikan, Hadeland; CO_3 present.
21(*S*) Silt from disintegrated Bleikan muscovite-schist.
21(*C*) Ca-saturated clay from disintegrated Bleikan muscovite-schist.

Note: Except for H_2O- and Ignition loss values, the data in the Table are from spectrochemical results, SiO_2 being estimated by difference.

for Cr, Ni, and Cu (Table 12); the fairly high content of Sr (800 p.p.m.) can be correlated with the calcite content and it appreciably exceeds Ba at 250 p.p.m. The extraordinary value for Rb (450 p.p.m.) leads to a value for K/Rb (at.) of 45, a figure normally associated with Rb-rich potash minerals.

Table 12

	S	20(*R*)	20(*S*)	20(*C*)	21(*R*)	21(*M*)	21(*S*)	21(*C*)	
Ga	5	15	10	15	4	65	40	30	Ga
Cr	1	170	250	200	10	40	20	30	Cr
Li	1	35	45	50	10	30	25	3	Li
Ni	1	50	80	80	10	*	15	15	Ni
Co	5	30	20	15	*	*	20	20	Co
Cu	10	75	80	90	*	*	*	*	Cu
V	10	340	140	140	170	260	50	70	V
Zr	10	160	70	80	300	*	20	*	Zr
Mn	10	1500	1900	3900	2400	310	5900	1000	Mn
Yt	15	*	*	*	45	*	15	*	Yt
Sr	10	800	170	*	400	15	800	*	Sr
Pb	15	*	*	*	*	*	15	*	Pb
Ba	10	250	100	10	800	4000	1000	250	Ba
Rb	50	450	*	*	440	1400	1800	1000	Rb
Cs	300	*	*	*	*	*	*	*	Cs
F	300	—	—	—	*	500	1500	*	F

20(*R*) Altered olivine-basalt, Movatn, Nordmarka, Oslo.
20(*S*) Silt from disintegrated Movatn olivine-basalt oven-dried basis.
20(*C*) Ca-saturated clay from disintegrated Movatn olivine-basalt oven-dried basis.
21(*R*) Muscovite-schist, Bleikan, Hadeland.
21(*M*) Muscovite from muscovite-schist, Bleikan.
21(*S*) Silt from disintegrated Bleikan muscovite-schist; oven-dried basis.
21(*C*) Ca-saturated clay from disintegrated Bleikan muscovite-schist; oven-dried basis.

3. *Mineralogy of the clay*

A striking similarity exists between the clay derived from the altered olivine-basalt and that derived from the Cornish serpentine; each contains the same five minerals, the former being richer in talc (35 per cent), poorer in chlorite (30 per cent), and similar in illite (20 per cent), montmorillonoid (5–10 per cent), and kaolin (5 per cent). The role of chlorite from both parent materials is probably much the same, especially in the formation of montmorillonoid, and again the presence of talc is at least partly due to its retention from the parent rock. The K_2O content of the basalt, however, causes less doubt about the in situ formation of illite and the K_2O percentage in the clay (0·85 per cent) approximate to that for a clay containing 20 per cent illite holding the conventional 6 per cent K_2O. The high MgO content of the clay (Table 11) is principally due to talc and chlorite; if 11 per cent is allowed as the contribution from 35 per cent talc, a content of about 20 per cent is implied for the chlorite. This is close to the MgO percentage in the silt (Table 11), which consists almost entirely of chlorite.

4. *Chemical changes on weathering*

The basalt resembles the monzonite, the other Mg-rich rock from Nordmarka, in retaining considerable Mg on weathering; relative to Al, Mg increases in the change rock → clay. Na, Ca, and K decrease as anticipated; Fe shows an unexpected decrease relative to Al, but this is partially explained by the resistance of iron-ore minerals from the parent material and their occurrence in the fine-sand fraction (as opposed to silt and clay) of the weathering products. Minor elements in the silt and clay (Table 12) are similar in concentration except for Sr and Ba, which reflect the superior feldspar and calcite content of the silt. In the change rock → silt → clay → the ratio Mg/Ni remains similar, but Ni/Co (at.) widens from 1·6 to 5·3, agreeing with general observations from the Cornish data.

Muscovite-Schist

1. *Description of the rock*

The rock is a typical schist with muscovite (20–30 per cent) and quartz (30–40 per cent) as principal primary minerals, and calcite (35–45 per cent) as a substantial secondary mineral. Biotite and feldspar are absent, but iron ore occurs in accessory amounts.

2. *Geochemistry of the rock*

The major element analyses (Table 11) show no unusual features, but amongst the minor elements (Table 12) Ga appears to be anomalously low; presence of considerable $CaCO_3$ may have influenced the spectrographic determination of this volatile element, since the content in the muscovite (65 p.p.m.) suggests a value between 13 and 20 p.p.m. for the rock.

3. *Geochemistry of the muscovite*

It is not to be expected that the minor-element concentrations of this metamorphic muscovite show much comparison with those of igneous muscovite; indeed, compared with data for the muscovite from the Cornish adamellite, only Ga is similar. Cr and V occur in substantially larger amounts in the muscovite from the schist, but considering the contents of the minerals fuschite and roscoelite, the tolerance of the lattice is scarcely tested.

4. *Mineralogy of the clay*

The interest of the clay is in its near-monomineralic nature; illite is the only recognized clay mineral, and quartz (1–2 per cent) is a minor accessory. The absence of any representative of the kaolin group illustrates the resistance of illite to further breakdown under the prevailing climatic conditions, and the chemical analysis of the clay (Table 11) is seen to represent that of K_2O-poor muscovite.

5. *Chemical changes on weathering*

The schist on weathering to clay loses its calcite, whilst its muscovite is slightly altered and its quartz remains intact. The chemical changes are thus loss of Ca,

Mg, and K, with Si sensibly constant relative to Al. Fe decreases from rock through silt to clay, but as with monzonite, the iron ore present in the parent material is resistant and occurs in the fine sand of the weathered products. F is lost from the muscovite on weathering to illite (Table 12), but due to the spectrographic sensitivity it is uncertain whether or not it loses more or less than the

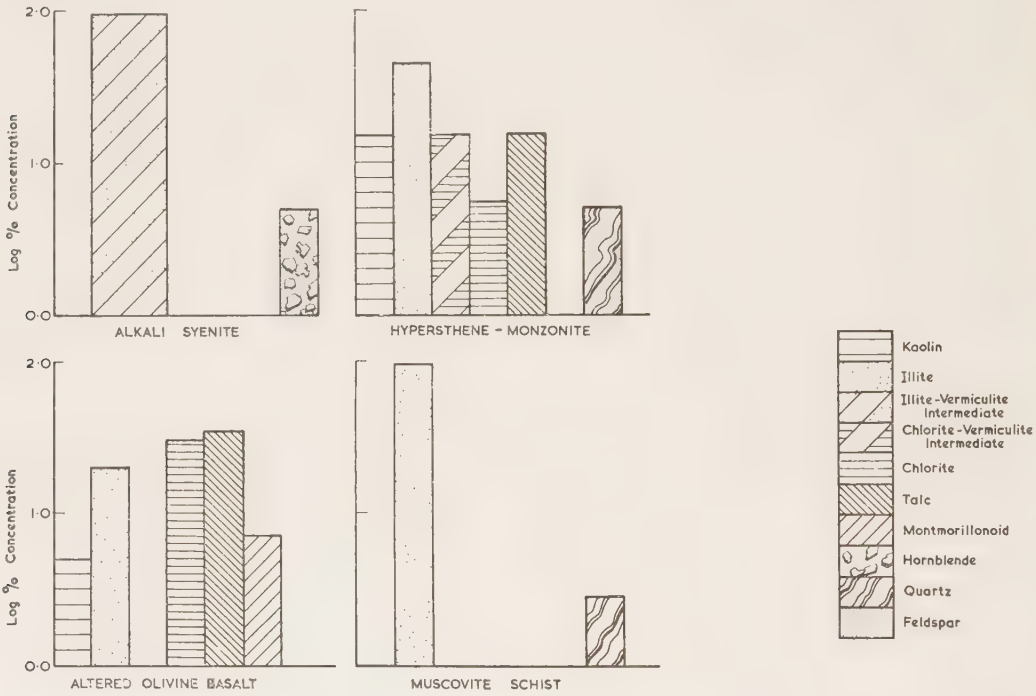

Fig. 3. Approximate mineralogical composition of Norwegian clays ($< 2\mu$) derived from weathering from various rocks. Free Fe-oxides removed.

biotite from the monzonite. The ratio Al/Ga (at.) increases from $8{\cdot}9 \times 10^3$ in the silt to $11{\cdot}4 \times 10^3$ in the clay compared with 5×10^3 (approximately) for the fresh muscovite; Ga is thus lost on weathering relative to Al as found for the Cornish examples. The difference between Sr in the silt (800 p.p.m.) and in the clay (below 10 p.p.m.) illustrates the calcite distribution in the two fractions. Ba is less drastically reduced in the clay compared with the silt, and it is evident that appreciable Ba is retained in the illite lattice from the muscovite.

Summary of Results and Conclusions

I. Minerals in the rocks and clays

Fig. 3 shows the distribution of the mineral species identified in the clays (after removal of free Fe oxides) derived by weathering of the four rocks. Only

illite is ubiquitous; kaolin, talc, chlorite, and vermiculite occur in two clays and montmorillonoid in one. Quartz, feldspar, and hornblende (and talc) are products of physical weathering. Feldspar, occurring in three of the rocks, weathers (chemically) to give kaolin in the clays from the monzonite and basalt; it produces no kaolin (i.e., less than 5 per cent) in the clays from the syenite, due to the much greater ease of weathering of the associated biotite whose products form over 90 per cent of the clay. Feldspar also produces illite in the clay from the basalt and possibly in that from the monzonite. These alterations are the same as those found for feldspars in Cornwall. Biotite weathers to give (in flakes) vermiculite or biotite-vermiculite intermediate and lepidocrocite. For the Cornish biotites it was suggested that the Mg content influenced the weathering product; thus the Mg-rich mica from the granodiorite produced chlorite (in flakes) and that from the adamellite (being Mg-poor) produced vermiculite. The biotite from the monzonite is certainly richer in Mg than that from the syenite, but no chlorite occurs in weathered flakes of either mineral and it is not proven that the chlorite in the clay from the monzonite derives from the biotite. The absence of lepidocrocite in weathered flakes of the biotites from Cornwall is a further distinction, and it is evident that climatic and drainage conditions as well as chemical composition are important factors in deciding the weathering fate of biotite. The two pyroxenes in the monzonite have uncertain weathering products, but it seems probable that they are associated with the formation of talc by their release of Mg and possible that the hypersthene produces chlorite-vermiculite intermediate mixed-layer material. Chlorite weathers to montmorillonoid above the Norwegian basalt as it did above the Cornish serpentine; impeded drainage conditions obtain at both sites.

II. Chemical composition of the rocks and clays.

The spectrochemical analyses of the Ca-saturated clays, derived by weathering from the syenite, monzonite, basalt, and muscovite-schist, are given in Tables 8 and 11. As expected (Reiche, 1950), the rocks lose Na, Ca, K, and Si relative to Al on weathering (according with the Cornish data), but Ti and Mn show no regular trend. Mg/Al increases in the change rock → clay when the rock is relatively rich in Mg (monzonite and basalt), and the high Mg content of the clays is in sharp contrast to those for clays derived from Mg-rich rocks in Cornwall (hornblende-schist and serpentine), and climatic conditions appear to be partly responsible. Although Fe/Al increases for the syenite and monzonite in the change rock → clay, the ratio decreases for the basalt and muscovite-schist; this is partly due to the latter rocks containing iron ore, which resists chemical weathering and does not contribute to the clay fraction.

The compositions of the rocks and clays are represented as before in a triangular diagram (Fig. 4). It is not apparent that the scatter of the clay-points is less than that for the rock-points, but in fact there is somewhat less variation in the Mg, Ca, Ti, and Na contents of the clays than of the rocks. Either the clays have been more recently derived from the Norwegian rocks than from the Cornish ones, or the climate in Nordmarka has been less favourable for chemical weathering than that in the Lizard area.

III. Minor elements in the minerals, rocks, and clays

The ratios for Al/Ga (at.) follow a pattern similar to those for the Cornish examples; the values are lowest for the minerals ($2{\cdot}7 \times 10^3$ for hornblende and $6{\cdot}3 \times 10^3$ for muscovite) and are close to those for the same minerals from the Lizard area. Bearing in mind that Ga in the muscovite-schist is probably at least 13 p.p.m., Al/Ga (at.) is higher in three of the clays and the same in the remaining clay than in the parent rocks. The ratios in the rocks are close to those of $8{\cdot}6 \times 10^3$ for acid and $17{\cdot}2 \times 10^3$ for basic rocks quoted by Sandell (1949), and they vary

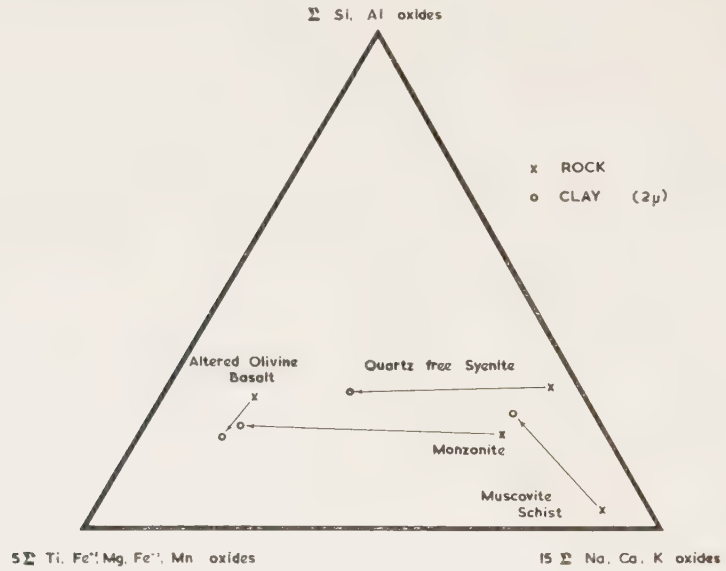

Fig. 4. Spectrochemical composition of Norwegian rocks and their 2-μ clay-weathering products. Molecular proportions of oxides.

from $5{\cdot}5 \times 10^3$ for syenite to $13{\cdot}7 \times 10^3$ for the monzonite; the clays have ratios ranging from $7{\cdot}3 \times 10^3$ to $17{\cdot}8 \times 10^3$. It can again be concluded that Ga is lost in the weathering process.

The ratio Mg/Ni decreases on weathering only for the muscovite-schist; in the other instances the ratio increases, contrasting to the Cornish observations; similarly Ni/Co does not generally increase. The conflicting trends are difficult to reconcile. The ratio K/Rb in the clays is smaller than that in the rocks when the alteration products of biotite or muscovite contribute substantially to the clay-mineral content (adamellite, syenite, and muscovite-schist). When illite in the clay has not been derived principally from mica (but from feldspar), Rb is lost and K/Rb increases in the change rock → clay (hornblende-schist, serpentine, monzonite, and basalt).

Acknowledgments—The writer is indebted to the Agricultural Research Council for a scholarship enabling him to initiate this study; also to Drs. Nockolds and Kvalheim for their stimulating criticisms and friendly advice.

References

Ahrens, L. H. (1952) *Geochim. et Cosmochim. Acta* **2,** 168.
Brown, G. (1953) *J. Soil Sci.* **4,** 220–225.
Brøgger, W. C. (1933) *Skr. Norske vid.-akad. Oslo,* (i) *Math.-nat. kl.* 1933 No. 1.
Butler, J. R. (1953) *Geochim. et Cosmochim. Acta* **4,** 157–178.
Kvalheim, A. (1947) *J. Opt. Soc. Amer.* **37,** 585–592.
Marel, van der H. W. (1951) *J. Sediment. Petrol.* **21,** 12–21.
Nockolds, S. R. (1947) *Amer. J. Sci.* **245,** 401–420.
Nockolds, S. R., and Mitchell, R. L. (1948) *Trans. Roy. Soc. Edinb.* **61,** 533–575.
Reiche, P. (1950) *Univ. N. Mex. Publ. in Geol.* No. 3, 1–95.
Sandell, E. B. (1949) *Amer. J. Sci.* **247,** 40–48.
Wager, L. R., and Mitchell, R. L. (1951) *Geochim. et Cosmochim. Acta* **1,** 129–208.
Walker, G. F. (1952) *X-ray Identification and Crystal Structures of Clay Minerals,* pp. 212–223. The Mineralogical Society, London (Ed., G. W. Brindley).

Geochimica et Cosmochimica Acta, 1954, Vol. 6, pp. 282 to 301. Pergamon Press Ltd., London

Contribution of metallurgy to the origin of meteorites

Part I—Structure of metallic meteorites, their composition and the effect of pressure*

Herbert H. Uhlig
Corrosion Laboratory, Department of Metallurgy, Massachusetts Institute of Technology, Cambridge, Massachusetts

ABSTRACT

The composition and structure of metallic meteorites accord with a mechanism of their formation by slow cooling from elevated temperatures under conditions of high pressure. These conditions produced the Widmanstätten pattern in 6–13 per cent Ni-Fe compositions. At some time in their history and at a temperature not higher than 300–400°C this pressure was suddenly changed, accompanied perhaps by a temperature rise followed by comparatively rapid cooling.

Approximate times necessary to form the Widmanstätten pattern at several temperatures are calculated. These are estimated from diffusion rates in nickel-iron alloys and from the time of heating required at high temperatures to erase the Widmanstätten pattern (twenty or more hours at 1000°C). From the calculated values it is concluded that within the age of the solar system (3×10^9 years) equilibrium could not have been achieved below 300–400°C.

In octahedrites, average observed composition of taenite (gamma phase, 30 per cent Ni) and of kamacite (alpha phase, 6 per cent Ni) is evidence according to the phase-diagram of equilibrium at a temperature of 500°C. Nevertheless, taenite variable in composition from edge to centre indicates final stages of Widmanstätten figure formation at a lower temperature range where restricted diffusion prevented homogeneity within the time available. This discrepancy is reconciled by effects of high pressure which lower the gamma-alpha transformation temperatures, and the corresponding temperatures for Widmanstätten figure formation. If the prevailing lower equilibrium temperature was about 300°C, the necessary pressure is calculated to be about 10^5 atmospheres. Pressures of this magnitude suggest conditions in the interior of a planetary body.

Pressure also accounts for absence of Widmanstätten patterns in meteorites containing more than about 12–13 per cent Ni. These alloys (nickel-rich ataxites) remained for the majority of their extraterrestrial existence in the gamma state. Subsequent fragmentation into smaller bodies released pressure and the alloys either transformed simultaneously into metastable α_2 phase, or cooled relatively rapidly through the transformation temperature, forming a mixture of alpha and gamma phases. Meteorites containing more than about 27 per cent Ni contain all taenite which accords with laboratory experience showing that 34 or more per cent Ni-Fe alloys resist transformation under all conditions of cooling or heat treatment.

Sudden release of pressure, as by changing distortional stresses or fragmentation of the parent body, accounts in major part for the metallographic structure called plessite. Reduction of pressure momentarily transplants gamma alloy to the alpha-gamma region of the phase diagram resulting in transformation to metastable α_2 phase which is an acicular or martensite-like transformation product analogous to structures produced in similar laboratory alloys by thermal quench. Heating of α_2 phase within the alpha-gamma region (or slow cooling from this region after transformation) results in a mixture of finely divided alpha and gamma phases either unresolved or granular as observed under the microscope. These products correspond to unresolvable, fine, and coarse plessite.

Acicular kamacite observed in some meteorites is also explained by sudden transformation occurring through pressure changes. Rapid cooling is not an equivalent explanation, because most original meteorite masses were too large to cool at the required rapid rate.

Most metals have definite structures which, like "fingerprints," are specific for purposes of identification. In addition, the structures may be useful for revealing past history of the metals, including origin, heat treatment, and fabrication.

To observe these structures, a microscope is focused on a surface of the metal previously polished and subsequently etched with chemical reagents. Areas show up rich in detail, the identification and interpretation of which make up the science of metallography. Such factors as crystal size and shape, appearance of slip bands

* Presented at symposium on "Origin of Meteorites," Am. Assoc. Adv. of Science, December, 1953, Boston, Mass.

and crystal twins, or islands of separate phases along crystal boundaries or within the crystals, are significant portions of the evidence that weave a singular pattern of past events. Each line straight or crooked, each band narrow or broad, and each shaded area bright or dull, means something in terms of present properties and former treatment. X-ray, hardness tests, and chemical analyses often supplement the microscope in extracting further facets of information that lie latent in the visible pattern. Applying the general techniques of metallography, therefore, can often be used to reveal how a metal like steel was produced, whether it was slowly or rapidly cooled from the molten state, and whether it was subsequently re-heated and, if so, to what temperature and how long. Its structure may divulge whether it was once deformed mechanically, and whether the force applied was gradual or sudden. Not all this information may be had from every specimen of metal or alloy, but some part of the record is usually accessible through the metallographic approach. The metallurgist in his capacity as historian parallels the botanist who reports weather-cycles hundreds of years ago by measuring the comparative width of tree-rings.

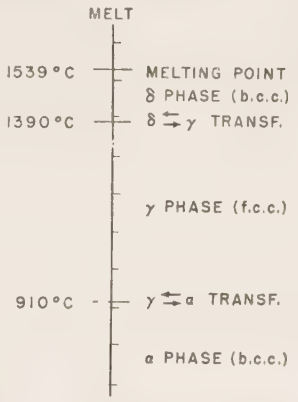

Fig. 1. Allotropic modifications of iron as a function of temperature.

The purpose of this paper is to outline the contribution which present-day metallurgy makes to our knowledge of the origin and history of meteorites. For example, were meteorites once part of a planet or asteroid that slowly cooled and then exploded or broke up by collision, as some astronomers believe? Were they subject to high pressures during the time they cooled? What was their probable temperature when fragmentation took place? These are some of the questions to which a study of meteorite structure can be directed.

Transformations in Iron

Metallic meteorites are essentially iron-nickel alloys (about 5 to 50 per cent Ni, averaging 8·5 per cent) containing small amounts of other metallic and non-metallic elements. A good starting-point for discussing their structure or metallography is the consideration of iron itself (Fig. 1). Iron in the liquid state solidifies sharply at 1539°C into a continuous, firmly inter-attached network of crystals called grains. The atoms of the grains are arranged in a regular lattice, individual repetitive units of which (cells) can be considered cubes. At the centre of each cube of atoms is located another iron atom; hence, the metal is said to be in the body-centred cubic lattice (Fig. 2). Iron of this lattice structure just below the melting point is called delta iron. As crystals of delta phase are cooled to 1390°C, the atoms rearrange themselves into an allotropic modification. Each cube loses the atom at the centre, and instead atoms take up new places at the middle of each six faces of the cube (Fig. 2). The new structure is called face-centred cubic, and iron of this structure is called gamma iron.

At 910°C the atoms revert to the body-centred cubic lattice. The new allotrope is called alpha iron, although its lattice is identical to the delta iron of higher temperatures. There are no further lattice changes on cooling below 910°C.

Transformation in Iron-Nickel Alloys

When nickel is added to iron, forming a nickel-iron alloy, nickel atoms are randomly distributed and can substitute for iron atoms in the two lattices just described. The solidification temperatures of the alloys are below that of iron, and the temperatures at which the gamma-alpha allotropic modification occurs are also shifted

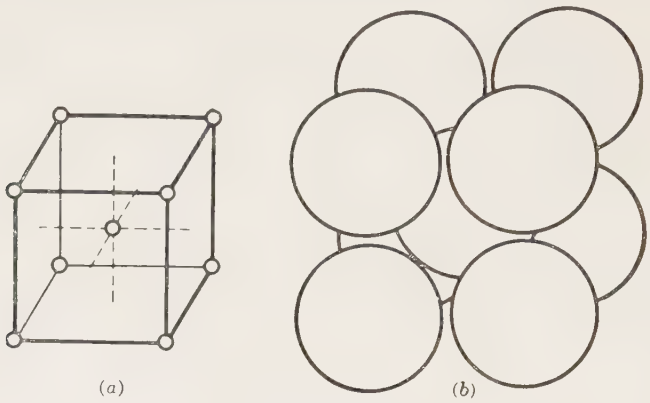

Body-centred cubic lattice.

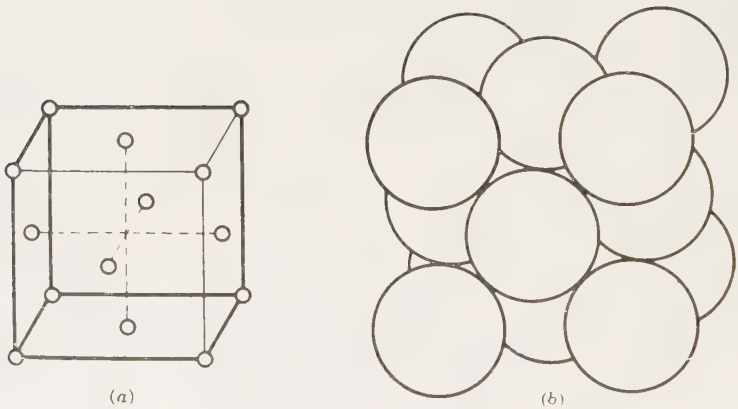

Face-centred cubic lattice.

Fig. 2. Unit cells of iron and nickel-iron alloys.

downward. Delta phase no longer exists above about 7 per cent nickel (Hansen, 1936). Our attention is profitably focused on the phase diagram below the gamma-alpha transformation, because at room temperature the metallographic structure of meteorites, or any other iron-nickel alloy, is determined largely by events occurring in this region. Effects of the delta-gamma transformation, for instance, are erased in short order both by the high temperatures prevailing for this transformation accompanied by high atom mobility, and by subsequent transformation of the gamma to the alpha phase.

The extent to which the gamma-alpha transformation temperature of the alloy decreases depends on the nickel content. For example, at 6 per cent nickel the

transformation occurs 150°C lower than for pure iron, or at about 760°C. An alloy of 10 per cent nickel transforms still lower at 700°C. Furthermore, instead of the gamma phase going to a single alpha phase, as occurs with pure iron, two phases are formed in equilibrium with each other. One phase is low in nickel, having the body-centred cubic (alpha) lattice, and the other is higher in nickel, having the face-centred cubic (gamma) lattice. As the temperature slowly decreases after initial transformation, the nickel content of both phases changes in a direction of

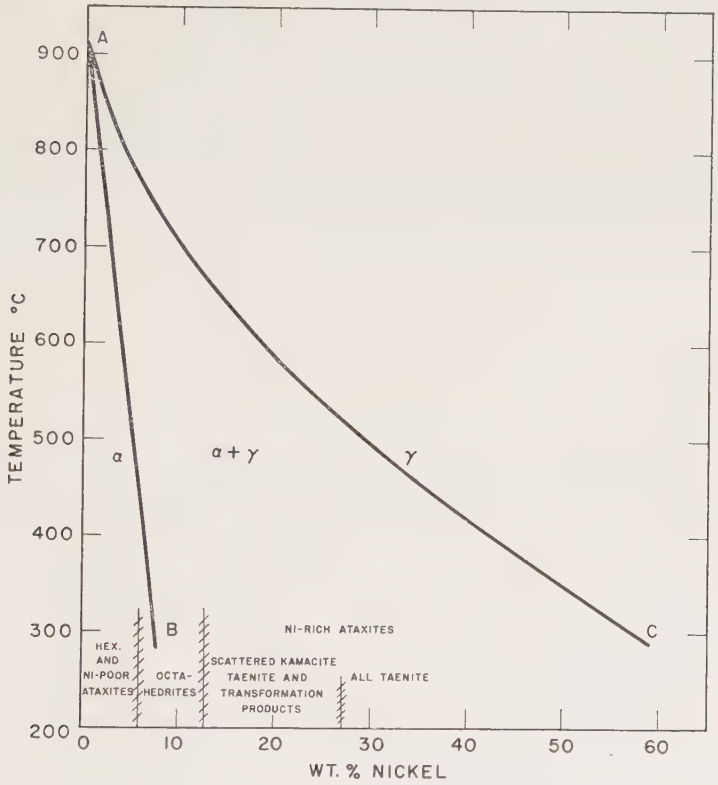

Fig. 3. Phase diagram for iron-nickel alloys at one atmosphere (Owen and Lui).

increasing nickel, the high-nickel phase increasing proportionately more in nickel than the low-nickel phase. Of course, the volume of each phase accommodates composition change, and it is obvious that if at any time in the cooling process the lower nickel-content alpha phase achieves the same nickel content as the original gamma phase from which it was formed, the volume of the latter must necessarily shrink to zero. In this event, the alloy becomes all alpha phase, and there is no further change in composition or structure as the temperature is lowered still further. Just above 400°C, for example, an alloy originally containing 6·5 per cent nickel is made up of a mixture of alpha phase, containing slightly less than 6·5 per cent nickel, and 42 per cent nickel gamma phase, but at 400°C the alloy becomes all alpha phase.

The equilibrium diagram of Owen and Liu (1949) shown in Fig. 3 depicts the

general phase relations just described. This supersedes the earlier phase diagram of Owen and Sully (1939). Line AC traces the initial transformation temperatures and compositions of the high-nickel (gamma) phase in equilibrium with the low-nickel (alpha) phase, the compositions of the latter being described by line AB. Iron-nickel alloys of compositions and at temperatures to the right of AC are always gamma-phase alloys, whereas those to the left of AB are all alpha-phase alloys. Compositions in the alpha-plus-gamma region exist as two-phase alloys, the composition of each phase at any single temperature being given by the boundary lines. The majority of meteorite compositions are well within the lower-temperature alpha-plus-gamma region of the equilibrium diagram.

With slow cooling of a nickel alloy, the alpha phase crystallizing from gamma phase at the transformation temperature (line AC) precipitates preferably along the 111 planes of the gamma phase. These are the planes of densest atomic packing and mark the octahedral planes of the gamma lattice. The precipitated alpha crystals consequently make up various sides of octahedrons, with residual gamma-phase alloy becoming higher in nickel, and smaller in volume. This crystallization pattern is the origin of the so-called Widmanstätten pattern (Fig. 4) in meteorites first observed by Alois von Widmanstätten in 1808. Meteorites having this structure are in the class called octahedrites.

With relatively rapid cooling, alloys transform at some temperature below the line AC into a distorted body-centred cubic lattice having the same proportion of nickel as the gamma lattice from which it originated. It is a metastable phase referred to as α_2 with acicular appearance under the microscope resembling martensite of quenched iron-carbon alloys. Sometimes the needles of the α_2 transformation product show vestiges of octahedral symmetry, but never on a scale comparable with nor as prominent as the oriented alpha and gamma phases of the Widmanstätten pattern. Heating of α_2 phase to some temperature in the alpha-gamma region causes it to decompose into alpha-plus-gamma phases in finely divided state, generally unresolved under the microscope, and which appears black when etched. Longer heating agglomerates the decomposition products into larger granular masses of alpha and gamma phases having microscopic size.

The weight of evidence is that octahedrite meteorites once cooled very slowly through the gamma-alpha transformation temperatures.* The Widmanstätten pattern is itself good evidence of this state of affairs, for had cooling through the transformation been rapid, followed by slow cooling, granular alpha and gamma phase would have resulted instead of the beautifully oriented bands that are found. Granular structures, when observed in meteorites, may be taken as evidence in fact that a rapid transformation once occurred. Ataxites, for example, often display a spherodized or granular structure (Fig. 5) which is typical of a laboratory alloy that has undergone sudden transformation followed by prolonged heat treatment above room temperature. Sometimes an acicular pattern in meteorites is observed (Fig. 6) which indicates rapid transformation to α_2 but without subsequent heat treatment necessary for decomposition of this phase.

* Owen (1940) proposes that the Widmanstätten pattern may have formed by slow decomposition of α_2 phase, but the imperfect orientation relations in this metastable phase make a mechanism of this kind unlikely. Decomposition of α_2, however, may well account for vestigial orientation patterns resembling microscopic Widmanstätten figures in the so-called plessite phase described below.

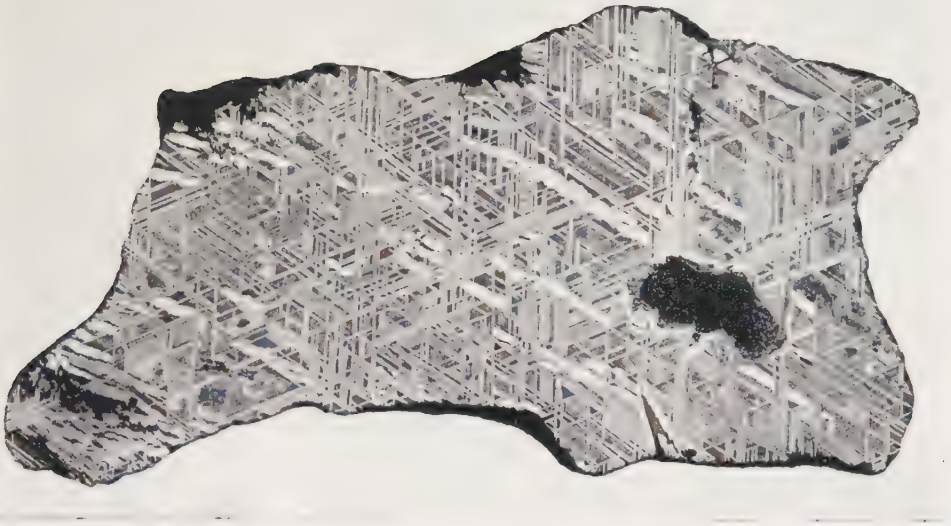

Fig. 4. Edmonton, Kentucky Octahedrite showing Widmanstätten pattern. 12·6% Ni. × 4/5 (Henderson and Perry) (reduced to $\frac{7}{10}$).

Fig. 5. A nickel-rich ataxite structure. Taenite areas in a ground mass of kamacite. Iquique, Chile, 16% Ni × 1000 (Henderson and Perry) (reduced to $\frac{8}{10}$).

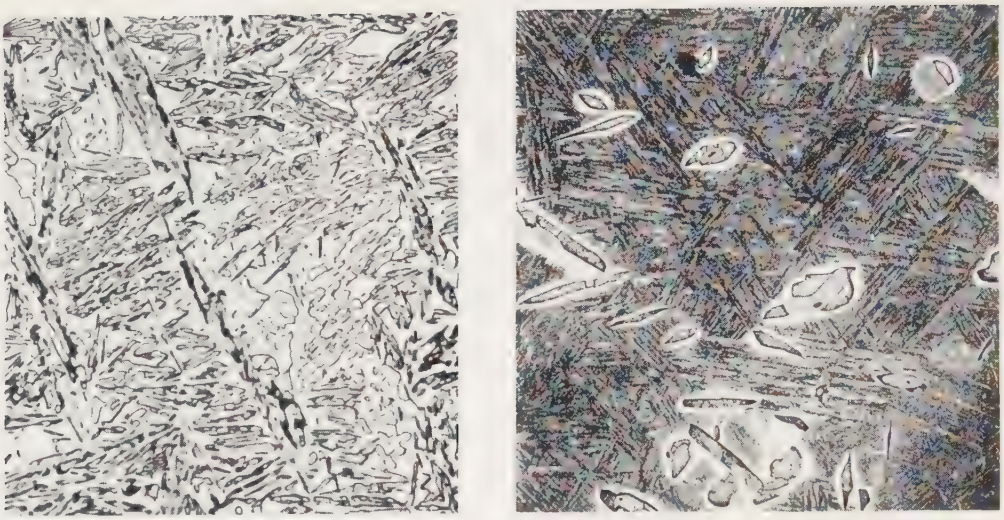

A *B*

Fig. 6. Acicular structures in nickel-rich ataxites (Perry, 1944).
A. Limestone Creek, 30·5% Ni + Co, × 600 (reduced to $\frac{7}{10}$).
B. Freda, N.D., 24·2% Ni + Co, × 60 (reduced to $\frac{7}{10}$).
Inclusions are kamacite and phosphides.

Fig. 7. Dexter meteorite 7·88% Ni, 0·036% Co, × 100 (reduced to $\frac{6}{10}$). Coarse plessite in centre area is surrounded by clear taenite. Dark areas are fine or unresolvable plessite. Remainder is acicular kamacite containing Neumann bands.

By way of further evidence that cooling occurred from high temperatures, Mehl and Derge (1937) proved by X-ray orientation studies the existence of a definite orientation of alpha phase in Canyon Diablo meteorite with respect to the parent-gamma phase. The (111) planes of gamma alloy were found parallel to the (110) planes of alpha alloy and the [110] direction in a particular (111)-gamma plane was parallel to a [111] direction in the corresponding (110)-alpha plane. This is in accord with the so-called Kurdjumow and Sachs relation, typical of a high-temperature transformation of gamma to alpha. Had the meteorite transformed at subzero temperatures, another phase orientation relation (Nishiyama) would have applied, but was not found.

It is also of interest that some meteorites a foot or more across were at one time single crystals of gamma-phase alloy, as shown by the continuous single Widmanstätten pattern extending from end to end of the specimen. Crystals of this size can only have resulted from long periods of heating at high temperatures before their transformation at lower temperatures.

Veining

Alpha-phase regions often contain a few single irregular lines that look like grain boundaries (Figs. 10 and 11), but in reality divide portions of the single crystal. These markings, singularly prominent in meteorite structures, are called veining and can be reproduced in the laboratory, particularly in large crystals. Although comparatively little is known about the details of their formation, the current explanation is that they represent an attempt of a large crystal, perhaps slightly distorted or stressed sometime in its history, to adjust itself with respect to slight lattice imperfections. The imperfections concentrate along the irregular boundaries that make up veining, the metal in between the boundaries representing a higher degree of crystal perfection. Each relatively more perfect subcrystal is oriented slightly differently from its neighbours, but all are part of the same single crystal. Impurities are also better accommodated along the boundaries than within the crystal, these often accentuating the outline of subcrystals. In meteorites, therefore, veining may have originated from some slight distortion during or after formation of the Widmanstätten pattern.

Transformations in Meteorites

In meteorites, the low-nickel or alpha phase is called kamacite, and the high-nickel or gamma phase is called taenite (Table 1). Plessite, also common to meteorites, is an intimate mixture of kamacite and taenite varying from areas unresolved under the microscope to readily resolved granular or lamellar areas (Fig. 7). With slow cooling from temperatures at which the meteorite is in the gamma phase, kamacite, therefore, will separate out according to the composition boundaries of Fig. 3, at the expense of taenite which becomes richer in nickel but smaller in volume. The kamacite precipitates out along the octahedral planes of taenite, as discussed before. It is this mode of crystallization continuing to relatively low temperatures over extremely long periods of time that reasonably accounts for the regular geometric patterns formed by etched and polished sections of octahedrites.

Table 1. *Terminology for metallic meteorites*

	Lattice	*Composition range % nickel*	*Remarks*
	PHASES IN METEORITES		
Kamacite	body-centred cubic (α)	Constant at about 6%	Composes all of hexahedrites and a part of octahedrites and some nickel-rich ataxites.
Taenite	face-centred cubic (γ)	Variable, but averages 30% Ni	Composes part of octahedrites and nickel-rich ataxites. Above 27% nickel, ataxites are all taenite.
Plessite	mixture of b.c.c. and f.c.c. ($\alpha + \gamma$), or acicular α_2		Found below 27% nickel.
	CLASSIFICATION OF METEORITES		
Hexahedrites	body-centred cubic (α)	about 5·5%	Uncommon variety (characteristic markings are Neumann bands).
Octahedrites	b.c.c. and f.c.c. ($\alpha + \gamma$)	approx. 6 to 13% nickel	Common variety (exhibit Widmanstätten patterns).
Nickel-poor Ataxites	body-centred cubic (α)	$<6\%$	Rare.
Nickel-rich Ataxites	mixture of b.c.c. and f.c.c. (except if nickel ~27%)	$>13\%$	Rare.

Should the overall nickel composition of a meteorite fall below that required for retention of taenite at the lowest temperatures where diffusion still operates, taenite of the Widmanstätten pattern will completely disappear as the alloy cools. Vestiges of the Widmanstätten pattern may persist, however, if the temperature for disappearance of taenite is too low for further marked grain growth. This situation accounts for so-called coarse octahedrites or brecciated hexahedrites. Their upper limit of nickel content is about 7 per cent (HENDERSON, 1941).* If the nickel content is somewhat lower than this value, taenite disappears at a higher temperature and the Widmanstätten pattern on further cooling now has time to grow more completely into single large crystals of kamacite giving rise to hexahedrites (5·5–5·6 per cent Ni).* In general, brecciated hexahedrites are expected to have a higher nickel content than hexahedrites.

With sufficient precaution of slow cooling, simulated Widmanstätten patterns in iron-nickel alloys can be reproduced in the laboratory. An early attempt was described by BENEDICKS (1910, 1926), who cooled a 12 per cent Ni-Fe alloy over a period of $2\frac{1}{2}$ days, obtaining a pattern having the expected appearance but visible only under the microscope. Later, MEHL and DERGE (1937) obtained a

* E. P. HENDERSON, Private communication.

better defined Widmanstätten pattern by slowly cooling a 27 per cent Ni-Fe alloy, the structure of which was clearly visible at 50× magnification. A similar experiment was performed by Buddhue (1948). Nickel-iron alloys comprising meteorites presumably cooled so much more slowly that their metallographic phases achieved larger dimensions, making them visible to the unaided eye, but in other respects the laboratory alloy pattern was similar to that in meteorites, including the Kurdjumow-Sachs lattice orientation of the gamma-alpha phases.

Classification of Meteorites

As was pointed out by Pfann (1917) and revised by Perry (1944, p. 47), structures and average compositions of metallic meteorites show that they can be divided into three general classes. If the nickel content is below about 6 per cent, the structure consists entirely of kamacite. The majority of meteorites in this class are called hexahedrites because of hexahedral symmetry produced by typical families of lines appearing on surfaces of etched specimens following the planes of the icositetrahedron (twenty-four sides). The latter is the natural crystal shape of the 112 planes of the body-centred cubic lattice for iron. These lines, which appear as bands under the microscope, are called Neumann bands, after Neumann who first observed them in 1848. Their origin is discussed in Part II.

Meteorites of higher nickel content ranging from about 6 to 13 per cent show the normal Widmanstätten pattern and, as mentioned above, are called octahedrites because kamacite and taenite are arranged with octahedral symmetry. They characteristically contain variable amounts of plessite as well. Octahedrites make up the majority of metallic meteorites which have fallen to the earth and have been subsequently recovered. Above 10 to 14 per cent of nickel, or according to E. P. Henderson,* 12 to 13 per cent Ni, the alloys may contain plessite and scattered kamacite fields. They no longer show a major Widmanstätten pattern and, hence, are called nickel-rich ataxites. Ataxites containing more than about 27 per cent nickel are all taenite. Nickel-poor ataxites also exist, falling within the kamacite composition region, but which fail to show Neumann bands. The hexahedrites and nickel-poor ataxites falling below 6 per cent nickel indicate, according to the phase diagram of Fig. 3, an equilibrium state achieved below 450°C. But the same phase diagram provides no obvious reasons for lack of a Widmanstätten pattern in alloys containing more than 13 per cent nickel. A 15 per cent nickel-iron alloy, for example, transforms at 640°C, and given sufficient time should develop a Widmanstätten pattern as readily as a 12 per cent alloy transforming at 675°C. Mehl and Derge (1937), as mentioned above, proved that an alloy containing as much as 27 per cent nickel transforms with an accompanying well-defined, even though microscopic, Widmanstätten pattern. The fairly sharp cutoff of octahedral etch figures at about 13 per cent nickel suggests, therefore, that some factor not common to laboratory alloys prevailed in meteorites. The diffusion of nickel in iron is not abnormally low above 13 per cent nickel, even taking into account impurities normal to meteorites, such as phosphorus and sulphur, which possibly decrease the diffusion rates. Owen and Burns (1939)

* Based on a critical examination of reported analyses. (Private communication.)

state that heat treatment of meteorites produces reactions closely resembling those taking place in artificially prepared pure nickel-iron alloys, indicating that no unusual metallurgical properties are imparted to meteorites by impurities. More plausible than a supposed effect of impurities is that 13 per cent alloys and above remained as gamma phase for the majority of their extra-terrestrial existence and cooled more rapidly through the transformation temperature than alloys of lower nickel content. The gamma-phase region for a 13 per cent Ni-Fe alloy at atmospheric pressure lies above 665 °C, and an alloy cooling relatively rapidly from this temperature would not form the usual Widmanstätten pattern, although a pattern of at least microscopic dimensions might develop. Areas in nickel-rich ataxites of less than 27 per cent Ni contain plessite and scattered areas of kamacite (Perry, 1944, pp. 46, 69), confirming past transformation in meteorites of this composition range and suggesting that phase change was more rapid than corresponded to the situation for octahedrites.* The acicular structure (Owen and Burns, 1939; Perry, 1944, p. 46) of some ataxites (Fig. 6) when observed in laboratory alloys is taken to indicate rapid transformation, such as occurs through rapid cooling, or cooling to sub-zero temperatures. It is inconceivable, however, that any large body of metal should cool sufficiently rapidly so as to transform to metastable alpha phase in the manner of small specimens of quenched laboratory alloys. A reasonable mechanism for formation of this structure in meteorites, therefore, favours sub-zero transformation. An alternative explanation is also possible, as is discussed below.

The temperatures of alloys above 13 per cent Ni need not have been so high as 665°C in order for them to remain in the gamma phase if one considers that high pressures may have prevailed simultaneously. Calculation shows that pressure lowers the transformation temperatures, or extends the gamma-phase region to lower temperatures. In fact, there is good evidence outlined below for believing that meteorites could not have established final equilibrium at so high a temperature as 500 to 600°, but instead at some lower temperature where diffusion rates are more restricted. The possible important part played by pressure, therefore, deserves further consideration, particularly if one accepts the idea that meteorites at one time may have been part of a large body composed of a nickel-iron core subjected to high gravitational forces.

Effect of Pressure

The extent of pressure-shift of gamma-alpha transformation temperatures and equilibrium boundaries of the phase diagram, depicted in Fig. 3, to lower values can be calculated from the heat of transformation, ΔH, and the change of volume, ΔV, by applying the Clausius-Clapeyron equation:

$$\frac{dp}{dt} = \frac{\Delta H}{T\Delta V}$$

* It has been suggested (e.g., Paneth, 1940, p. 21) that ataxite structures originated from heating the specimen to some high temperature sufficient to wipe out the Widmanstätten pattern, as by passing near the sun. This explanation, although adequate to explain some observed structures, fails to account for nickel-rich ataxites being found only within the composition range lying above 12–13 per cent Ni. Why are not 6–12 per cent Ni alloys also ataxites, at least occasionally?

The heat of gamma-alpha transformation has been measured for pure iron ($\Delta H = -3{\cdot}9$ cal/gram), but not for iron-nickel alloys. Making use of the specific volumes of gamma iron (0·1310 cc/gm) and alpha iron (0·1321 cc/gm) at 910°C, $dp/dt = -124$ atmospheres/°C, or −0·0081°C/atmosphere.* In other words, the gamma-alpha transformation temperature for iron is lowered 0·0081°C for one atmosphere increased pressure. For nickel-iron alloys, the value is expected to be the same order of magnitude for the reason that although the volume change for iron-nickel alloys is larger (ΔV for 10 per cent Ni-Fe - 0·0017 cc/gm at 600°C (Marsh, 1938, pp. 122-3)),this effect is offset by a lower transformation temperature (700°C for 10 per cent Ni-Fe) and a higher ΔH. Heat of transformation of iron at lower temperatures, for example, compared with the value at 910°C increases 6·4-fold at 630°C and 8·2-fold at 430°C (Darken and Gurry, 1953, p. 397). Differing compressibilities of the two phases and variation of ΔH with pressure also alter the quantitative situation, especially where the pressures are high. It is well within reason, considering all factors, to associate pressures of 10^4 to 10^5 atmospheres with a depression of the Ni-Fe transformation temperatures in the order of two or three hundred degrees.

Vogel and Heumann (1946), using the simplified Clausius-Clapeyron equation, calculated that a 10 per cent Ni-Fe alloy, normally transforming at 700°C, transforms instead at 400°C under a pressure of about 5×10^4 atm. They consider the Widmanstätten pattern to form only sluggishly at the latter temperature, and when the pressures are higher (and corresponding temperatures lower) not at all. Their conclusion is that formation of octahedral patterns under pressure is unlikely, and that meteorites are fragments of small cosmic bodies. They do not take into account, however, the long times which are actually available to form octahedral patterns at temperatures in the neighbourhood of 300 to 400°C, and which are actually necessary to explain the observed dimensions and compositions of the two-phase structure, as shown below. Furthermore, a better approximation of the pressure required to produce a 200°C depression of the transformation temperature is larger than their estimated value for a 300°C change when the Clausius-Clapeyron calculation is corrected for increasing values of ΔH at lower transformation temperatures. Accordingly, the necessary pressure to depress the transformation temperature from 500°C to 300°C using data of Darken and Gurry (1953), considering the volume change constant, is actually $2{\cdot}5 \times 10^5$ atm. This is an extreme pressure belonging to the interior of a relatively large mass.

Fig. 8 shows the estimated qualitative location of equilibrium composition boundaries for the nickel-iron alloy system as affected by these high pressures. An alloy cooling from temperatures in the gamma region begins to transform at L instead of P, accounting for taenite of composition L and equilibrium kamacite of composition O. As the structure cools slowly, the taenite and kamacite eventually reach compositions of N and M at 300°C, below which any further change is extremely slow because of restricted diffusion, as shown by laboratory experiments and also by calculations of the diffusion rates at this temperature.

* F. Birch (1940) found the experimental value to average −0·0088°C/atm., with which the calculated value is in satisfactory accord.

Explanation of Phase Compositions

It follows that a 25 per cent Ni alloy transforming above 500°C at 1 atm. would, under conditions of high pressure, transform with great difficulty, if at all, in the lower-temperature region. Furthermore, with the existence of very high pressures, temperatures appreciably below 665°C suffice to keep a 13 per cent or higher nickel alloy entirely in the gamma phase (Fig. 8). These relations are in the right direction for explaining the observation that meteorites containing approximately 13 per cent or more nickel no longer contain the Widmanstätten pattern.

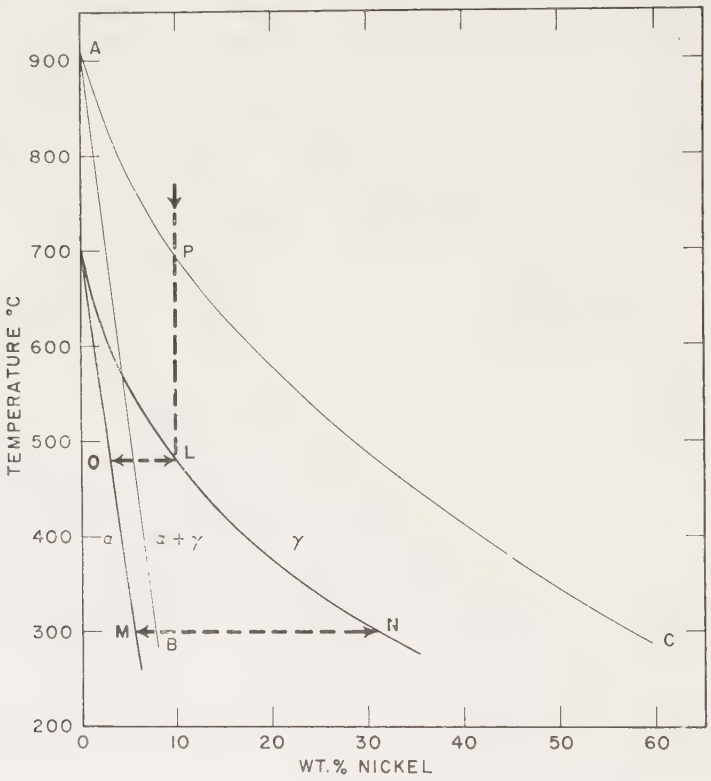

Fig. 8. Estimated phase diagram for iron-nickel alloys under high pressure. Light lines trace 1 atm. boundaries.

Another consideration also enters. The fact that meteorites above approximately 27 per cent Ni are all taenite (gamma phase) and show no evidence of having transformed, agrees, perhaps unexpectedly, with laboratory experience concerning alloys of this order nickel content. When a laboratory alloy reaches about 34 per cent Ni, which according to the phase diagram should transform at 460°C, 100 per cent gamma phase is retained on cooling to room temperature, or quenching to sub-zero temperatures (Owen and Sully, 1939; Mehl and Derge, 1937; Hoselitz, 1944), and the alloy completely resists change for long periods of heating (several days) in the alpha-plus-gamma region. Accordingly, the compositions of laboratory alloys and of meteorites are almost identical at which

gamma phase is completely retained on cooling. This correlation with laboratory experience implies that alloys transforming at or below 460°C may be expected to resist transformation under any conditions, perhaps including long periods of time below the transformation temperature, whereas alloys transforming above 460°C do so readily. The factor of pressure, therefore, may conceivably prevent transformation of $>$ 13 per cent Ni alloys (which at 10^5 atm. transform below 460°C (see Fig. 8)), even though the alloys cool slowly through the pressure-depressed transformation temperatures, just as the 34 per cent Ni alloy at 1 atm. cools without change below 460°C. Hence, the Widmanstätten pattern, for this reason, is absent in alloys containing considerably less than 34 per cent Ni. The pattern once formed may, of course, continue to grow below 460°C, since its formation then depends on crystal growth of phases already fully nucleated.

If, therefore, the high-pressure phase diagram is appropriate to meteorites, as seems reasonable, the composition of taenite first in equilibrium with kamacite at the initial transformation temperature depends only on the overall nickel content of the alloy, but the final taenite composition depends on both the pressure and the particular lower temperature at which final equilibrium was established, and not on the overall nickel content. The higher the pressure, the lower is the nickel content of taenite corresponding to temperatures for which diffusion is just operable within the time available. The kamacite composition, on the other hand, is less sensitive to temperature and is expected, therefore, to be less sensitive to pressure effects.

Diffusion in Taenite and Kamacite

The diffusion rate of nickel in iron decreases exponentially with decrease of temperature, so that the rate falls off very rapidly in going from a region of observable atom mobility, at perhaps 400°C in short-time laboratory experiments, to a region only 100° lower. Hoselitz (1944) estimated that small particles of nickel-iron alloys reach equilibrium in one year at 365°C, but require forty years at a temperature of 300°. Equilibrium in unstressed larger specimens would, of course, require much longer times.

If we assume (as justified below) that the Widmanstätten pattern is essentially "frozen" on reaching 300° where diffusion is severely restricted within the times assigned to the age of the solar system (3×10^9 years), the usual atmospheric pressure phase diagram (Fig. 3) indicates that a taenite of 57 per cent Ni co-exists in equilibrium with kamacite of 8 per cent Ni. However, the taenite phase of most meteorites averages only about 30 per cent Ni (Farrington, 1915, p. 134; Cohen, 1894, p. 103; Owen and Burns, 1939). At atmospheric pressure, equilibrium between 5·5 per cent Ni kamacite and 30 per cent Ni taenite is achieved at a temperature of 500°C (Fig. 3), a temperature at which diffusion is readily observed in laboratory experiments. Hence a taenite or kamacite phase might be expected to become homogeneous given the long times at this temperature associated with Widmanstätten figure formation. It is important to note, therefore, that taenite as observed in meteorites is characteristically inhomogeneous from edge to centre (Perry, 1944, pp. 15, 61; Smith and Young, 1939) and seldom of uniform composition, which alone is adequate evidence that taenite was formed under conditions

of restricted diffusion. Kamacite, by comparison, even though occupying a larger volume than taenite, appears to be relatively homogeneous in nickel, and the X-ray pattern correspondingly indicates achievement of equilibrium, contrary to the situation for taenite (Owen and Burns, 1939). Since calculations described below show that the difference in diffusion rates in taenite and kamacite becomes much greater as the temperature is lowered, the available evidence, therefore, lends weight to the attempted achievement of *equilibrium in octahedrite meteorites at some temperature below* 500°C. Considering the observed average composition of taenite at 30 per cent Ni and kamacite at 6 per cent, equilibrium, therefore, can only have been achieved under conditions of high pressure. The prevailing pressures, furthermore, must have been sufficient to account for depression of the transformation temperatures to values so low that concentration gradients in taenite were not eliminated in the time available. This depression was in the order of 200°C, if one accepts the assumption that the Widmanstätten pattern at 300°C or below no longer changes within the time we are concerned with. The corresponding pressures in these cases according to the calculations described above are about 10^5 atm. This agrees with our previous discussion of factors entering the cut-off of Widmanstätten patterns at 13 per cent Ni. The evidence of pressure entering as a significant factor in meteorite structures is also plausible from the characteristics of plessite, kamacite, and nickel-rich ataxites, as is outlined below.

Evidence of variable-composition taenite shows up in both etching patterns and hardness measurements. The centre of taenite after etching is often dark compared with a light coloured border or may consist of dark plessite (Perry, 1944, P. 42–1, 42–4, 43–1, and 43–2). In Fig. 9, however, the centre of etched taenite of Dexter is light, and the border dark. By indenting a microscopic pyramidal diamond into the metal under fixed and reproducible conditions of load, the relative hardness of the various areas can be measured. The softer the metal, the larger are the dimensions of the impression; hence, measured length of the impression can be taken as an arbitrary gauge of hardness. Measurements of this kind in Dexter meteorite are shown in Figs. 9, 10, and 11. The etched taenite band of Fig. 9, light in colour, averages 399 in the hardness-numbers scale (Knoop hardness), whereas the darker areas average 359. Hardness measurements of kamacite, on the other hand, show less or no corresponding variation in going across a field, and also the etch-pattern by comparison is uniform.

Greater observed homogeneity in the kamacite phase, despite its larger volume, is logically related to the more rapid diffusion of nickel in alpha-phase alloys than in gamma-phase alloys, the quantitative difference of which can be calculated for a variety of temperatures. Measurements of diffusion rates of nickel in gamma alloys have been reported, but have not been determined for alpha-phase alloys where the necessarily lower temperatures make experimental techniques difficult. However, a quantitative estimation of the rate in alpha-phase alloys can be obtained from the self-diffusion rate data for iron in both alpha and gamma phases obtained by employing radioactive iron isotopes to mark the extent of diffusion. The diffusion constant $D(\mathrm{Ni},\gamma)$ in $\mathrm{cm}^2/\mathrm{sec}$ is given by $(0{\cdot}344 + 0{\cdot}012 \times \text{wt. per cent Ni})e^{\frac{-67{,}500}{RT}}$, where R is in calories per mole (Wells and Mehl, 1941). For a

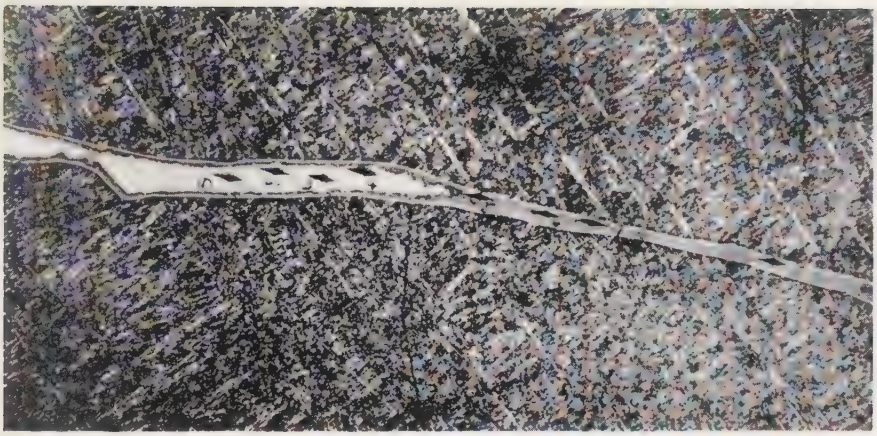

Fig. 9. Dexter meteorite, × 100 (reduced to $\frac{7}{10}$). Showing inhomogeneous taenite band. Knoop hardness values left to right for light-coloured taenite are 409, 382, 409, 395, and for darker taenite 347, 359, 370, 359. Broad parallel markings through acicular kamacite are Neumann bands, and the diamond impressions were produced by the hardness tester.

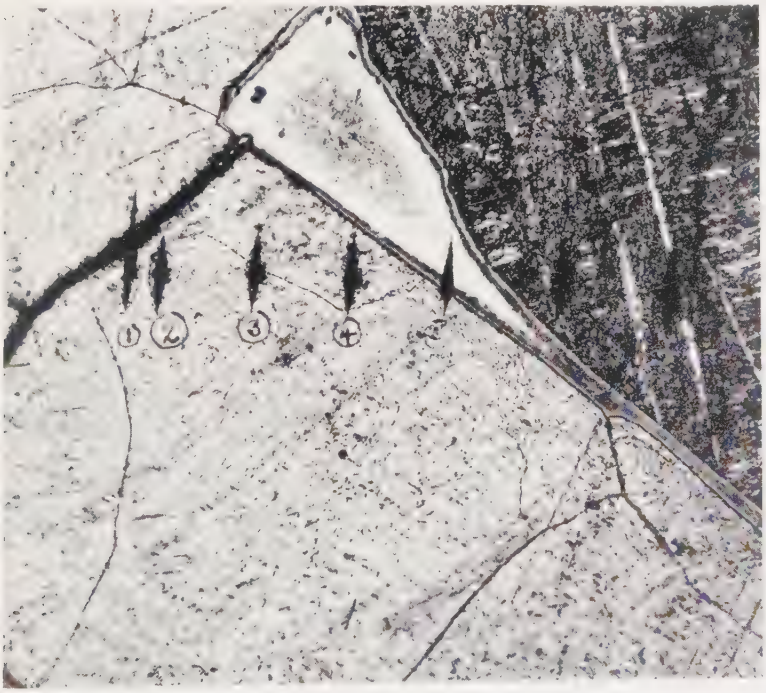

Fig. 10. Dexter meteorite, × 100. Taenite area, upper centre, shows darkly etched edges and also a slightly darker centre. Appearance of the latter suggests transformation. Knoop hardness numbers for diamond impressions left to right are (1) · · ·, (2) 373, (3) 353, (4) 373, (5) 419, (6) 359, (7) · · ·.

Fig. 11. Dexter meteorite, × 100 (reduced to $\frac{5}{10}$). Vertical band is taenite on either side of which is kamacite, the latter etching light or dark depending on crystal orientation. Knoop hardness numbers reading left to right are: 340, 340, 353, 387, 323.

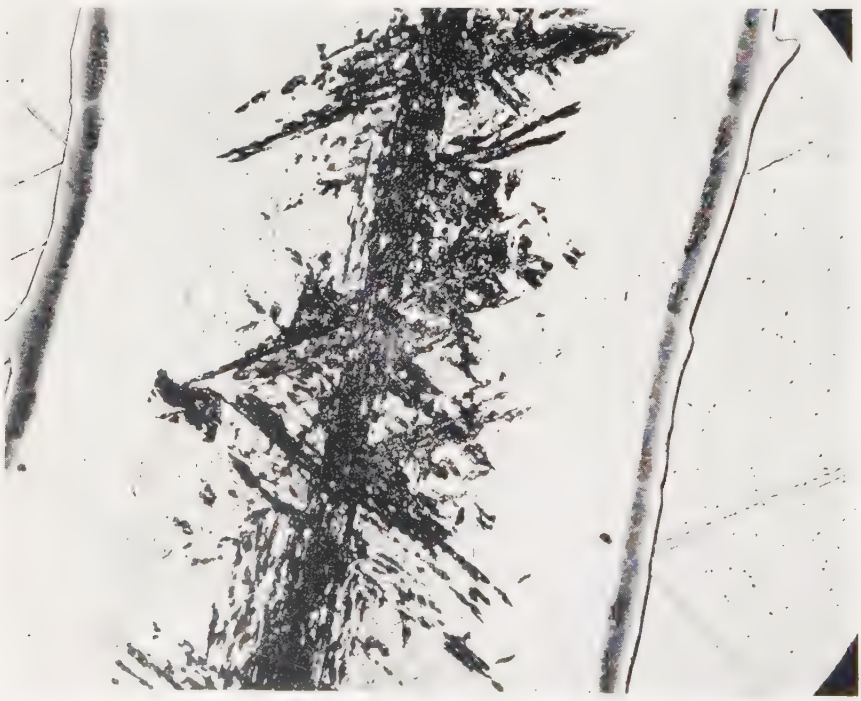

Fig. 12. Vestigial Widmanstätten pattern within taenite lamella. Edmonton, Kentucky, 12·6% Ni. 100 (Henderson and Perry) (reduced to $\frac{5}{10}$).

10 per cent Ni alloy, the precise composition being unimportant to the final conclusions, the coefficient of this expression is equal to 0·46 and

$$D(\mathrm{Ni},\gamma) = 0{\cdot}46e^{\frac{-67{,}500}{RT}} \tag{1}$$

The self-diffusion rate constants for iron* in alpha and gamma iron are given by:

$$D(\mathrm{Fe},\alpha) = 6{\cdot}2e^{\frac{-59{,}800}{RT}} \tag{2}$$

$$D(\mathrm{Fe},\gamma) = 0{\cdot}84e^{\frac{-68{,}900}{RT}} \tag{3}$$

Making the reasonable assumption that the constants in the diffusion equation for nickel in alpha iron are related to similar constants for gamma alloys as are the constants for self-diffusion of iron, one calculates:

$$D(\mathrm{Ni},\alpha) = 3{\cdot}4e^{\frac{-58{,}600}{RT}} \tag{4}$$

This equation establishes that diffusion of nickel is more rapid in alpha phase than in gamma, which follows the similar behaviour for comparative diffusion rates of hydrogen and carbon in alpha and gamma iron. From equations (1) and (4), the ratios of $\frac{D(\mathrm{Ni},\alpha)}{D(\mathrm{Ni},\gamma)}$ are calculated and are summarized in Table 2. In other words, nickel at 300°C diffuses in alpha phase 15,000 times more rapidly than in gamma phase for the same concentration or activity gradient of nickel. Looked at another way, if the diffusion of a given quantity of nickel across 1 cm² of kamacite requires one year, the time required for the same amount of nickel to diffuse across 1 cm² of taenite requires 15,000 years.†

The inhomogeneity of taenite compared with kamacite is less surprising in view of these calculations. At the same time, it is obvious that final equilibrium

Table 2. Comparative diffusion constants for nickel in alpha (kamacite) and gamma (taenite) phase 10 per cent Ni-Fe *alloys cm²/sec*

Temp.	$D(\mathrm{Ni},\gamma)$	$D(\mathrm{Ni},\alpha)$	*Ratio* $D(\mathrm{Ni},\alpha)/D(\mathrm{Ni},\gamma)$
700°C	$3{\cdot}6 \times 10^{-16}$	$2{\cdot}4 \times 10^{-13}$	670
500°C	$4{\cdot}6 \times 10^{-20}$	$8{\cdot}5 \times 10^{-17}$	1850
400°C	$6{\cdot}5 \times 10^{-23}$	$3{\cdot}0 \times 10^{-19}$	4600
300°C	$9{\cdot}1 \times 10^{-27}$	$1{\cdot}35 \times 10^{-22}$	14,900

* M. Cohen, private communication.

† The amount of nickel or iron diffusing a short distance across 1 cm² of surface is approximated by the expression $C_0 \frac{\sqrt{Dt}}{\pi}$ where C_0 is the surface concentration, D is the diffusion constant, and t is the time. For equal amounts of substance diffusing into two phases 1 and 2 for which D_1 and D_2 apply, the relation $D_1 t_1 = D_2 t_2$ holds. The same relation appears to be valid for any general solution of Fick's diffusion equation.

of kamacite with taenite is unlikely at a temperature as high as 500°C, where diffusion is five million times more rapid in gamma phase and is 600,000 times more rapid in alpha phase than at 300°C; otherwise, taenite would have become homogeneous in the time during which the Widmanstätten pattern formed. Hence, taenite of 30 per cent Ni must have formed, at least in part, at lower temperatures, implying the prevalence of high pressures.

It is the general impression that nickel is usually higher at the edges of taenite than in the centre (Perry, 1944, p. 15, Pl. 43–1). The darkly etched centre portion, often showing evidence of transformation (plessite) compared with untransformed light-coloured borders, correlates with a composition gradient of this kind (Fig. 7). Curie temperature (magnetic) and X-ray measurements confirm that nickel is higher in narrow bands than in broad bands of taenite of the same meteorite (Smith and Young, 1939). Perry states that this order of nickel concentration has been shown by quantitative nickel coloration (Perry, 1944, p. 15).

But hardness measurements, such as those of Dexter (Fig. 9) and those recorded by Dalton (1950, 1951) on Canyon Diablo and Bristol, Tennessee, show edges of taenite softer than the centre. Since the hardness of nickel-iron alloys appears to increase with nickel content (Marsh, 1938, p. 387), the supposition is that edges of taenite are sometimes *lower* in nickel than the centre. It may be significant in this regard that the etched centre areas of taenite in Dexter are light compared with a dark border, which is the reverse of the usual situation. Because indirect approaches to nickel composition of this kind are affected by impurities, it would be far better to rely on chemical analyses before reaching a final conclusion in this matter. There is no doubt that a systematic correlation of nickel content in taenite (and kamacite) with distance from the taenite-kamacite interface is needed, and that the analyses, difficult though it is to obtain them, will materially aid meteorite studies.

If nickel is higher at the borders of taenite than in the centre, this situation accords with slow cooling of meteorites, producing taenite of lower nickel content at first, enclosed by a continuous border of increasing nickel content as the temperature decreases.

Assuming, on the other hand, that the nickel composition is sometimes lower at the edges, the history of meteorites in this class may correspond to a secondary heat treatment for temporary periods under conditions of higher temperature or higher pressure. Both factors acting alone or simultaneously induce diffusion of nickel from taenite to kamacite, which would be manifest especially in taenite, where diffusion rates are low, by a border containing less nickel.

Time for Widmanstätten Pattern to Form

Since diffusion rates determine the time it takes for the Widmanstätten pattern to form, it should be possible to calculate the time of formation at any temperature from known diffusion rates of nickel or iron in alloys of the two metals, provided the time is known at one temperature. Although the time of formation at a given temperature is unknown, the time for erasing the Widmanstätten pattern at high temperatures has been determined within broad but reasonable limits. Fraenkel and Tammann (1908) reported that the characteristic pattern of Damara octahedrite

meteorite (7·8 per cent Ni) disappeared, as shown by etching characteristics, after an average of about twenty hours heating at 1000°C. Vestiges of the taenite outline remained, indicating that perhaps the actual required time is somewhat longer. Since the time and temperature necessary to erase the Widmanstätten pattern are those necessary to diffuse nickel from taenite into kamacite (all of which at 1000°C becomes gamma phase), it is reasonable that the time to form the pattern by the reverse processes of diffusion should be related. Using the previously described equation for the diffusion of nickel in gamma nickel-iron alloys, the calculated times for erasing the Widmanstätten pattern (or forming it) at various temperatures are given in Table 3.

Table 3. *Calculated times to form Widmanstätten figure in Damara meteorite* (7·8 *per cent* Ni)

Temp.	$D(\mathrm{Ni}, \gamma) cm^2/sec$	*t(hrs)*	*t(years)*
1000°C	$1{\cdot}23 \times 10^{-12}$	20 (meas'd)	
800°C	$8{\cdot}7 \times 10^{-15}$	$2{\cdot}8 \times 10^{3}$	0·32
500°C	$4{\cdot}4 \times 10^{-20}$	$5{\cdot}6 \times 10^{8}$	$6{\cdot}4 \times 10^{4}$
400°C	$6{\cdot}2 \times 10^{-23}$	$4{\cdot}0 \times 10^{11}$	$4{\cdot}5 \times 10^{7}$
300°C	$8{\cdot}7 \times 10^{-27}$	$2{\cdot}8 \times 10^{15}$	$3{\cdot}2 \times 10^{11}$

The values listed for $D(\mathrm{Ni}, \gamma)$ are slightly different from those of Table 2, because of lower nickel content. The calculated values of time assume that diffusion of nickel in gamma phase or taenite essentially controls the overall rate of diffusion. At lower temperatures where gamma phase co-exists with alpha phase, more rapid diffusion in alpha phase may, of course, shorten the overall time associated with formation of the Widmanstätten figure, and, hence, the method used to calculate times listed in Table 3 may give somewhat high values. Nevertheless, any decrease in times taking into account diffusion rates in alpha phase will be offset to some extent by the effect on diffusion of impurities and high pressures. The present calculated values are consistent with the view that if up to 10^9 years were available, equilibrium in octahedrites was established at 300 to 400°C and definitely not below 300°C.

Plessite Formation and Transformed Kamacite and Taenite

Since plessite is composed of a mixture of finely divided taenite and kamacite, its composition lies between taenite and kamacite. The presence of plessite in meteorites has formerly been difficult to account for based on the expected order of events outlined by the phase diagram. This difficulty persuaded some investigators (Pfann, 1917; Osmond and Cartaud, 1904; Hanson and Hanson, 1920) to reconstruct the phase diagram for iron-nickel so that it included a eutectoid field analogous to finely divided, darkly etched eutectoids known in several other alloy systems. But careful and repeated examination of the nickel-iron diagram has consistently failed to disclose the supposed eutectoid, and instead has verified the diagram shown in Fig. 3.

Derge and Kommel (1937) suggest that plessite was formed by later transformation of the first-formed low-nickel region of taenite. Perry also subscribes to this view. This implies successful transformation in the centre areas of taenite, leaving untransformed the outer edges which can transform only sluggishly, if at all, because of higher nickel content. Accordingly, a taenite border is usually observed to surround plessite areas. Also, in agreement with this view, if the cooling and concurrent decomposition of low-nickel taenite are relatively slow, a simulated Widmanstätten pattern may form on a smaller scale within the observed taenite bands. This also is sometimes observed (Fig. 12). The small-scale irregular patterns revealing vestigial Widmanstatten designs can probably also be explained by decomposition of α_2 phase (Owen, 1940).

If the cooling is rapid in astronomical terms, on the other hand, or the transformation occurs at sub-zero temperatures, acicular α_2 phase forms resembling the appearance of martensite (Fig. 6). If an acicular phase of this kind is retained for a short time at above room temperatures in the alpha-gamma region it decomposes into a structureless, finely divided alpha-gamma mixture which etches darkly. Such areas are typical of many plessite areas. Owen and Burns (1939) found that the acicular phase of meteorites they examined transformed to plessite when heated only eight days at 300°C. Longer heating or heating at higher temperatures is expected to produce a coarser structure of granular taenite and kamacite.

Sub-zero transformation of taenite, therefore, is an additional possible mode of formation for the acicular phase, which, in turn, is the parent substance of the structureless and granular types of plessite. Sudden cooling through the transformation temperature, on the other hand, cannot be considered an equal possibility. The sudden cooling of a large metallic mass is certainly not feasible, any more than is the sudden heating of the interior of a meteorite on its passage through the Earth's atmosphere. Ingots of steel produced in modern steel mills weighing six to eight tons require a day or so to cool down from the melting point to atmospheric temperatures. Larger masses require still longer times, compelling, in any case, a slow cooling rate.

One factor, however, that can easily precipitate phase changes in large or small masses is sudden alteration of pressure. The phase boundaries of the phase diagram are quickly shifted up or down, producing the right conditions for sudden transformation. And, if the temperature at which these changes occur is sufficiently high, the acicular phase so produced is tempered or heat-treated in varying degrees to form a structureless or granular mixture of taenite and kamacite. The higher the temperature or slower the cooling after sudden transformation, the coarser does the mixture of phases become. The entrance of pressure into the detail of possible events in meteorite history, therefore, explains the observed plessite structures without introducing variations of the currently known phase diagram, or necessitating improbable cooling rates, or heating and cooling cycles.

For example, if an alloy (Fig. 8) under pressure finds itself suddenly at much lower pressures (e.g., through breaking up of a larger body into small fragments for which gravitational forces are less), kamacite remains in the kamacite region of the low-pressue diagram and, hence, is stable to further change. But taenite in equilibrium is now suddenly in the alpha-gamma region, and aided by sizable

mechanical shock waves attending change of pressure, it will, therefore, transform to acicular α_2 phase similar to transformation occurring on quenching a gamma alloy to the appropriate temperature within the alpha-gamma region. Only the taenite in centre portions of this phase may transform, assuming the nickel content to be actually lower than the borders, since we have seen that taenite above about 34 per cent Ni resists transformation under any conditions. If all this occurs at above room temperature or is accompanied by a rise of temperature, as seems likely, the acicular α_2 phase will later decompose into plessite.

A further fact enters supporting pressure transformation as a source of plessite. This concerns the observed increase of fine plessite areas in meteorites as the overall nickel content increases (Perry, 1944, pp. 6, 17). Calculations show* that for conditions of equilibrium in a gravitational field, concentration of nickel is higher near the centre of the alloy mass compared with the outer periphery. But the pressures are also greatest in the centre, and corresponding pressure changes can, therefore, have greater metallurgical effect whenever such a mass breaks up into smaller fragments. A nickel concentration gradient of this kind, therefore, correlates with larger areas of pressure-transformed taenite in the higher-nickel alloys. This conclusion also suggests that transformation temperatures for the high-nickel alloys were depressed to lower temperatures than for the lower-nickel compositions.

The factor of pressure also accounts for the otherwise difficult-to-explain acicular kamacite phase sometimes found, as in Dexter (Figs. 7, 9, 10, 11). This structure, as discussed above, may connote sudden transformation of gamma phase, producing a martensite-like phase of body-centred cubic lattice, or may originate from precipitation of taenite from super-saturated kamacite, as is discussed in Part II. In either case, the transformation may develop by increase of pressure (Fig. 8) and sudden release of that pressure (e.g., by the changing distortional strains in a large body, or impact followed by fragmentation). The alloy moves from the alpha region of the phase diagram to either alpha-plus-gamma or all-gamma phase, and thereupon to alpha phase again as lower pressures are resumed. Any changes of pressure in a large mass, contrary to similar possibilities of temperature change, can be conceivably rapid enough to produce the observed acicular transformation. If a low-temperature heat treatment follows the pressure changes, acicular kamacite will tend to become somewhat blurred as seen under the microscope, owing to a tendency of the alloy to revert to non-acicular kamacite again, but not to plessite, since the alloy remains in the alpha-phase region. In Dexter

* The simplified expression for change of mol fraction N of nickel with change of height h in a gravitational field is given by:

$$\frac{dN}{dh} = N(\overline{V}\rho - W_1)\frac{g}{RT}$$

where V is the partial molal volume of nickel, ρ is the density of the alloy, W_1 the atomic weight of nickel, g the gravitational constant applying to the conditions considered, R the gas constant, and T the absolute temperature (Brewer, 1951). At, for example, 400°C, assuming all gamma phase, the partial molal volume from lattice constants of the 20-40 per cent Ni-Fe alloy is 6·9 cc, and $\rho = 7{\cdot}9$ g/cc for 8 per cent Ni-Fe or 8·0 g/cc for 30 per cent Ni-Fe. Since $\overline{V}\rho$ equal to about 55 is less than W_1 equal to 58·7, $\frac{dN}{dh}$ is negative, or the mol fraction of nickel tends to decrease going away from the centre of the alloy mass.

meteorite, the time and temperatures after sudden transformation were sufficient to cause only slight diffusion.

Further evidence of sudden pressure changes as postulated above is provided by the presence of Neumann bands in hexahedrites and in the kamacite of octahedrites. These form characteristically by reason of impact or sudden fracture in the body-centred cubic lattice of iron at room temperatures. They are discussed next in Part II.

Acknowledgment

Appreciation is expressed to E. P. Henderson for many stimulating discussions on meteorites and for several of the figures. Discussions with Morris Cohen were especially helpful, as well as suggestions by Benjamin Averbach. Photomicrographs of Figs. 7, 9, 10, and 11 were prepared by Mrs. Constance Craven, formerly of the General Electric Research Laboratories. Specimens of the Dexter meteorite were made available by the American Museum of Natural History.

References

Benedicks, C. 1910 Synthese du fer meteorique. *Nova Acta Regiae Soc. Sci. Upsaliensis* (4), **2**, No. 10, 1–26

Benedicks, C. 1926 *Meteoric iron and invar. Metallographic Researches*, McGraw-Hill Book Co., New York, pp. 99–150.

Birch, F. 1940 The alpha-gamma transformation of iron at high pressure and the problem of the earth's magnetism. *Amer. J. Sci.* **238**, 192–211.

Brewer, Leo 1951 The equilibrium distribution of the elements in the earth's gravitational field. *J. Geol.* **59**, 490–497

Buddhue, J. D. 1948 Synthetic metallic meteorites. *Pop. Astron.* **56**, 105–108

Cohen, E. 1894 Untersuchungsmethoden und Charakteristik der Gemengtheile. *Meteoritenkunde*, I Heft, 340 pp.

Dalton, F. 1950 Microhardness testing of iron meteorites. *J. Roy. Astron. Soc. Canada* **44**, No. 5. 185–195

Dalton, F. 1951 Microhardness testing of iron meteorites. *J. Roy. Astron. Soc. Canada* **45**, 162–166

Darken, L., and Gurry, R. 1953 *Physical Chemistry of Metals*. McGraw-Hill Book Co., New York, 535 pp.

Derge, G., and Kommel, A. R. 1937 The structure of meteoritic irons. *Amer. J. Sci.* (5) **34**, 203–214

Fraenkel, W., and Tammann, G. 1908 Über meteorisches Eisen. *Z. Anorg. Chem.* **60**, 416–435

Farrington, O. C. 1915 *Meteorites*. Chicago, The author, 233 pp.

Hansen, M. 1936 *Zweistofflegierungen*. Springer, Berlin, 696 pp.

Hanson, D., and Hanson, H. 1920 The constitution of the nickel-iron alloys. *J. Iron Steel Inst.* **102**, 39–64

Henderson, E. P. 1941 Chilean hexahedrites and the composition of all hexahedrites. *Amer. Mineral.* **26**, 546–550

Hoselitz, K. 1944 The iron-nickel phase diagram by magnetic analysis and the effects of cold-work. *J. Iron Steel Inst.* **149**, 193–211

Marsh, J. S.	1938	*Alloys of Iron and Nickel.* McGraw-Hill Book Co., New York, **1**, 593 pp.
Mehl, R. F., and Derge, G.	1937	Studies upon the Widmanstätten structure, VIII—The gamma-alpha transformation in iron-nickel alloys. *Trans. A.I.M.E.*, **125**, 482–500
Osmond, F., and Cartaud, G.	1904	Sur les fers meteoriques. *Revue Metallique*, **1**, 69–79
Owen, E. A.	1940	The structure of meteoritic iron. *Phil. Mag.* (7) **29**, 553–567
Owen, E. A., and Burns, B.	1939	X-ray study of some meteoritic irons. *Phil. Mag.* (7) **28**, 497–519
Owen, E. A., and Liu, Y. H.	1949	Further X-ray study of the equilibrium diagram of the iron and nickel system. *J. Iron Steel Inst.* **163**, 132–137
Owen, E. A., and Sully, A.	1939	The equilibrium diagram of iron-nickel alloys. *Phil. Mag.* (7) **27**, 614–636
Paneth, F. A.	1940	*The Origin of Meteorites.* Halley Lecture, Clarendon Press, Oxford, 26 pp.
Perry, S. H.	1944	The metallography of meteoric iron. *Bull. U.S. Natl. Museum*, No. 184, 1–196
Pfann, E.	1917	Über den inneren gefügeaufbau der meteorischen nickeleisen. *Internationale Zeit. für metallographie* **9**, No. 2, 65–81
Smith, S. W. J., and Young, J.	1939	The Widmanstätten structure of octahedral meteoritic iron. *Nature* **143**, 384–385
Vogel, R., and Heumann, T.	1946	Über die Bildungsmöglichkeiten der Widmannstättenschen Struktur des meteorischen Eisens unter hohem Druck. *Nachrichten der Akad. der Wissenschaften Göttingen, Math. Phys. Klasse, Heft* 2, 123–125
Wells, C., and Mehl, R. F.	1941	Rate of diffusion of nickel in gamma iron in low-carbon and high-carbon nickel steels. *Trans. A.I.M.E.* **145**, 329–339

Book review

SYDNEY J. JOHNSTONE: **Minerals for the Chemical and Allied Industries.** Chapman and Hall Ltd., London, 1954, 652 pp. Price (bound) 75s.

THIS new work on economic minerals covers a field which has hitherto been rather neglected in text-book literature. It sets out to provide a conspectus of information on the grades and qualities of mineral products that are acceptable to various branches of industry; and it will certainly achieve its purpose of establishing closer liaison between producers of crude minerals and the consumers concerned with industrial utilization. The author was for many years Principal of the Mineral Resources Department of Imperial Institute, in which capacity one of his duties was to find markets for the mineral products of Colonial and some Dominion territories, a task that demanded an extensive knowledge not only of the sources whence minerals are derived but also of the techniques employed in their processing and of the specific requirements of potential buyers. On retirement, he has condensed in this volume the accumulated practical experience of an official lifetime.

Each of the seventy-one chapters deals with a single industrial mineral or a related group of mineral commodities, ranging from platinum to perlite, from selenium to slate waste. Only the mineral fuels, iron ores, gold, industrial diamonds, and gemstones are omitted. Under each heading information is given on the principal ores and their geographical sources, on the methods of process metallurgy used in their beneficiation, on their industrial uses, and on market specifications. The latter topics are given the greater space, the specifications drawn from guides issued by the British Standards Institution, the American Society for Testing Materials, and the U.S. National Stockpile authorities being the most novel part of the work.

Within its scope the text is unusually comprehensive, and there are few errors or noteworthy omissions. A statement that "nepheline-syenite has piezo-electric properties but is not used for this purpose as the crystals are usually small and imperfect" will give rise to some bewilderment. In the chapter on uranium, there is a little confusion between the grade of ores and that of picked concentrates: apart from Congo production, no run-of-mine output has ever averaged more than about one per cent U_3O_8, and today a fifth of this value in non-refractory ore is marketable. Contrary to current official usage on both sides of the Atlantic, the name columbium is employed in preference to niobium. But in a work of such a wide range it is remarkable that such a uniformly high standard of accuracy and modernity has been achieved. Whilst principally of value to producers and consumers of minerals, the volume will be found useful in the practice and teaching of economic geology; and as it is the only work of its kind it should find a place in every geological and chemical library.

C. F. DAVIDSON

CORRECTION

H. G. THODE, R. K. WANLESS, and R. WALLOUGH: *The origin of native sulphur deposits from isotope fractionation studies*, Vol. 5, pp. 286 to 298:

On Fig. 1, on p. 287, "SO_4" should appear at the left-hand end of the middle line of the figure, and "H_2S" should appear at the right-hand end. These symbols were unfortunately omitted when the block was made.

IMPORTANT ANNOUNCEMENT

From Volume 7 onwards (the first number will be published in January 1955) the subscription rates for *Geochimica et Cosmochimica Acta* will be as follows:

Class A: The present rate of £4 10s. ($12.60) per volume, which will continue to apply to University libraries, research laboratories, institutions, Government offices, etc.

Class B: **A reduced price of £3 10s.** ($9.80) per volume, for individual subscribers who can certify that they require the journal for their personal use only.

It is hoped that the introduction of the Class B subscription will encourage many for whom the regular price is too high, to become personal subscribers to the journal.

This journal does not receive financial assistance from any outside body, and relies for its finances solely on the revenue from subscriptions. In the present circumstances it is quite impossible to reduce the regular subscription price, but it is the publishers' aim to make the journal as widely available as possible.

Scientific journals are produced in small numbers and soon go out of print. As time passes their value is enhanced, and therefore they represent not only an interest for the present but a good investment for the future.

PAPERS ACCEPTED FOR PUBLICATION

The following is a list of papers which will appear in the early issues of Volume 7. This does not necessarily include all papers accepted for publication:

HERBERT H. UHLIG: Contribution of metallurgy to the origin of meteorites. Part II—The significance of Neumann bends in meteorites.

HOWARD A. POWERS: Composition and origin of basaltic magma of the Hawaiian Islands.

F. E. SENFTLE and J. T. BRACKEN: Theoretical effect of diffusion on isotopic abundance ratios in rocks and associated fluids.

HIROSHI ONISHI and E. B. SANDELL: Geochemistry of arsenic.

G. J. WASSERBURG and R. J. HAYDEN: A^{40}–K^{40} dating.

RALPH STAIR: The spectral transmissive properties of some of the tektites.

14Sep

PERGAMON PRESS LTD.

Spectrochimica Acta

An international research journal

This journal is devoted to the applications of optical spectroscopy to chemical problems, *i.e.*, the subject of spectrochemical analysis, the importance of which increases year by year. Original papers are published dealing with the basis, technique, instrumentation and results of qualitative and quantitative analysis by means of ultra-violet, visible and infra-red emission and absorption spectra.

Contributions appear in English, French or German, with summaries in English. Reports of national and international congresses and colloquia and reviews of important books are also included.

Issued in alternate months (*Vol. 7, No. 1—February, 1955*)

Price per vol. (six issues) £5 15*s.* 6*d.* ($16) *including postage*

Recently published

QUANTITATIVE SPECTROCHEMICAL ANALYSIS OF SILICATES

by L. H. AHRENS, M.A., D.Sc., F.R.I.C.

This book is based almost entirely on recent research of the author and his co-workers at the Massachusetts Institute of Technology, most of which appears here for the first time. A scheme of DC arc analysis of the naturally occurring silicates (minerals, rocks, meteorites, soils and sediments) is described, in which an attempt is made to reach an effective compromise between accuracy, sensitivity, speed and cost of analysis. This is achieved in 3–7 separate operations by means of which some 35 elements (including all alkali metals, fluorine and the so-called major constituent elements, if desired) are determined. Wide concentration ranges from ppm or so to several per cent covered.

Not only spectrochemists and silicate analysts in general, but all those concerned with the composition of silicates—mineralogists, petrologists, geochemists, cosmochemists, ceramicists and others—will find much of its content that will be of use to them.

120 *pp.* 28 *diagrams.* 7 *plates.* 25*s. net*

Prospectus available on request

242 MARYLEBONE ROAD · LONDON N·W·1

PRINTED AT THE PITMAN PRESS, BELFAST, NORTHERN IRELAND